Flexible, Reconfigurable and Wearable Antennas Integrated with Artificial Magnetic Conducting Surfaces

by

Saud Saeed

A Dissertation Presented in Partial Fulfillment
of the Requirements for the Degree
Doctor of Philosophy

Approved August 2017 by the
Graduate Supervisory Committee:

Constantine A. Balanis, Chair
Joseph C. Palais
James T. Aberle
Martin Reisslein

ARIZONA STATE UNIVERSITY

December 2017

ABSTRACT

Flexibility, reconfigurability and wearability technologies for antenna designs are presented, investigated and merged in this work. Prior to the design of these radiating elements, a study is conducted on several flexible substrates and how to fabricate flexible devices. Furthermore, the integration of active devices into the flexible substrates is also investigated. A new approach of designing inkjet-printed flexible reconfigurable antennas, based on the concept of printed slot elements, is proposed. An alternate technique to reconfigure the folded slot antenna is also reported. The proposed radiator works for both Wireless Local Area Network (WLAN) and Worldwide Interoperability for Microwave Access (WiMAX) applications. The flexible reconfigurable antenna is also redesigned to resonate at both (2.4/5.2 GHz) for WLAN devices and its Multiple-Input Multiple-Output (MIMO) configuration is reported. Two orthogonal elements are used to form the MIMO antenna system for better isolation.

The wearability of the proposed flexible reconfigurable radiator is also discussed. Since wearable antennas operate close to the human body, which is considered as a lossy tissue, an isolation between the radiating elements and human body is required to improve the radiation characteristics and to reduce the Specific Absorption Rate (SAR). The proposed antenna is redesigned on an Artificial Magnetic Conductor (AMC) surface that also functions as a ground plane to isolate the radiator from the human body. To examine its performance as a body-worn device, it is measured at different positions on the human body. Furthermore, simulations show that the SAR level is reduced when using the AMC surface. The proposed wearable antenna works for both Wireless Body Area Network (WBAN) and WiMAX body-worn wireless devices.

Electromagnetic bandgap (EBG) structures are used to suppress surface wave propagation in printed antennas. However, due to the presence of vias, not all of them can be utilized in flexible radiators. Thus, a Perforated High Impedance Surface (PHIS) is proposed which suppresses the surface waves without the need of vias, and it also serves as a ground plane for flexible antennas. The surface wave suppression and the antenna applications of the proposed PHIS surface are discussed.

I dedicate this dissertation to my beloved parents and my wife.

I also dedicate this dissertation to my close and very special friends: Abdulrahman bin Saeed, Ali Alaseem, Abdulrahman Alaseem, Hotham Altwaijry, Sattam Alsubaiee, Abdulaziz Alhussien, Abdullah Alkudsi, Ali Alrajhi, Khaled Aljaloud, Khalid Almegbel, Mohammed Alzaid, Badr Alharbi, Hamad Alshalawi, Mohammad Mahzari, Ramadan Salim, Nafati Aboserwal, Abdulhamid Altheyab and Abdulaziz Aldaej.

ACKNOWLEDGMENTS

In the name of Allah, the Most Merciful and Beneficent. All the thanks goes to Allah almighty, who has granted me the health and knowledge to accomplish and achieve my Ph.D. degree in Electrical Engineering.

I would like to thank my family for their endless support and prayers during my study abroad. Special thanks goes to my brother Abdulrahman bin Saeed and my uncle Mohammed Alaseem for their endless support during my study. I extend my appreciation and thanks to my other brothers and sisters. I am deeply thankful to my wife Sarah Aljwair and my daughters: Leen, Noof and Dana for their encouragement and support.

I would like to deeply acknowledge my adviser Prof. Constantine Balanis and to express my sincere appreciation to him for his excellent guidance, encouragement, support and valuable suggestions. It is my pleasure to be his student and work with him throughout my study and research at the Arizona State University (ASU). His great assistance and advice when writing my journal articles and the dissertation are deeply acknowledged and appreciated.

I would like to thank the committee members Prof. Joseph C. Palais, Prof. James T. Aberle and Prof. Martin Reisslein for their helpful comments and suggestions. Special thanks goes to Craig Birtcher for his assistance and support during the experimental work of my research.

I would like to express my thanks and appreciation to all my labmates and friends at ASU: Dr. Ahmet Durgun, Dr. Alix Rivera-Albino, Dr. Nafati Aboserwal, Dr. Sivaseetharaman Pandi, Dr. Wengang Chen, Dr. Yousef Dashti, Mikal Amiri, Anuj Modi, Subramanian Ramalingam, Ziyad Alharbi, Fahad Almofawez, Omar Alotaibi and Akhilesh Thyagaturu. I also would like to thanks my friends at King Abdulaziz City for Science and Technology (KACST): Dr. Hussein Shaman, Dr. Waleed Alomar,

Turki Alanazi, Mohammed Alharbi, Khalid Almegebl, Meshaal Alyahya and Turki Alhazani. I would like to thank Dr. Joseph Costantine and Dr. Youssef Tawk for their support. I also thank Dr. Russell I. Heigh and Dr. David A. Etzioni from Mayo Clinic Hospital in Arizona for their encouragement and support.

I would like to thank the Ministry of Education in Saudi Arabia, Saudi Arabian Cultural Mission (SACM) in United States and Prince Sattam bin Abdulaziz University in Saudi Arabia for their generous financial support and administrative support.

TABLE OF CONTENTS

CHAPTER Page

LIST OF TABLES

LIST OF FIGURES

Figure Page

Figure Page

Figure Page

Figure Page

Figure Page

Figure Page

Chapter 1

INTRODUCTION

1.1 Research Motivation and Significance

In recent years, wireless communication systems have advanced rapidly. Moreover, the size of these systems have become smaller and smaller due to the swift progress in electronic technology. Therefore, these advances result in an increasing demand for affordable, compact, lightweight, and easy to integrate antennas. With the advancement in wireless technology, other demands arose for antennas designed to deal with other requirements, such as their capacity and environmental conditions. Today, antennas are being used in a wide spectrum of applications, such as personal communication, medical, military, entertainment, and space applications. As a result, a substantial amount of research has been performed to discover new technologies in designing antennas that meet the demands of the new wireless systems. Therefore, this research has investigated and merged the properties of flexibility, reconfigurability, and wearability of planar printed antennas. The resulting antenna elements are then integrated with Artificial Magnetic Conductors (AMC) to improve their radiation characteristics.

During the past decade, flexible, reconfigurable and wearable antennas have received an intensive research interest due to the potential that they could be used in many applications because of their attractive features that can improve the performance of wireless systems when compared with conventional radiator elements. For instance, flexible wearable antennas can be used in wearable medical sensors or

other health care environmental applications. Advances in technologies have led to new applications, such as flexible mobile devices or flexible RFID tags for sensing, tracking, automatic payment solutions, access control, and other applications. For military systems, flexible antennas can be used as conformal antennas coated to the aircraft to reduce the complexity of the aircraft structure and its visibility signature to radar systems.

Antennas are critical components of any wireless system, but individually their radiation characteristics may be fixed. Thus, some wireless systems have more than one antenna to perform the multiple functions of the system. This results in an increase in the size and cost of the system. Reconfigurable antennas are the solution to overcome this problem. They can extend the functions and applications of basic antennas due to the ability to change their radiation characteristics. Reconfigurable antennas are needed for many applications, such as cognitive radio, MIMO technology, and space communication. These advantages have led the author to design a flexible reconfigurable antenna system that is suitable for conformal wireless devices that is also reconfigurable so that its radiation characteristics can be changed.

Electromagnetic Bandgap Structures (EBGs), which are also referred to as Artificial Magnetic Conductors (AMCs) or High Impedance Surfaces (HISs), are widely documented in the literature where they have been shown to improve the radiation characteristics of antennas, obtain low profile radiators and suppress the Surface Waves (SWs) in printed antenna systems. Another advantage is using these surfaces in wearable antenna designs that operate close to the human body which may otherwise result in impedance mismatch and high Specific Absorption Rate (SAR). AMC surfaces can be used as isolators to overcome this problem and to improve the radiation efficiency of wearable antennas. Conventional EBG/AMC surfaces with metallic vias can be used to suppress SWs in printed antenna systems. However, the metallic

vias increases the complexity of designing flexible EBG surfaces and using them for flexible antenna applications. The demand for flexible EBG surfaces that suppress SWs without vias, while still maintaining the surface wave suppression, is increasing. As a result, this work investigates the potential of designing flexible EBG surfaces for flexible and wearable antenna applications.

1.2 Research Contributions

The main contributions and advances of this work are the following:

- Developed a compact antenna that is flexible and also reconfigurable for conformal WLAN/WiMAX wireless devices. The proposed antenna is based on the concept of folded slot antennas, and it is fabricated using inkjet-printing technology. A new technique to reconfigure the antenna is based on only one RF switch (PIN diode) with a simple bias circuit. The antenna is designed, simulated, fabricated and tested for both flat and cylindrically curved configurations. The MIMO configuration is also reported.

- Created a compact antenna design that merges wearability, flexibility and reconfigurability of antenna designs into one design. It is designed on an AMC surface to isolate it from the human body in order to reduce the SAR level and to improve its performance. The flexibility of the antenna is examined, and it is also measured on a model of a human body to demonstrate its performance.

- Designed a flexible EBG/AMC surface without the need of metallic vias. The surface is referred to as a flexible Perforated High Impedance Surface (PHIS), and it can be used for both surface wave suppression and low profile antenna applications.

1.3 Dissertation Organization

This dissertation consists of seven chapters:

- Chapter 1 includes the importance and the main original contributions of this work.

- Chapter 2 reviews the research related to flexible, reconfigurable and wearable antennas.

- Chapter 3 presents the inkjet-printed flexible reconfigurable antenna. It includes the radiator design and reconfiguration concepts, and also incorporates the results and discussion of the new proposed design.

- Chapter 4 introduces the wearability of flexible reconfigurable antenna. It includes all the design procedures of wearable antennas and also antennas mounted on AMC surfaces. The radiation characteristics of the antenna is presented, and its flexibility and wearability test are discussed in Chapter 4.

- Chapter 5 presents the flexible EBG/AMC surface. It includes the design procedure of perforated HIS surfaces, and the reflection phase and surface wave suppression analysis.

- Chapter 6 incorporates the conclusions of the research.

- Chapter 7 incorporates the potential future work of the current research.

Chapter 2

RESEARCH OVERVIEW

This chapter reviews the concept of flexibility, wearability and reconfigurability of antenna designs. Since the choice of the substrates and the antenna types is the critical part when designing flexible antennas, a comparison between the commercially available flexible substrates and fabrication technologies are discussed. The previous work on flexible and wearable antennas is also reported. The chapter reviews the reconfiguration techniques, such as the electrical tunable techniques, of reconfigurable antenna designs. The basic concept of a PIN diode (RF switch) and its bias circuit is explained.

2.1 Flexible and Wearable Antennas

The importance of antennas being flexible and wearable has received much interest from both industry and academic research. Recent advances in thin-film materials being used as flexible substrates have made flexible electronics possible. These advances have been merged with advances in fabrication technologies, such as inkjet printing, to be used in fabricating flexible electronics and antennas. Flexible electronic devices, as a newly introduced technology, require flexible antennas to make them wireless. Thus, the efficiency of those devices relies on the radiation characteristics of the antennas. An example of a wearable flexible electronic device is displayed in Fig. 2.1. The proposed flexible folded slot antenna in this work is shown in Fig. 2.2. Flexible antennas are convenient for wearable medical devices, where they can be used for wearable sensor devices on the human body to measure the patients temperature.

Figure 2.1: Flexible Circuit: Flexible Wireless Temperature Sensor System [1].

2.1.1 Literature Review on Flexible and Wearable Antennas

The choice of the substrate type for flexible electronic circuits and antennas is a challenging task. When the substrate is flexible, it is deformable to be mounted on conformal structures. However, the substrate flexibility is not the only criteria for choosing a flexible substrate. A designer of flexible antennas must consider and investigate the other properties of the material such as the electrical, mechanical, chemical, optical, thermal, and surface roughness properties [2]-[3]. For example, a paper substrate is a flexible material but it has a high loss when compared with

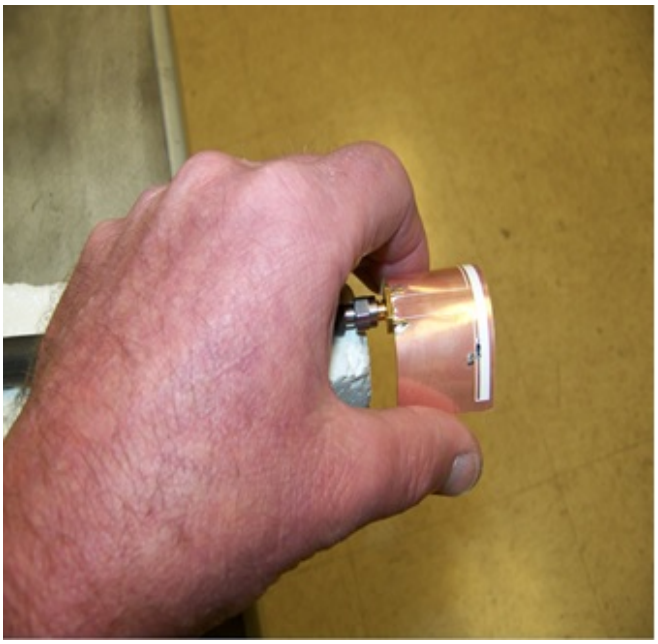

Figure 2.2: The Proposed Flexible Folded Slot Antenna Printed on PET Material.

other substrates, which affects the radiation efficiency of the antenna. Based on the applications, the flexible substrate has to be chosen carefully in order to maintain an efficient antenna design. This section reviews several examples of flexible antenna designs.

In [4], a flexible wearable dipole antenna was designed and fabricated on a fabric material using conductive threads, as shown in Fig. 2.3, to make it attachable to human clothes. The locations on the human body at which conventional rigid printed antennas can be worn are limited. This is not the case when designing antennas on fabric substrates. However, the fabric substrate suffers from absorbing fluids which may affect the performance of the antenna.

In [5], a flexible antenna designed on a paper substrate was proposed. The paper material is cost-effective but it is fragile, and frequent or high levels of bending result in cracks and associated electrical discontinuities. The dielectric constant of the paper is $\epsilon_r = 3.4$, and the loss tangent is $\tan(\delta) = 0.065$, which is considered a high loss type

Figure 2.3: Flexible Antenna Printed on a Fabric Substrate [4].

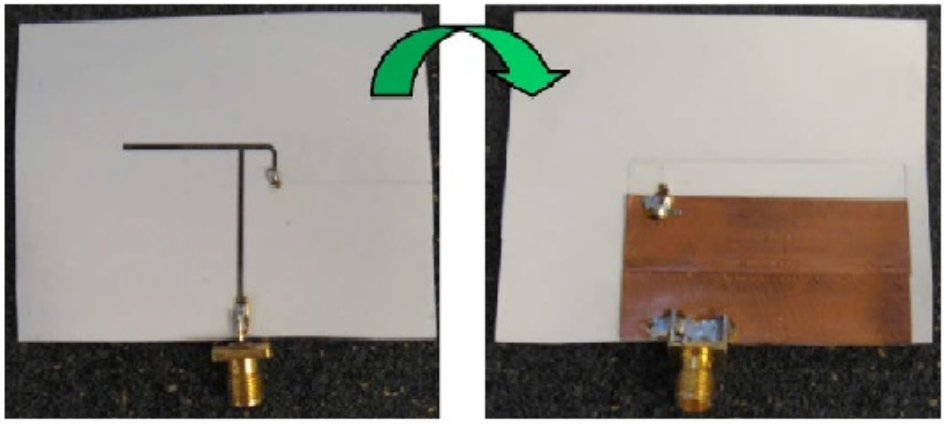

Figure 2.4: Flexible Antenna Printed on a Paper Substrate [5].

of substrate compared to other commercially available flexible materials. The compact (46 mm×25 mm) paper-based antenna displayed in Fig. 2.4 was designed at 2.45 GHz for WLAN applications, and it was fabricated using inkjet-printing technology.

In [6], flexible bowtie antennas were proposed and fabricated on Polyethylene Naphthalate (PEN) film, as shown in Fig. 2.5, which is used as a flexible substrate.

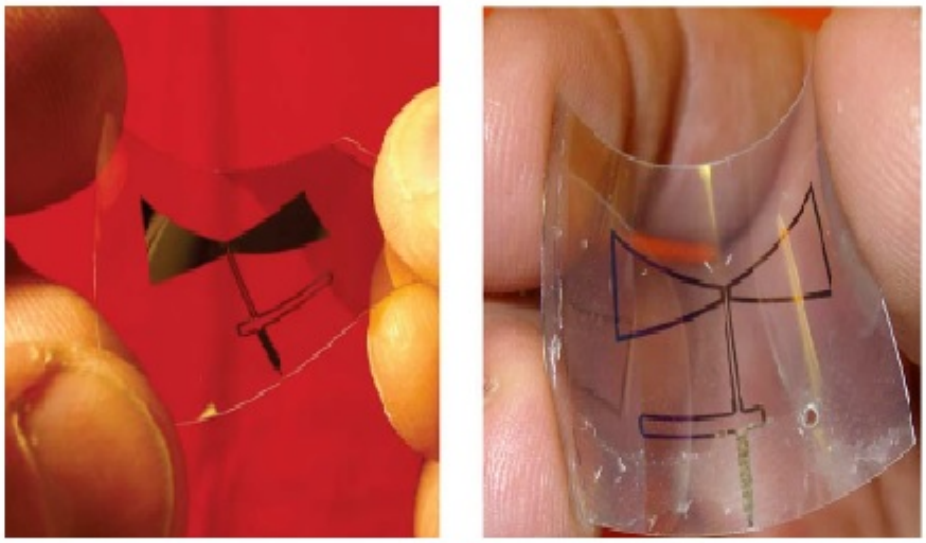

Figure 2.5: Flexible Antenna Printed on a PEN Substrate [6].

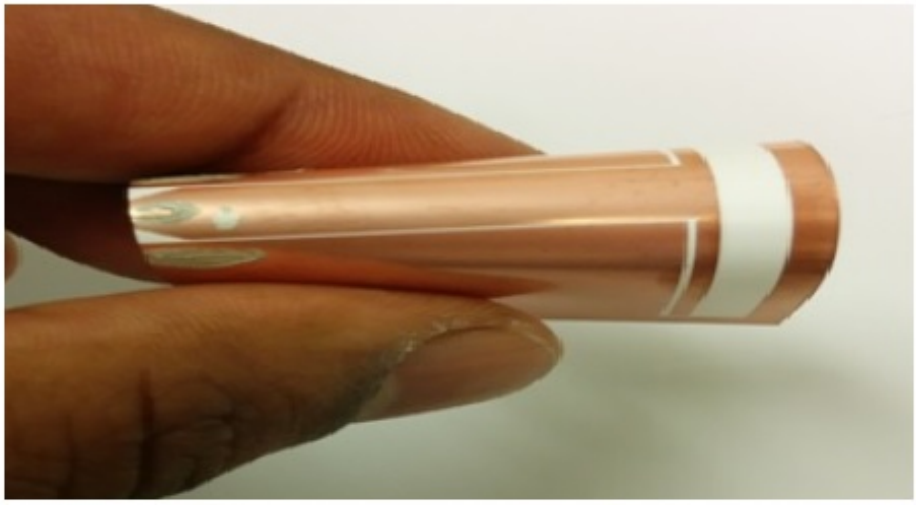

Figure 2.6: Flexible Antenna Printed on a PET Substrate.

Two antennas were designed: a bow-tie and an outlined bow-tie. It was observed that the outlined bow-tie antenna, which has reduced metallization, has almost the same radiation characteristics as the solid bow-tie antenna. The resonant frequencies of the solid and outlined bow-tie antennas are 7.66 and 7.4 GHz, respectively. The

size of both antennas is (39 mm $\times$ 25 mm). Another flexible design that is based on the fluidic antenna design was reported in [7]. The antenna is fabricated on Polydimethylsiloxane (PDMS), which is also considered a flexible substrate. PDMS has a low dielectric constant ($\epsilon_r = 2.67$) and a high loss tangent [$\tan(\delta) = 0.0375$].

The Kapton polymide and Polyethylene Terephthalate (PET) films are also recommended materials for flexible designs. They are chosen because of the balance between the electrical and mechanical properties of the substrate. For example, PET substrate has a low loss tangent [$\tan(\delta) = 0.008$] compared with the paper substrate. Also, to maintain the flexibility of the antennas, these films are available at very low thicknesses, such as 0.05 mm and 0.1 mm; the dielectric constant is around ($\epsilon_r = 3$), and the mechanical strength is excellent. Flexible antennas fabricated using Kapton polymide and PET material were previously reported in [8]-[9]. Fig. 2.6 shows a flexible antenna printed on PET material.

In this work, we are interested in designing flexible printed antennas for conformal and wearable applications. It is observed from the literature that the selection of the antenna type is also a challenging task. The microstrip antenna is a well-known type of printed radiator [10]. However, it is not recommended to be used in flexible configuration because flexible substrates are exceedingly thin, resulting in very narrow frequency bandwidths. It is also recommended to avoid multi-layers of substrates in designing flexible antennas, which is the case of aperture coupled antennas. Printed or planar monopoles and dipoles are an attractive antenna type for flexible antennas because of their compact size and ease of fabrication [3], [10]. In addition, their radiation pattern is omni-directional, which is required by most wireless systems. However, for body-worn antennas, the back radiation is not preferred since it may increase the SAR level. Moreover, the human body is a lossy tissue so that it may absorb some of the energy and affect the radiation efficiency of the antenna. Thus, an

isolation surface between the antennas and the human body is required to improve the radiation efficiency and to reduce the SAR level. More details are discussed in Chapter 4 about the proposed wearable antenna in this work and its integration with an AMC surface to reduce the SAR level and to improve its radiation characteristics.

2.1.2 Fabrication Technologies for Flexible Antennas

Inkjet-printing fabrication technology is used to fabricate flexible antennas. It is a very simple and inexpensive technique, and it is widely used by manufacturing companies. This fabrication technique is an additive process which is based on depositing copper ink droplets of a certain size onto a flexible substrate [3], [11]; it is unlike photolithography, which is mainly based on removing the unwanted part from the conductive layer of the substrate. The resulting pattern on the substrate has a high quality and resolution. There are different types of conductive inks, such as silver, gold, and copper, which affect the quality of the printing. Another factor that is important for the printing quality is the characteristics of the substrate, such as the thermal properties. This fabrication technology is a fast process and does not require a clean room environment.

Another fabrication technology is photolithography, which is a technique that is based on removing the unwanted parts using a photoresist and etching technique [3]. This technology is widely used for printed circuit boards, and it can be used to fabricate complex geometries of printed antennas and circuits. It is not a fast process like inkjet printing, and it is a multi-step process with a low productivity technique when it is compared with inkjet printing technology.

2.2 Reconfigurable Antennas

Antennas are a very significant part of any wireless system, since without antennas no wireless connectivity can be provided. Therefore, the performance and reliability of any wireless communication system rely on the radiation characteristics of antennas. Many types of antennas, such as dipole, monopole, loop, microstrip, reflector, slot and horn radiator elements are commercially available for wireless systems. There are some requirements or standards for each wireless system, such as the capacity of the system or the environment conditions. Therefore, some wireless systems have more than one antenna to meet system requirements, since the radiation characteristics of certain elements are basically fixed [12]. As a result, the cost and the complexity of the systems might be increased. The use of reconfigurable antennas is the appropriate solution to overcome this problem.

Reconfigurable antennas, proposed in 1983 by D. Schaubert [13], can be defined as a multifunctional type of antenna which is able to change its radiation characteristics such as the frequency of operation, polarization, and radiation pattern [12]. When the radiation characteristics of antennas are changeable, this may help to accommodate changes in the operating requirements of any wireless system. When reconfigurable antennas are compared with broadband antennas, they have other advantages, such as compact size, the same radiation characteristics for all frequency bands, and the ability to provide the frequency selectivity of the system, which help to reduce the co-site interference from other wireless systems [14]. However, there are some issues and challenges with the design of reconfigurable antennas and how to integrate them into a wireless system while maintaining the reconfigurablity and the functionality of the antenna. The main goal of using reconfigurable antennas is to reduce the number

of them needed for a wireless system. This may help with the reduction of the system complexity, cost, size, and weight.

Many reconfiguration techniques have been proposed for antennas. Based on these techniques, a plethora of reconfigurable, tunable and active antenna designs are proposed in the literature. Planar antennas, which are printed on circuit board substrates, are the recommended antenna type to be used for reconfigurable designs. They are recommended because of their simplicity in incorporating active devices to the antenna design structure. The main reconfiguration technique is to redistribute the current on the antennas, allowing them to change their radiation characteristics [15]. RF components such as PIN diodes are able to connect or disconnect the radiator parts of the radiating element to change the function of the antenna. For instance, PIN diodes are used as switches between the radiator parts in order to redistribute the current and to change the electrical length of the antenna. Once the electrical length of the antenna is varied, the frequency of operation will change. Different reconfiguration techniques for antennas are addressed in this section.

Because of the ability to change their properties, reconfigurable antennas are needed in advanced wireless systems. Reconfigurable antennas can be used in many applications, such as radar, mobile communication, space, cognitive radio, and MIMO technology wireless systems. For example, a cognitive radio antenna system consists of two antennas: one is the sensing antenna, which is an ultra-wide-band (UWB) antenna, while the second antenna is the reconfigurable antenna, which is used for frequency selectivity.

Designers of reconfigurable antennas are required to address the requirements of the operating systems. These requirements are needed to determine:

- Reconfiguration property, such as operating frequency bands or pattern.

- Antenna type for the design requirements.
- Reconfiguration technique that will be used to reconfigure the antenna while maintaining the design requirements.

2.2.1 Reconfiguration Mechanisms for Antennas

In terms of changing the radiation characteristics, reconfigurable antennas can be divided into four groups [16]:

- Reconfiguration of the operating frequency.
- Reconfiguration of the radiation pattern.
- Reconfiguration of the polarization.
- Reconfiguration of the antenna in term of frequency, radiation pattern, and polarization.

In the literature, many reconfiguration techniques have been proposed to reconfigure the antenna radiation characteristics. The main idea of these techniques was to redirect the surface current on the antennas in order to change their radiation characteristics. Another way of reconfiguring an antenna is to change the feeding network or the structure of the antenna. The reconfiguration techniques can be summarized into four groups [16]:

- Electrically reconfigurable antennas using electronic RF switches such as PIN-diodes, varactors, and RF-MEMS.
- Optically reconfigurable antennas using optical switches.

- Physically reconfigurable antennas by altering the physical structure.
- Material-based reconfigurable antennas by using materials like ferrite.

In this work, we used the concept of electrically reconfigurable antennas. In our case, we used one PIN diode to design a flexible reconfigurable antenna. The way the switches are integrated into the antenna structure is critical in designing reconfigurable antennas because the designer is required to overcome the complexity of the system. Some design issues that are involved in designing reconfigurable antennas include the biasing network for activating/deactivating the switches, non-linearity issues of the switches, and losses or interference that might be created by the switches and the biasing lines that are used to control the activation of the RF switches.

Having explored the different reconfiguration techniques of reconfigurable antennas, our plan is to use the electrical reconfiguration technique. The next step is to show examples of designing reconfigurable antennas using the electrical reconfiguration technique; the first example uses a PIN diode to reconfigure the element. A PIN diode works in two states. When the diode is forward biased, the state is ON, and when the diode is reversed biased, the state is OFF. In [17], a meander line antenna with non-uniform five turns, was proposed. It was reconfigured by using a PIN diode to change the electrical length of the meander line in order to tune the operating frequencies between 4G LTE and other wireless communication applications. Fig. 2.7 shows the proposed antenna in [17]. The second example uses RF-MEMS to reconfigure an antenna. In [18], a reconfigurable rectangular spiral antenna was presented. Four RF-MEMSs were integrated on the same substrate, and they were used to connect the five sections of the antenna structure. The antenna spiral arm length increased from U to NU, as shown in Fig. 2.8, and the RF-MEMS were used to control the length of the spiral arm.

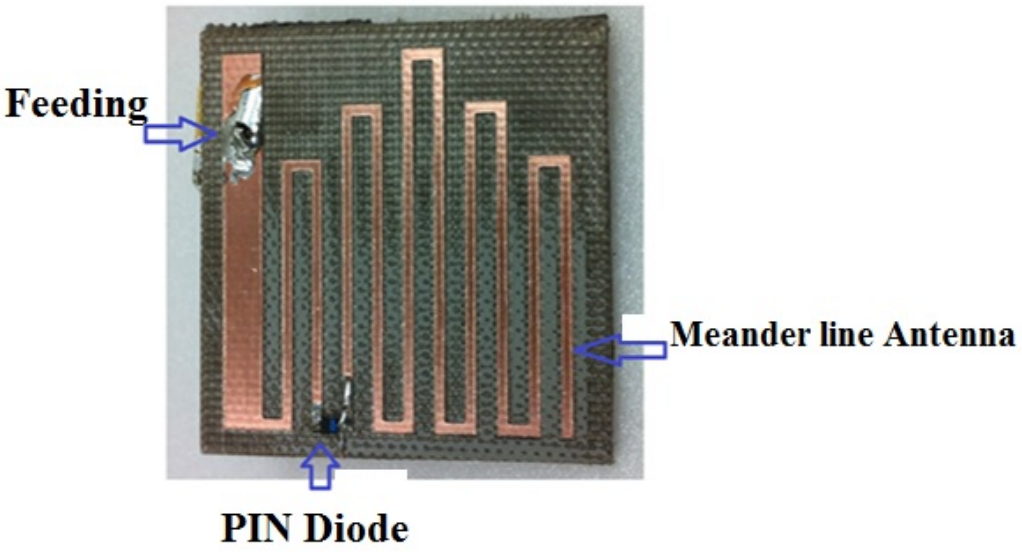

Figure 2.7: The Proposed Antenna System in [17].

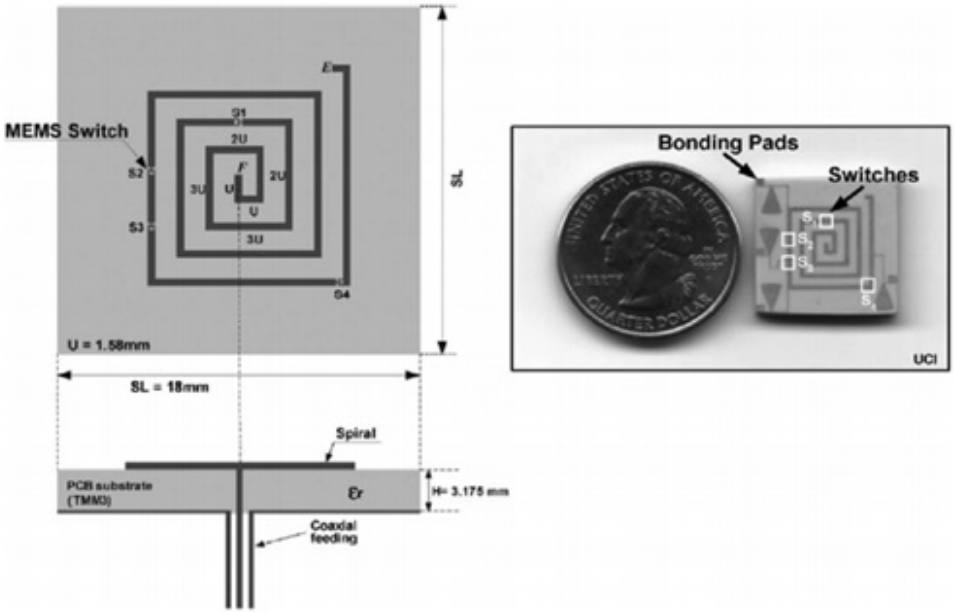

Figure 2.8: The Proposed Antenna System in [18].

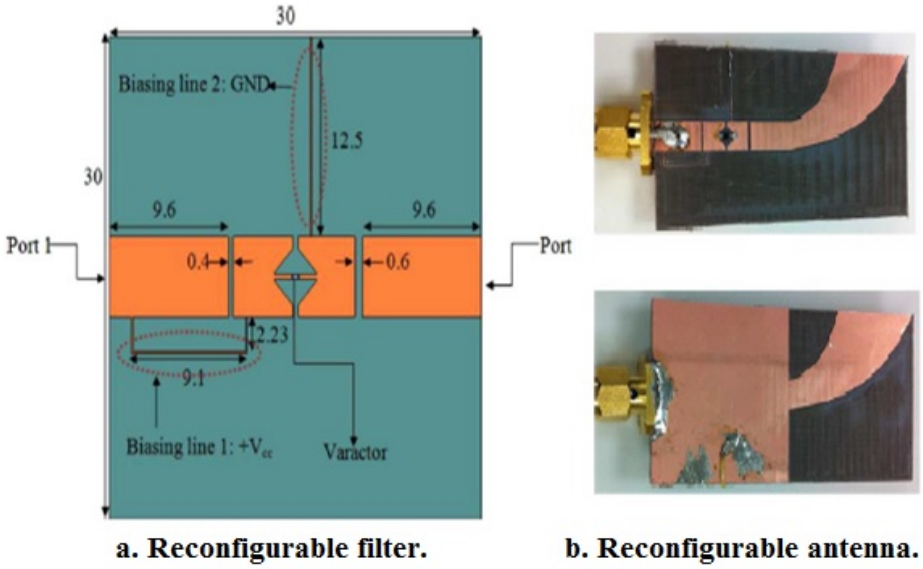

Figure 2.9: The Proposed Antenna System in [19].

a new technique based on using varactor diode for reconfiguring antennas is proposed in the third example [19]. A tunable bandpass filter was designed by changing its total capacitance using the varactors. The varactor diode operation is based on p-n junction diode concept, and once the applied voltage changes, its capacitance changes. The reconfigurable bandpass filter is added to the feed line of the antenna to make it reconfigurable. This technique is unique since no bias lines or active components are added to the antenna surface. Fig. 2.9 displays the proposed reconfigurable antenna of [19].

2.2.2 PIN Diodes

Since this research project investigated the possibility of using PIN diodes to reconfigure a flexible antenna, a brief and basic description of the PIN diode is presented here. According to [20], a PIN diode is a semiconductor device that can be used for

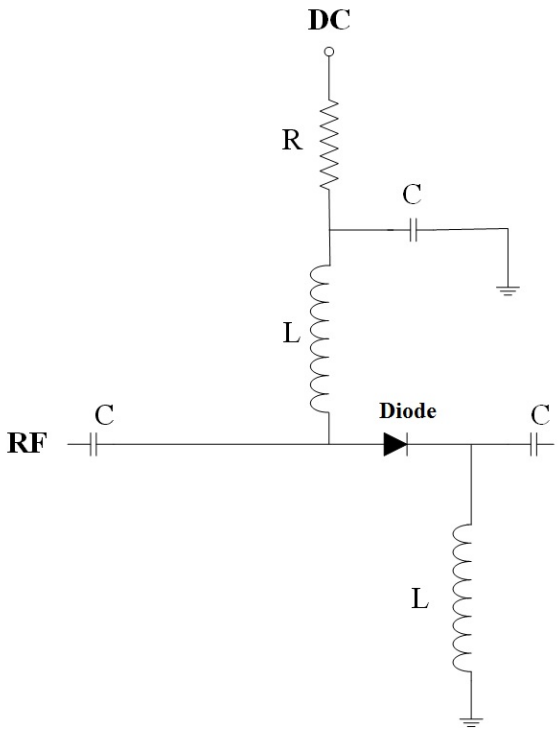

Figure 2.10: Bias Circuit Configuration of the PIN Diode.

microwave frequency applications as an RF switch or attenuator. The forward-biased current is used to control the resistance value of the PIN diode, and the PIN diode is known as a current-controlled resistor. When using a PIN diode for RF applications, as an RF switch or attenuator, it is important to consider the distortion of the RF signal and the non-linearity issue for the PIN diode. Also, the bias circuit is another issue when using the PIN diode for reconfigurable antennas. A diode has two terminals, anode and cathode. To bias the PIN diode, the anode has to be connected to a DC voltage source and the cathode to the ground. The general bias circuit of the PIN diode is shown in Fig. 2.10.

If the PIN diode is activated, which is the case when forward biased, the holes and electrons are injected to the I-region, as shown in Fig. 2.11(a), which results in decreasing the resistance of the I-region into a value of resistance (Rs). Based

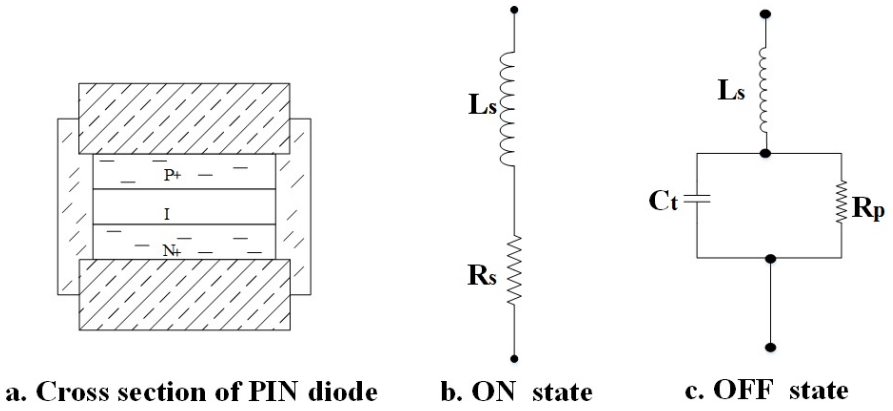

Figure 2.11: Equivalent RLC Circuit for PIN Diode.

on that, the PIN diode has a small value of resistance (Rs) when the PIN diode is activated. Fig. 2.11(b) shows the equivalent circuit for the PIN diode when it is forward biased. The resistance (Rs) is a function of the forward biased current (IF). The inductance (Ls) is a small parasitic element that depends on the geometry of the PIN diode package, and it has little effect on the PIN diode. When the PIN diode is deactivated, which is the case when reversed biased, there are no charges in the I-region, and the diode appears as a capacitor (Ct) in parallel with a resistance (Rp). When the I-region has no charges, it becomes a high resistive region, so the value of the resistance (Rp) is high. Fig. 2.11(c) shows the equivalent circuit for the PIN diode when it is reversed biased. More information about the PIN diode theory is available in [20].

2.3 Printed Slot Antennas

As discussed earlier, the choice of the antenna type that can be used for both flexible and reconfigurable antenna designs is challenging. In this work, printed slot antennas are chosen as the reference antenna, and this section reviews the theory and the design procedure of slot antennas. Moreover, it explains the concept of slot antennas and their complementary dipole antennas. Printed slot antennas can be fabricated with different feeding configurations like microstrip feeding line or Coplanar Waveguide (CPW) feeding line techniques. Examples of designing printed slot antennas and folded slot antennas are presented with simulation results computed by EM simulation software, such as High Frequency Structure Simulation (HFSS).

2.3.1 Slot Antennas

A conventional slot antenna, which is considered as an efficient radiator, is a half-wavelength ($\lambda/2$) slot on a flat metal sheet. Fig. 2.12(a) shows an example of a slot antenna in a rectangular form cut in a flat metal sheet. The length (Ls) of the slot is $\lambda/2$ at the resonance frequency and the width (Ws) is very small (Ws $<<$ λ). The maximum currents are at the two edges of the slot and the currents spread out on the metal sheet, resulting in equal radiation from both sides of the flat sheet [21]. The maximum electric field is perpendicular to the longer dimensions of the slot. For instance, if the slot is horizontal, the electric field, which is perpendicular to the slot, is vertically polarized. Using an extension of Babinet′s principle by Henry Booker [22], the impedance and pattern of a slot can be predicted from its complementary dipole. Fig. 2.12(b) shows the complementary dipole of the slot antenna. As a result, for a medium with an intrinsic impedance of (η), the impedance of the slot (Z_s) and its complementary dipole impedance (Z_d) are related by:

$$Z_s \times Z_d = \frac{\eta^2}{4} \tag{2.1}$$

The input impedance of the half-wavelength dipole in free space at resonance is around 73 Ω. Thus, the input impedance of the half-wavelength ($\lambda/2$) slot, using (2.1), is given by:

$$Z_s = \frac{\eta^2}{4Z_d} = \frac{(377)^2}{4 \times 73} = 500\Omega \tag{2.2}$$

The impedance of a slot is a function of distance from its center. At the center, as shown in Fig. 2.13(a), the input impedance is approximately 500 Ω (a large discontinuity relative to common 50 Ω transmission lines). Thus, the off-center feed, as shown in Fig. 2.13(b), can be used to improve the matching. Using the same extension as Booker′s, we can conclude that the pattern of the slot is similar to the dipole, but the electric and magnetic fields are interchanged [21].

2.3.2 Microstrip Slot Antennas

Before we discuss the microstrip-fed slot antenna designs, it is beneficial to discuss the structure of microstrip antennas. Microstrip (patch) antennas have three layers [10]. The top layer is the patch (conductive material), while the middle layer constitutes the dielectric material (substrate). The bottom layer is the ground plane (conductive material). Fig. 2.14 displays a microstrip antenna fed by the microstrip feeding line technique. The bandwidth is very narrow for microstrip antennas, and for better bandwidth and efficiency, it is recommended to use a thicker substrate, which is not preferable for flexible antennas as discussed. The width of the microstrip feed line is related to the substrate thickness and the dielectric constant. This results

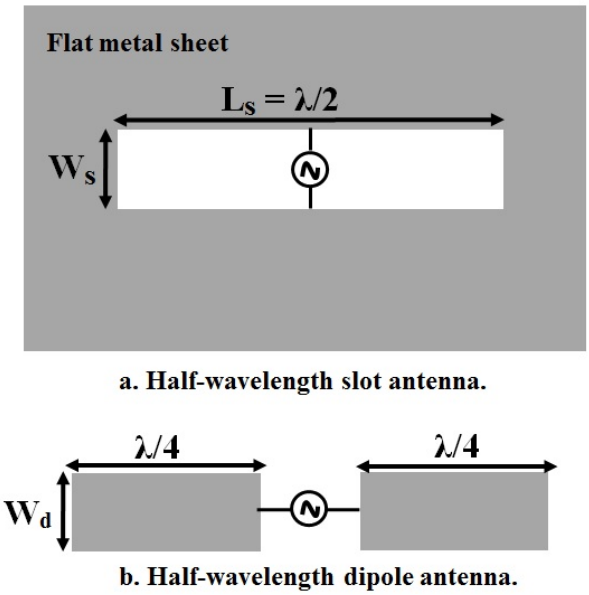

Figure 2.12: A Half-wavelength ($\lambda/2$) Rectangular Slot in a Flat Metal Sheet and Its Complementary Dipole.

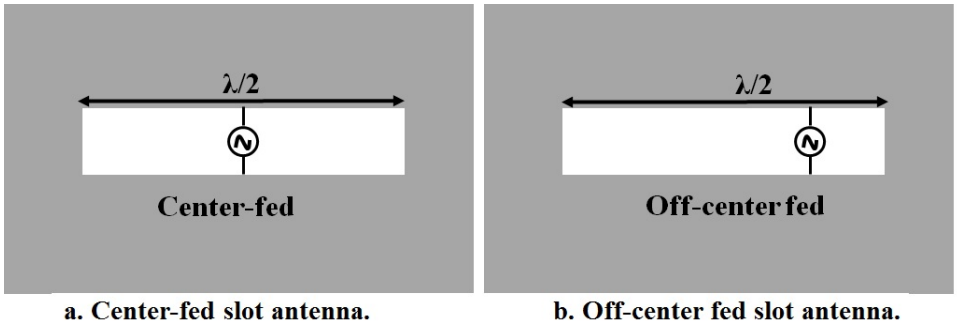

Figure 2.13: Slot Antennas: a) Center-fed. b) Off-center Fed.

in a very small width of the 50 Ω feeding line when printed on a very thin flexible substrate, such as PET material. This complicates the fabrication process for flexible antennas.

Microstrip-fed slot antennas (MSAs) have advantages over microstrip antennas, such as larger bandwidth, ease to fabrication, and bidirectional and unidirectional radiation patterns. A microstrip-fed rectangular slot antenna is briefly described as

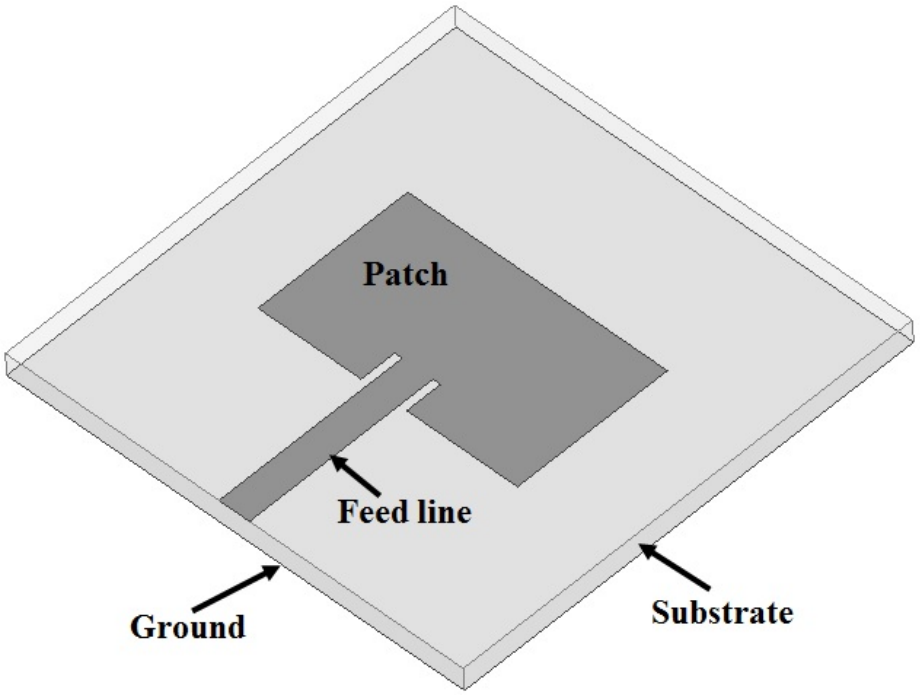

Figure 2.14: Microstrip Antenna Fed by Microstrip Feed Line.

a slot (perforation) on a ground plane of a microstrip line and the slot is normal to the strip conductor of the printed microstrip feed line [23]. Fig. 2.15 displays the structure of a microstrip-fed rectangular slot antenna and the antenna is center-fed. The slot is excited by the fields of the microstrip line, and the strip conductor is extended beyond the slot edge with a quarter-wavelength length (Lm) and terminated by an open circuit for better matching. Another feeding technique uses the same strip conductor to excite the slot, but the slot edge is short-circuited to the strip conductor, which complicates the fabrication process. Thus, this feeding technique is not recommended for thin flexible antennas. As mentioned in the previous section, the slot antenna has a high impedance when it is fed at the center. From the literature [23]-[26], many matching techniques have been proposed to reduce the slot impedance and to avoid the matching network for the slot antennas.

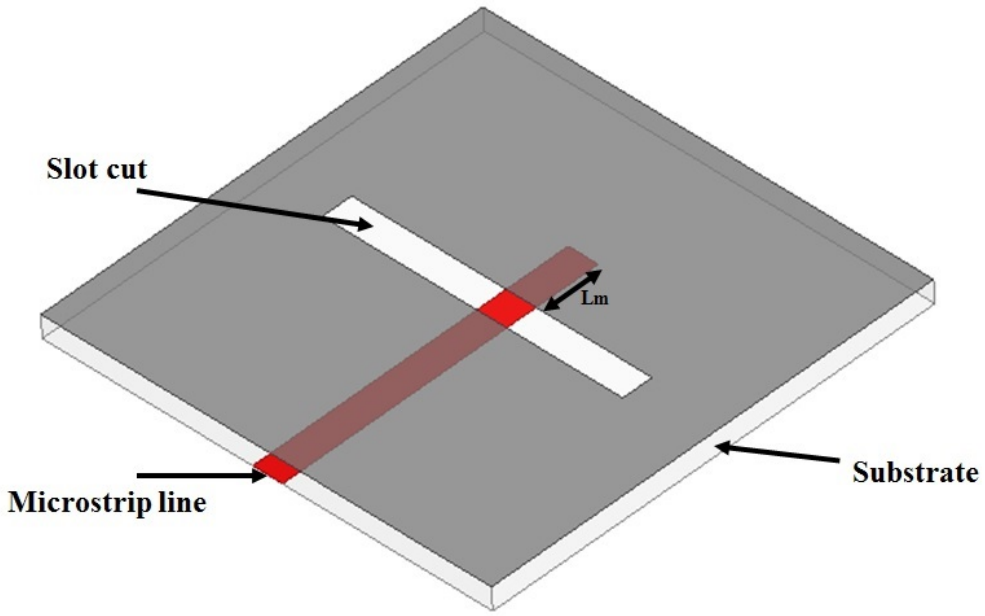

Figure 2.15: Microstrip-fed Rectangular Slot Antenna.

To discuss and study the radiation characteristics of a microstrip-fed rectangular slot antenna, the proposed design in [26] is redesigned to resonate at 2.4 GHz. Fig. 2.16 shows the geometry of the design, which was mainly based on a rectangular slot placed at the middle of the ground plane. Since the impedance of the slot is high, a matching technique is required to match the slot antenna to the 50 Ω feed line. For better matching, the antenna is approximately fed by a 97 Ω open-circuited microstrip line followed by the main 50 Ω feed line, where both are printed on the opposite side of the ground. The antenna was designed using FR4 substrate (ϵ_r= 4.4 and h = 0.6 mm). The length of the slot is a half-guided wavelength ($\lambda_g/2$) at the 2.4 GHz resonant frequency, and the width of the slot needs to be optimized for better matching. The maximum current is concentrated in the slots edges, as shown in Fig. 2.17, which exhibits the same current distribution of the conventional

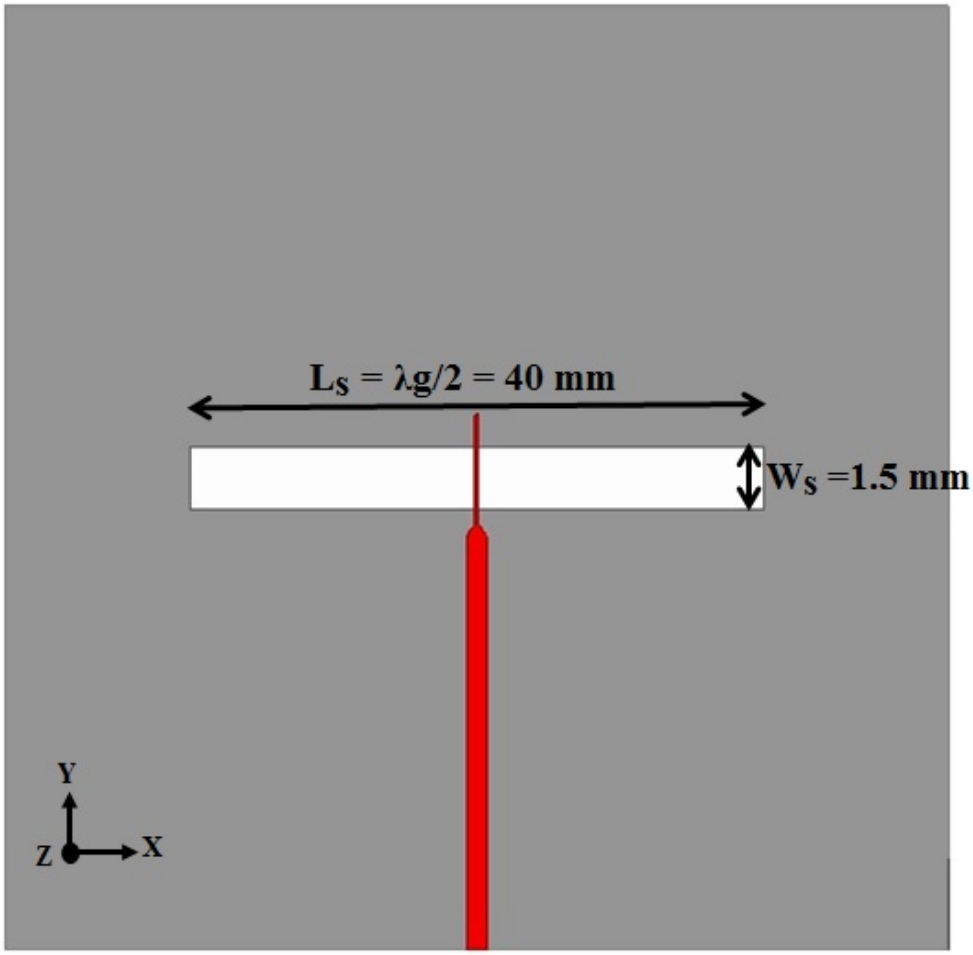

Figure 2.16: Geometry of the Design of Microstrip-fed Rectangular Slot Antenna with a Matching Technique.

half-wavelength slot antenna and demonstrates the concept of the slot antenna in terms of its complementary dipole. Fig. 2.18 displays the reflection coefficient of the rectangular microstrip-fed slot antenna at the 2.4 GHz resonant frequency of the antenna and it is well matched ($S_{11}\sim$ -15 dB). Figs. 2.19 to 2.20 display the radiation patterns of the antenna for both the E plane and H plane at 2.4 GHz. The radiation pattern for both planes exhibits the same radiation pattern of the conventional slot antenna, where the E plane (YZ plane) is perpendicular to the horizontal slot and is

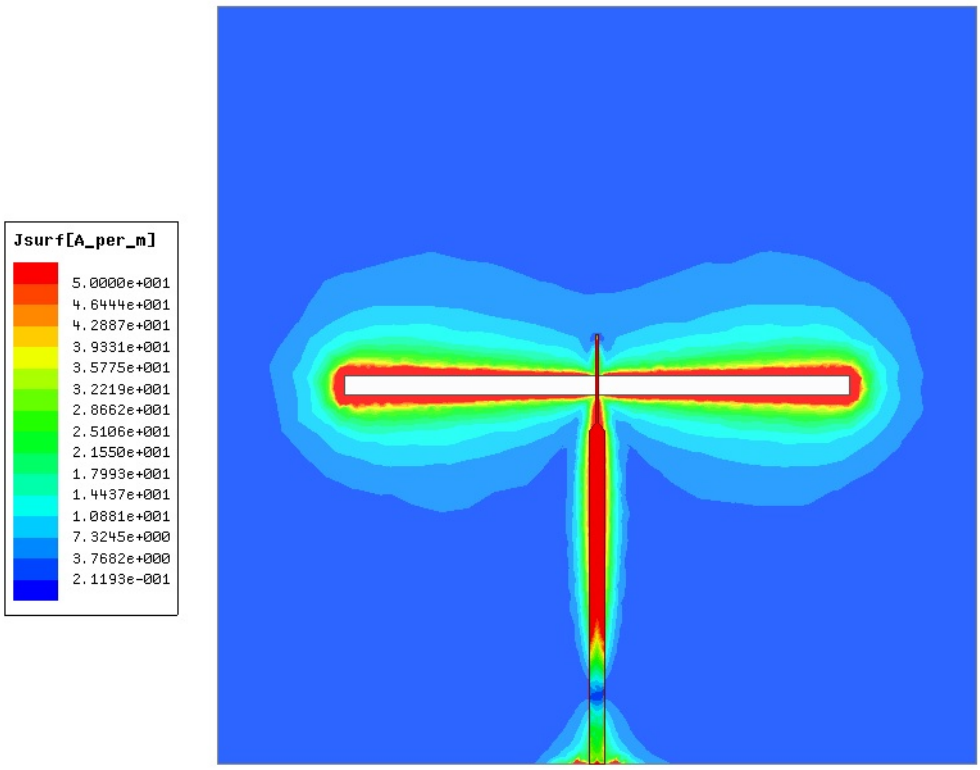

Figure 2.17: The Maximum Current Distribution on the Slot Edges.

vertically polarized. However, for the horizontal dipole, the E plane is parallel to the dipole and is horizontally polarized.

2.3.3 CPW-Fed Printed Slot Antennas

The microstrip line feeding technique for slot antennas is not recommended when designing flexible antennas because it suffers from the need for careful alignment of the etching and printing on both sides of the substrate [23]. Moreover, it requires using holes and short pins when incorporating or integrating active devices with the antenna structure, which is not possible or preferable for flexible and reconfigurable antennas. This problem can be solved by the use of CPW feed configuration, where both the ground plane and the feed line are printed on the same side of the substrate. This

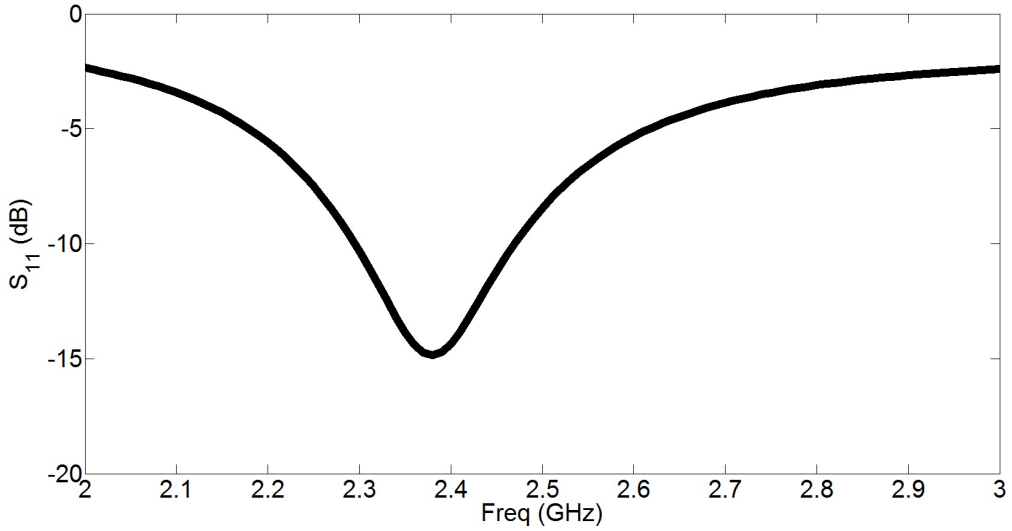

Figure 2.18: The Simulated Reflection Coefficient of the Design.

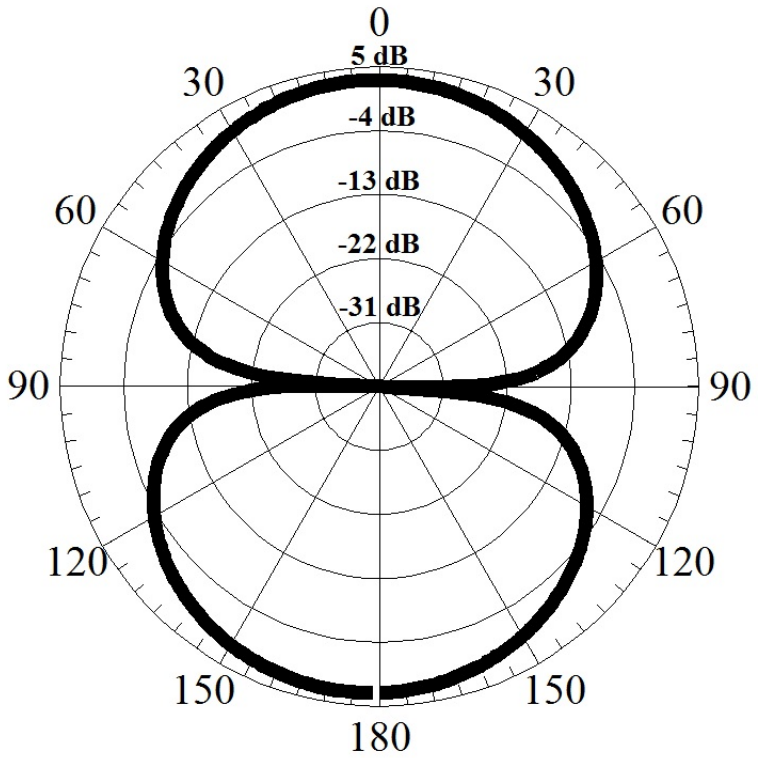

Figure 2.19: E-plane (YZ) Radiation Pattern of the Slot Antenna at Resonance (2.4 GHz).

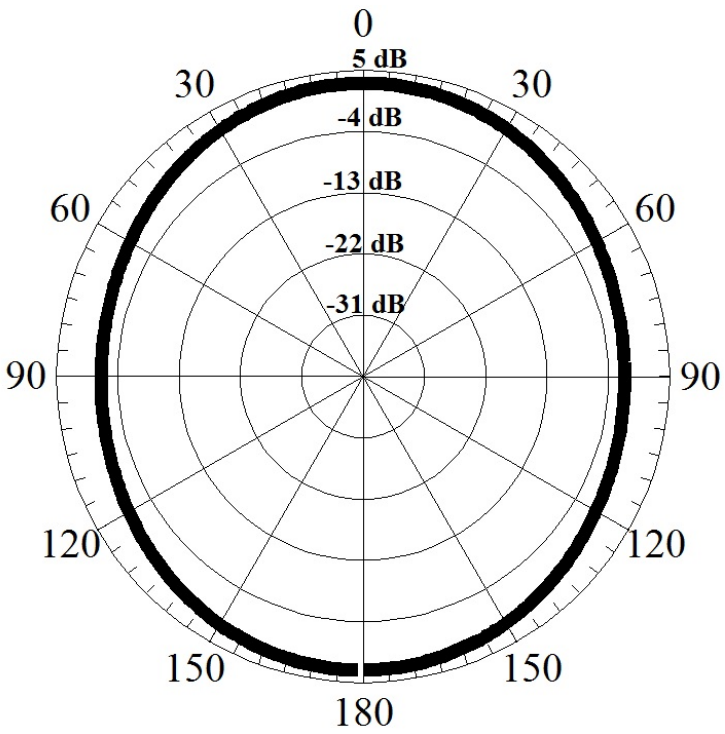

Figure 2.20: H-plane (XZ) Radiation Pattern of the Slot Antenna at Resonance (2.4 GHz).

is necessary for flexible antennas and to integrate active devices for reconfigurable antennas. Fig. 2.21 illustrates the schematic of a CPW transmission line, which consists of three conductors printed on a dielectric substrate as follows: the central conductor is the feeding line, while the others represent to the ground. The width of the slot between the feeding line and the ground is denoted by S, while the width of the feeding line is denoted by W. Those parameters, along with the thickness and dielectric constant of the substrate, impact the characteristic impedance of the CPW feeding line.

This section presents an example of a printed slot antenna with CPW feeding configuration. The antenna design is based on the concept of folded slot antennas. The radiation resistance of the slot is very high, around 500 Ω in free space, as

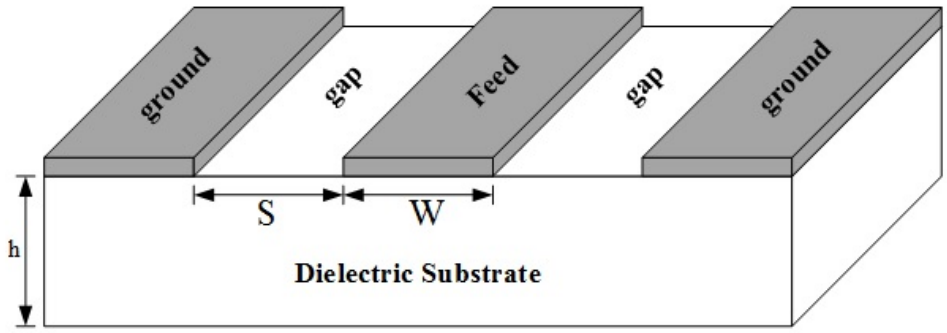

Figure 2.21: Schematic of a CPW with Substrate of Finite Thickness.

discussed. Thus, the matching of the slot antenna to the characteristic impedance of the 50 Ω CPW feed line is required. The input impedance of the half-wavelength dipole at resonance is around 73 Ω, and for some applications, like TV, a twin-lead transmission line, which has high characteristic impedance around 300 Ω, is used. Thus, it is required to increase the impedance of the dipole which leads to the folded dipole design. A folded dipole antenna can be used as a step-up impedance transformer of the half-wavelength dipole [10]. A folded dipole gives two equal parallel paths of currents with a length of half-wavelength, and the impedance is a factor of four times the impedance of the half-wavelength dipole. This technique may be extended to N parallel currents, and the impedance of the folded dipole (Z_{fd}) is scaled as: $Z_{fd}= Z_d \times N^2$, where N represents the number of the parallel current paths. Since the dipole antenna is the complement of the slot antenna, based on an extension of Babinet′s principle, the folded dipole antenna is the complement of the folded slot antenna, as shown in Fig. 2.22. In contrast to the folded dipole with N parallel current paths, the folded slot antenna, as shown in Fig. 2.22(a), consists of N parallel slots, and the length of each slot is a half-wavelength. The folded slot antenna can be used as a step-down impedance transformer, where the impedance of the folded

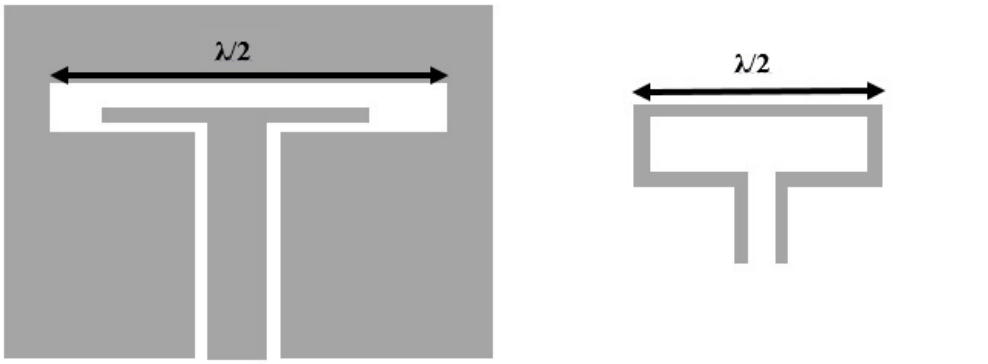

Figure 2.22: Folded Slot Antenna and Its Complementary Folded Dipole Antenna.

slot (Z_{fs}) in free space is scaled by: $Z_{fs}= Z_s/N^2$, where N represents the number of the parallel slots [27]. As a result, if the number of the parallel slots increases, the input impedance of the slots decreases, which is needed for proper matching to the 50 Ω CPW feed line of the slot antenna. However, this relation is limited to other parameters, such as the thickness and the dielectric constant of the substrate for printed antennas, which are functions of the antenna impedance.

HFSS numerical simulations were used to design a folded slot antenna with CPW feeding configuration to demonstrate the concept of reducing the slot impedance. A stub inside the slot, as shown in Fig. 2.22(a), is symmetrical with respect to the slot and the CPW feeding line, and is used to reduce the impedance of the slot antenna by increasing the number of the slots [27]. Fig. 2.23 illustrates folded slot antennas with different numbers of slots. HFSS was used to predict the impedance of a single slot, and then we evaluated the influence of the additional slots on the slot impedance. The folded slot antenna was simulated for two, three, four, and five slots. The antenna was designed on a very thin PET flexible substrate (ϵ_r = 3 and h = 0.1 mm). The antenna was designed to resonate at 2.4 GHz, where the resonance approximately occurs when the outer circumference of the slot is about one guided wavelength (λ_g).

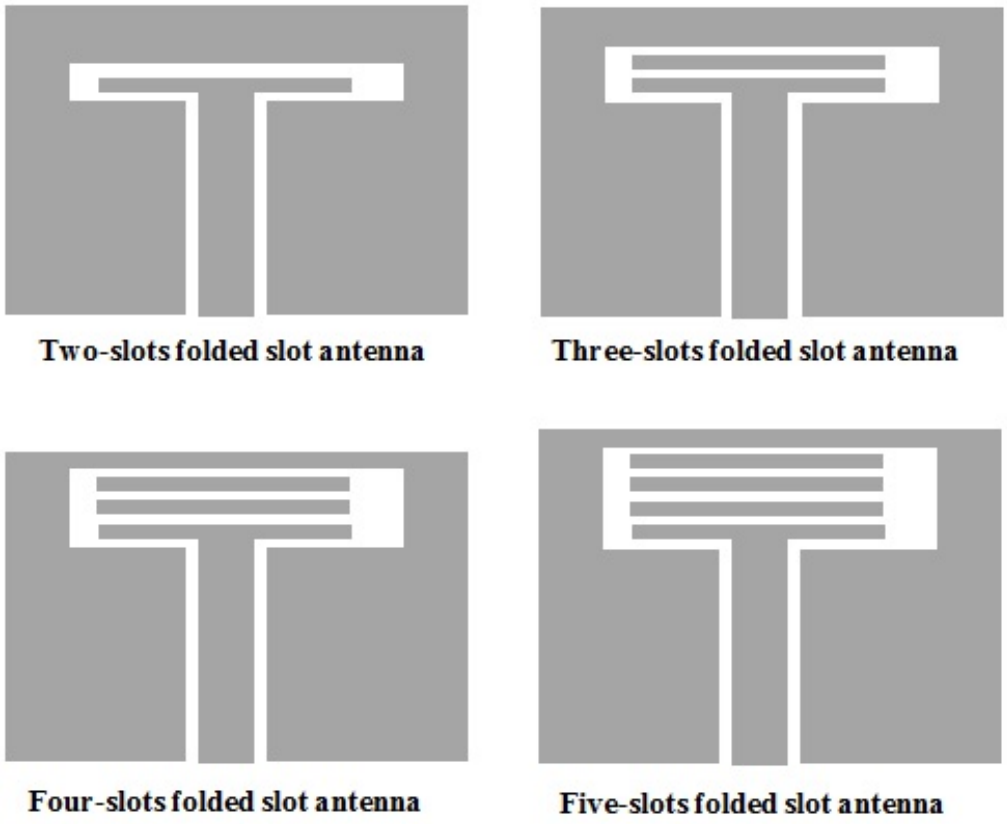

Figure 2.23: Folded Slot Antenna with Multiple Number of Slots.

The effective dielectric constant (ϵ_{eff}) for the CPW feed line, when printed on PET substrate, is ($\epsilon_{eff} = 1.23$). The length of the slot is about ($\lambda_g/2$) at 2.4 GHz. Fig. 2.24 shows the simulated reflection coefficients of a folded slot antenna with a multiple number of slots, while Fig. 2.25 displays the simulated impedance of the slot antenna with a multiple number of slots.

As expected, the simulation impedance of the one slot is about 210 Ω at the resonant frequency of 2.4 GHz. The simulated reflection coefficient using one slot is not well matched ($S_{11} >$ -5 dB) at resonance. It was observed, as displayed in Fig. 2.25, that the slot impedance decreases from 210 Ω to almost 50 Ω for a folded slot antenna with five slots, which is an excellent match for the 50 Ω feeding line. The simulated reflection coefficient of the five-slot antenna is well matched

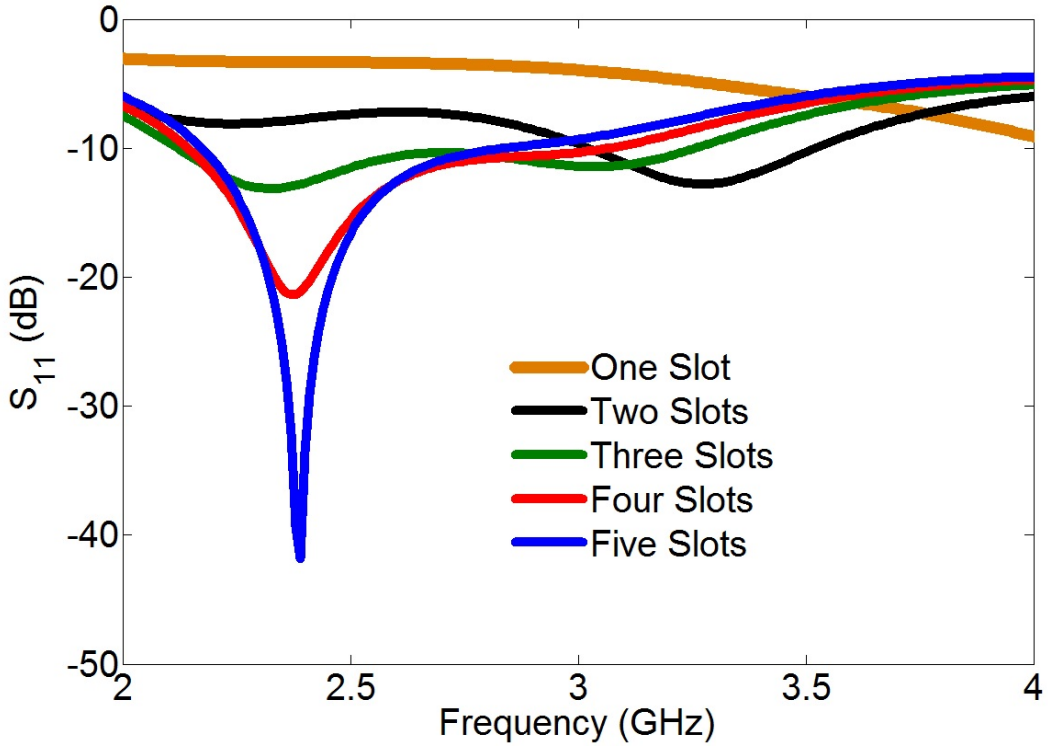

Figure 2.24: Simulated Reflection Coefficients with Different Number of Slots.

(S_{11} < -40 dB) at resonance. This is extremely helpful for some slot antenna designs in order to improve the matching. However, the argument for increasing the number of slots cannot be carried too far since this leads to an increase in the antenna size and complicates the fabrication process. The impedance of a folded slot antenna is controlled by changing the width of the slot. The slot widths (Wa) and (Wb), as shown in Fig. 2.26, are equal, with a value of W, and the folded slot antenna is symmetrical in respect to the CPW feed line. According to [28], by increasing the width Wb, the input impedance can be reduced and matched to the 50 Ω feeding line without increasing the antenna size, as happens for the multiple-slots matching technique. Fig. 2.27 shows the reflection coefficients of the folded slot antenna with different widths for Wb. Fig. 2.28 displays the real impedance of the folded slot antenna with different widths for Wb. It was observed from both the simulated

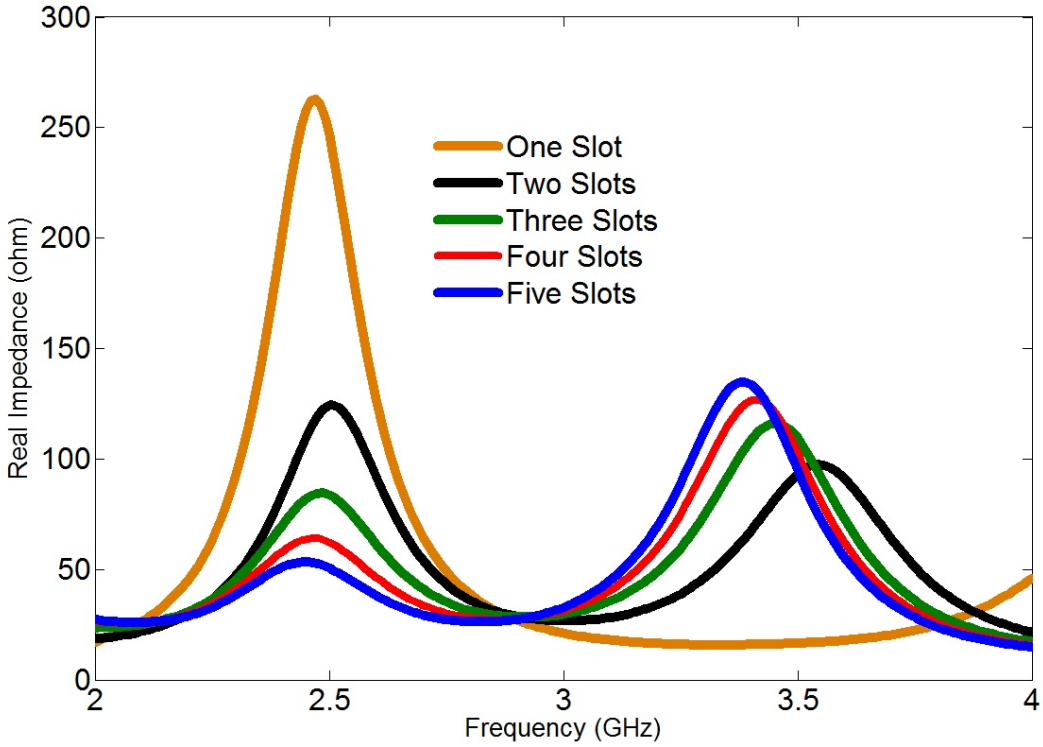

Figure 2.25: Simulated Real Impedance with Different Number of Slots.

reflection coefficient and the real impedance that the impedance is reduced if the width Wb increases, and the antenna is well matched at the resonant frequency of 2.4 GHz. The radiation characteristics of the optimized design that is used as the reference folded slot antenna is discussed in the next chapter.

Figure 2.26: Symmetrical CPW-Fed Folded Slot Antenna.

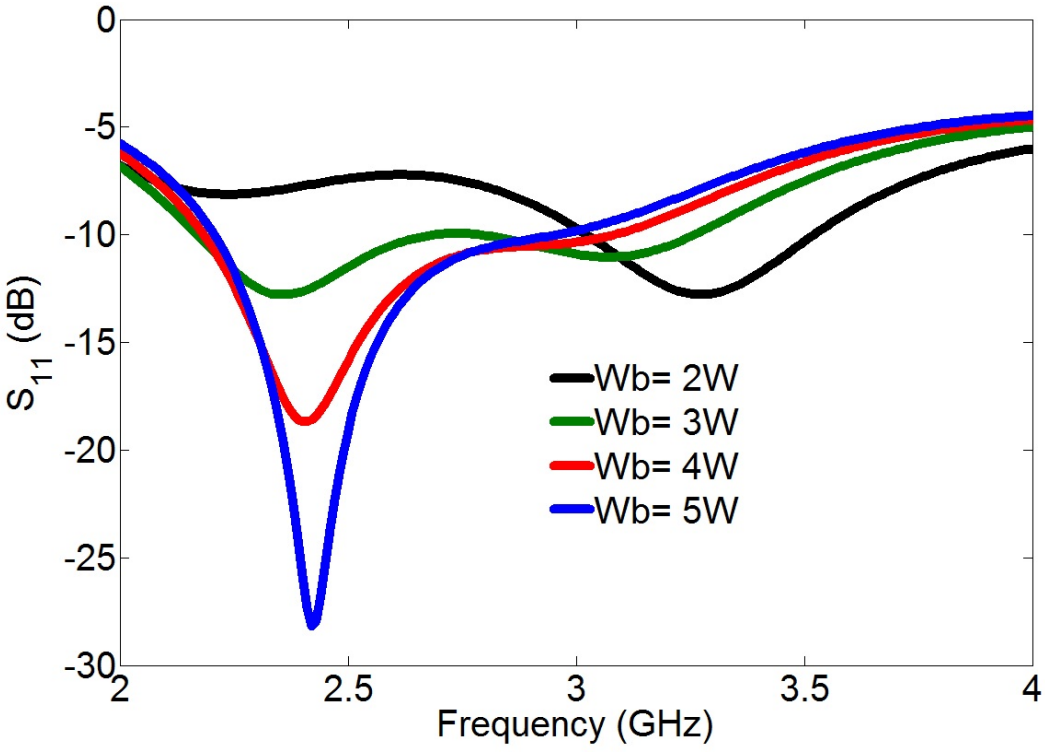

Figure 2.27: Simulated Reflection Coefficients of Different Width Values for (Wb).

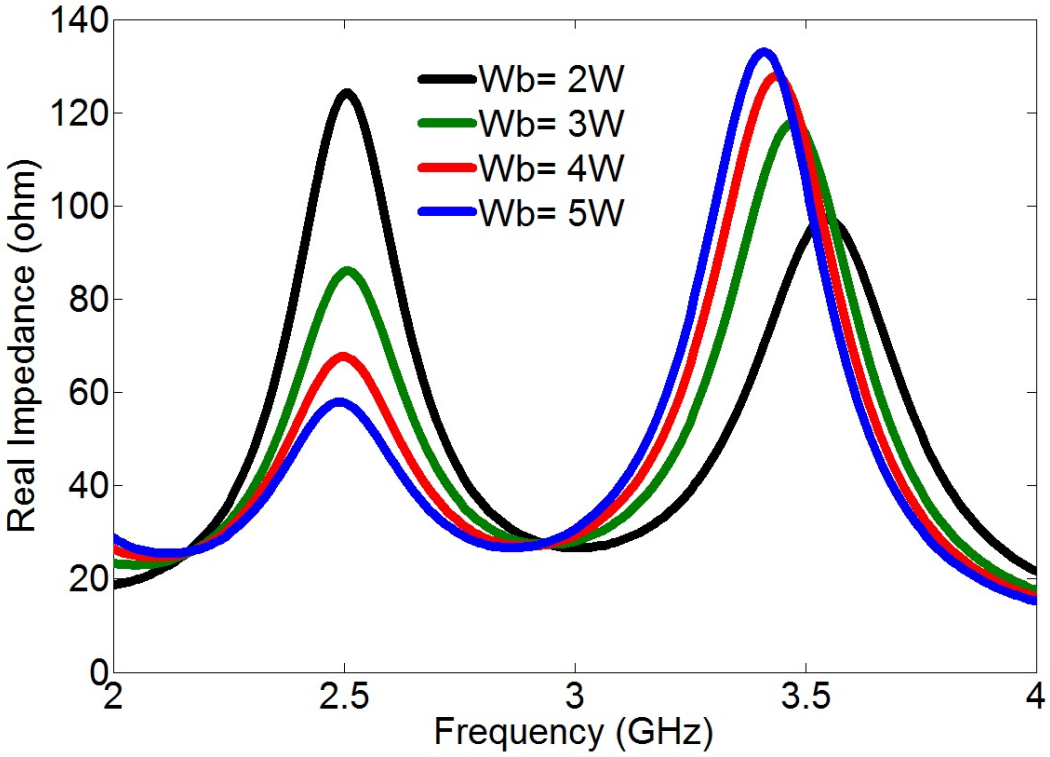

Figure 2.28: Simulated Real Impedance of Different Width Values for (Wb).

Chapter 3

INKJET-PRINTED FLEXIBLE RECONFIGURABLE ANTENNA

This chapter reports on the proposed flexible reconfigurable antenna for this project. The device is designed on a flexible PET substrate and inkjet-printing technology is used to fabricate the prototype. One PIN diode is incorporated on the antenna surface to redirect and redistribute the surface current resulting in a reconfigurable antenna in terms of frequency and polarization. When the PIN diode is forward biased (ON), the antenna has a single band at 2.42 GHz for WLAN wireless devices. However, when the PIN diode is reversed biased (OFF), the antenna is dual-band with different polarizations at 2.36 GHz and 3.64 GHz for WLAN and WiMAX wireless devices, respectively. The proposed antenna is simulated, fabricated and tested for both flat and curved geometries, such as circumferential and axial cylindrical configurations, with good agreement between measurements and simulations.

3.1 Introduction

Flexible antenna designs, with fixed radiation characteristics, have received a lot of attention. However, designs with flexibility and reconfigurability are of interest in many applications. Therefore, in this chapter both flexibility and reconfigurability were integrated to design an antenna that is flexible to be used for conformal applications and reconfigurable in its radiation characteristics (resonant frequency and polarization). Based on the design requirements of the operating systems, the design methodology can be summarized in three main steps:

- Determine the antenna type that can be used for both flexible and reconfigurable antenna designs.
- Determine a flexible substrate and fabrication technology.
- Determine the reconfiguration technique for your antenna design that maintains both the flexibility and reconfigurability for that antenna design.

According to the literature review, printed antennas, such as monopoles with CPW feeding techniques, are preferred in flexible antenna designs since both the radiating element and the ground plane are printed on the same side of the substrate, which reduces the complexity of the fabrication process. Moreover, there is no need for vias and short pins when incorporating active devices with the antenna structure, which is desirable for flexible reconfigurable radiators printed on very thin substrates. As a result, a single folded slot antenna with CPW feeding configuration [29]-[30], was chosen as the reference for the proposed design because of the wide bandwidth and low impedance, when compared with other slot antennas. In [30], a broadband and dual-band folded slot antenna was designed based on off-center CPW feeding technique to adjust the stub length inside the slot. Here we present another technique based on RF switches, such as a PIN diode, to redirect and redistribute the current on the internal stub and to resonate the stub inside the slot.

Slot and folded slot antennas with CPW feeding have been reconfigured by altering the slot length to change the resonant frequency [14], [31]-[33]. In [32], PIN diodes were used to change the antenna resonant frequency by changing the slot length, and the design does not require a bias circuit. However, via holes and DC wires were used to activate the PIN diodes, which may degrade the flexibility of flexible antennas printed on very thin substrates. In [33], a dual-band reconfigurable folded slot antenna was designed by using the same technique. This previous technique

results in a reconfigurable antenna in terms of resonant frequency only. However, the proposed antenna here is flexible and reconfigurable in terms of both resonant frequency and polarization. One PIN diode is inserted to the stub to redirect and redistribute the current, and no via holes, short pins or DC wires are connected to the antenna surface, which preserves the flexibility of the proposed design.

The main contributions in this chapter are the following:

- A compact flexible and reconfigurable antenna for WLAN and WiMAX conformal wireless devices is proposed.
- An alternate technique to reconfigure folded slot antennas is proposed, which is based on one PIN diode to redirect and redistribute the current on the stub, resulting in a reconfigurable antenna.
- A reconfigurable antenna in terms of both resonant frequency and polarization.
- The proposed antenna systems are designed, simulated and tested.

3.2 Flexible Folded Slot Antenna

This section presents the design of the optimized flexible antenna printed on Polyethylene Terephthalate (PET) film. The dielectric constant of the substrate is 3, while the loss tangent is 0.008, and the thickness is about 0.1 mm (0.004 in.). First, a CPW-fed single band folded slot antenna, which has a single band when fed at the center, was designed and optimized using HFSS. It resonates when the perimeter of the slot is about one guided wavelength (λ_g), where λ_g is the guided wavelength of the 50-ohm CPW feed line. Fig. 3.1 shows the optimized folded slot antenna and its dimensions are listed in Table 3.1. Fig. 3.2 displays the simulated curved

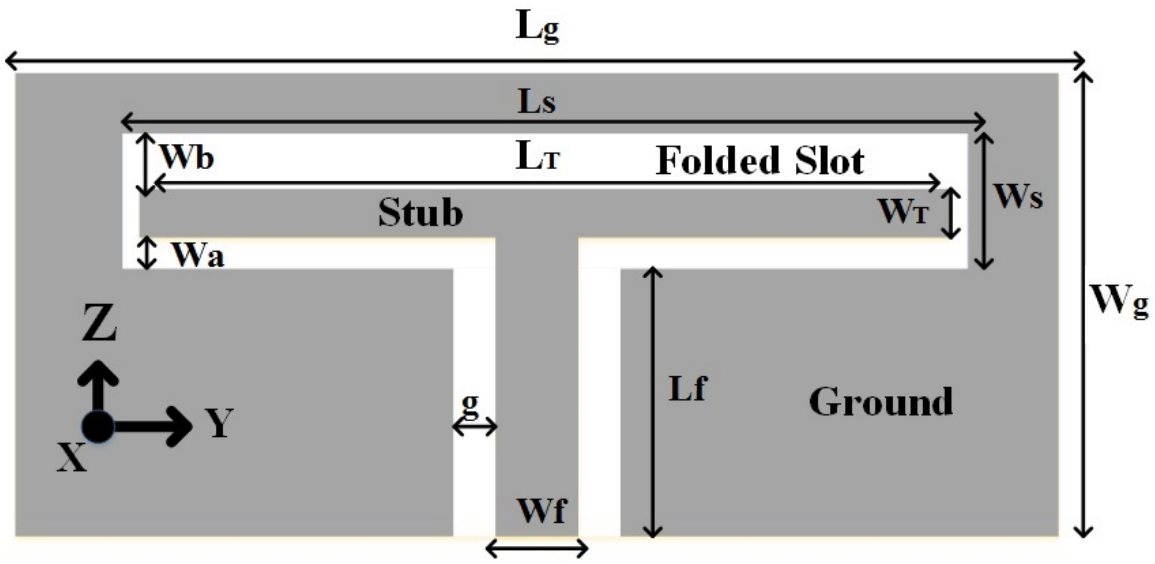

Figure 3.1: Geometry of Single Folded Slot Antenna.

antenna in HFSS which was simulated to ensure that the reference antenna can be used for curved structures. The reflection coefficients of different lengths (Ls) of the folded slot are shown in Fig. 3.3. The optimized antenna has single band resonant frequency at 2.4 GHz and its simulated reflection coefficient, for both flat and curved configurations, is displayed in Fig. 3.4.

The stub is used to reduce the impedance of the slot, and the stub itself is not radiating. It was observed that for a single band folded slot antenna, the stub inside the slot is not radiating, since it is symmetrical with respect to the feed line but with 180 degrees phase difference between the left and right horizontal sections of the stub. Therefore, the radiation from the right section of the stub cancels the radiation from the left section of the stub and thus the radiation of the antenna is primarily due to the slot. To verify this assertion, the direction of the simulated current distribution on the stub is illustrated in Fig. 3.5 to show that both sides of the stub have an equal amount of current, but they are out of phase; this results in a non-radiating stub inside the slot. Fig. 3.6 displays the maximum currents on the folded slot antenna

Table 3.1: Dimensions of the Proposed Flexible Folded Slot Antenna

Parameters	Dimensions (mm)	Parameters	Dimensions (mm)
Lg	59	Lf	25.5
Wg	31	Wf	6
Ls	53	g	0.2
Ws	4.75	Wa	0.5
Lt	52	Wb	3.25
Wt	1		

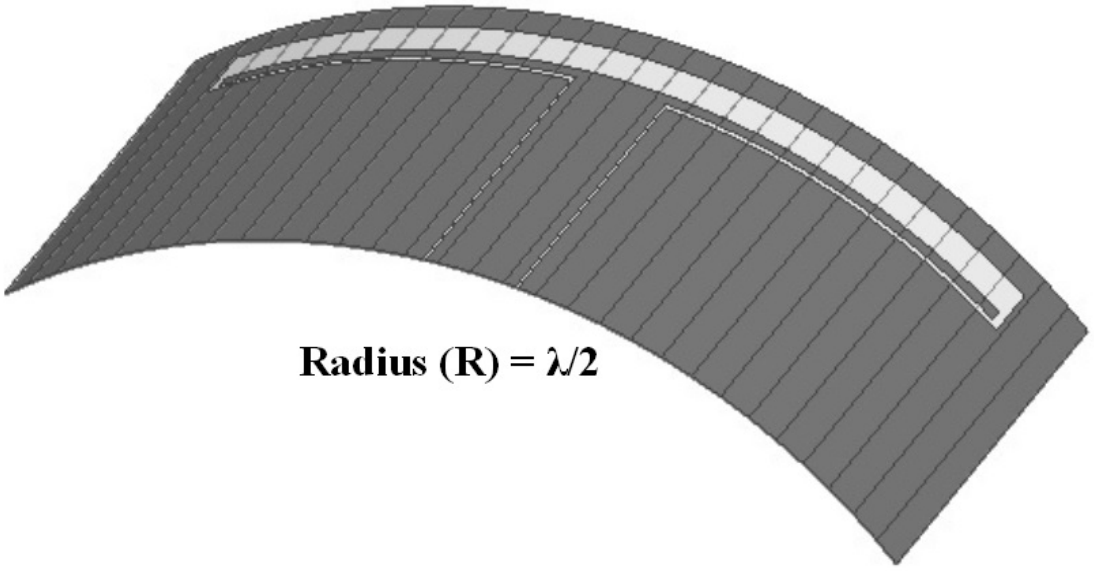

Figure 3.2: Geometry of the Simulated Curved Single Folded Slot Antenna in HFSS.

which concentrate on the slot edges, which proves that the optimized antenna exhibits the same behavior of the conventional slot antenna, as discussed in Chapter 2.

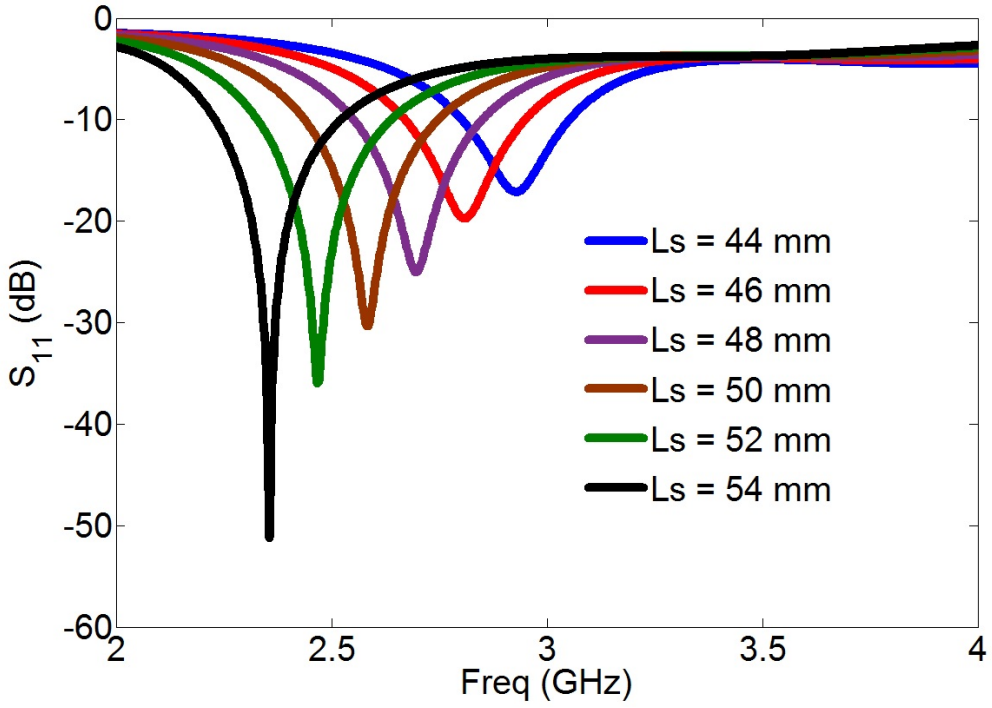

Figure 3.3: Reflection Coefficients of Different Lengths (Ls) of the Folded Slot Antenna.

After the antenna design was optimized using HFSS, it was fabricated on the PET flexible material using inkjet-printing technology provided by CIT Technology Ltd., Cambridge, England and using a MetalJet6000i inkjet printer. The printer has 360 dpi (dots per inch) resolution, and is used to deposit the catalytic ink onto the PET substrate. After that, the printed substrate is placed into a copper plating solution to produce the copper metal on the PET substrate, which has a total thickness of 1.5 μm and the conductivity of the copper metal is about 2×10^7 S/m, which corresponds to a sheet resistance of 0.03 ohms/square. Fig. 3.7 shows the fabricated flexible antenna, and a good agreement between the measured and simulated reflection coefficients at 2.42 GHz was achieved as shown Fig. 3.8.

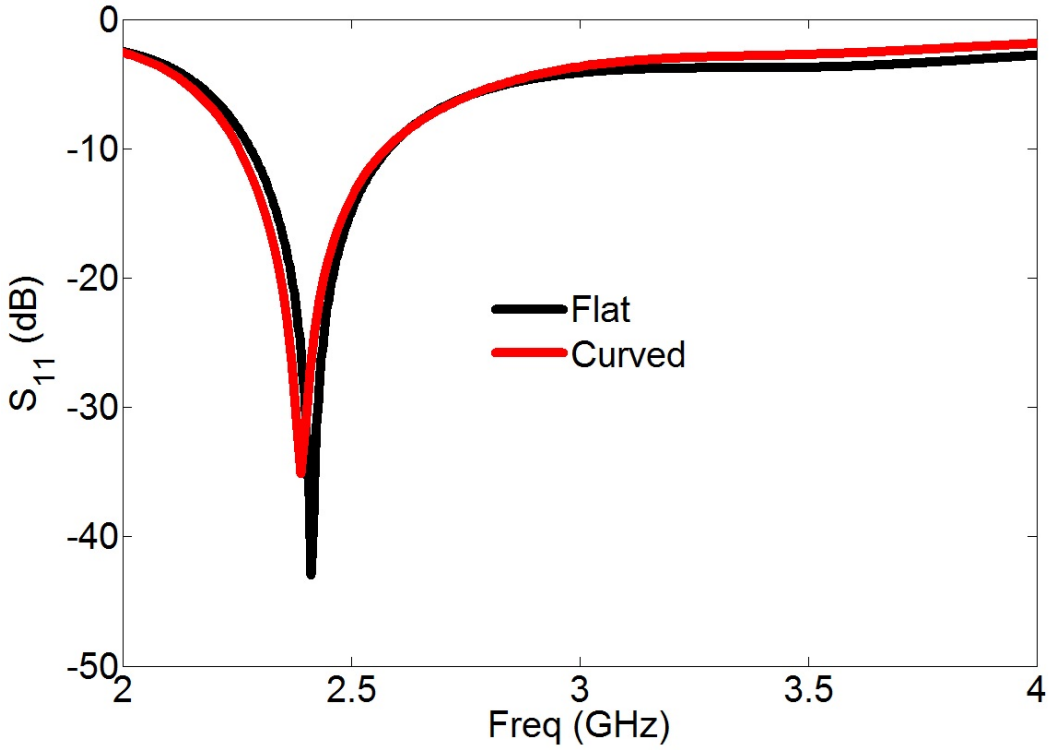

Figure 3.4: Simulated Reflection Coefficient of the Optimized Flat/Curved Folded Slot Antenna.

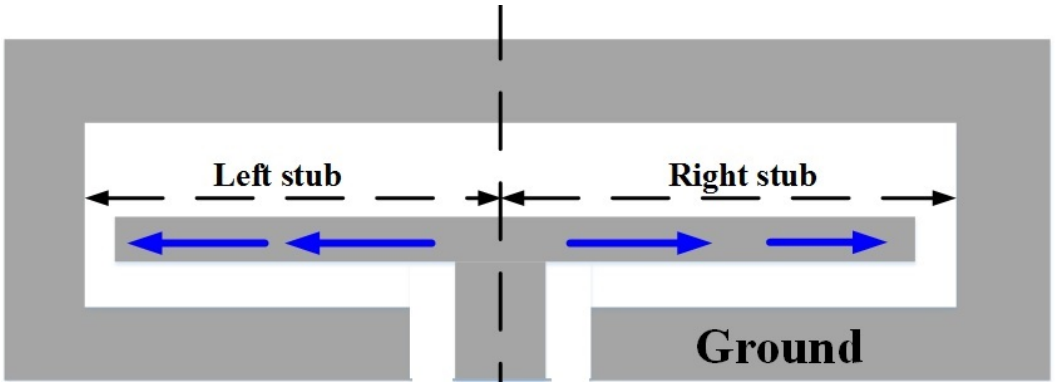

Figure 3.5: Current Directions on the Symmetric Stub Inside the Slot.

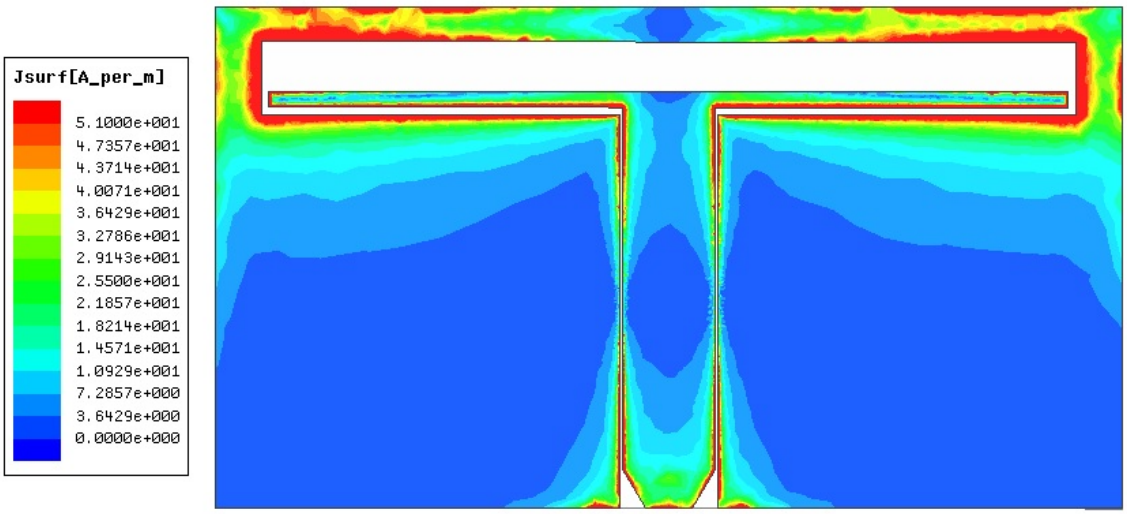

Figure 3.6: Simulated Maximum Current Distributions at 2.4 GHz Resonance.

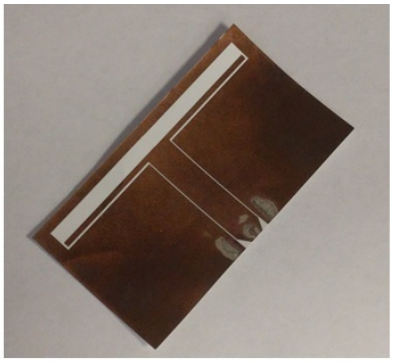

a. Flat antenna.

b. Flexed antenna.

Figure 3.7: The Fabricated Prototype of the Proposed Flexible Antenna.

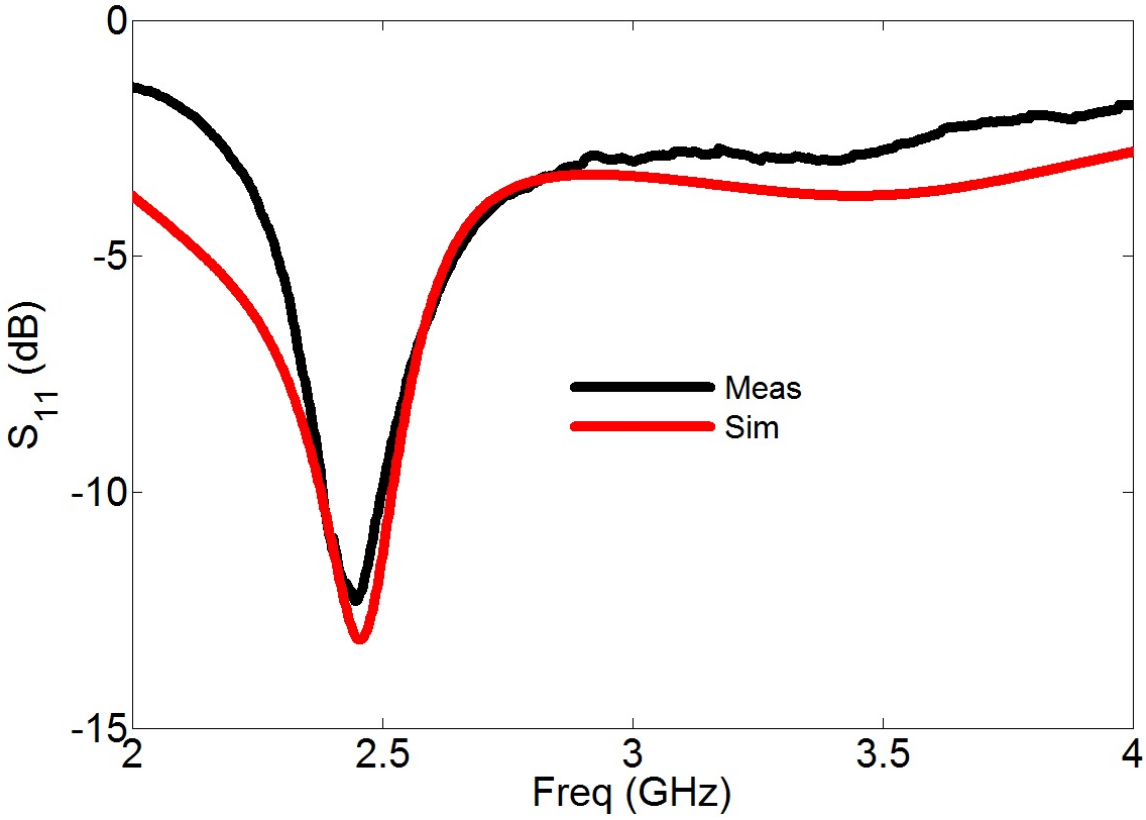

Figure 3.8: Simulated and Measured Reflection Coefficients of the Fabricated Flexible Flat Antenna.

3.3 Flexible Reconfigurable Antenna

After the proposed flexible folded slot antenna was designed, fabricated and examined, the next step is to discuss the reconfiguration of the reference folded slot antenna. The previous work on reconfigurable folded slot antennas is mainly based on changing the slot length in order to change the resonant frequency of the antenna. Fig. 3.9 displays the reconfigurable folded slot antenna presented in [32], where four PIN diodes were used to change the length of the slot, which resulted in changing the resonant frequency of the slot antenna. This reconfiguration technique is used for a frequency reconfigurable antenna, and it requires via holes and DC feed lines

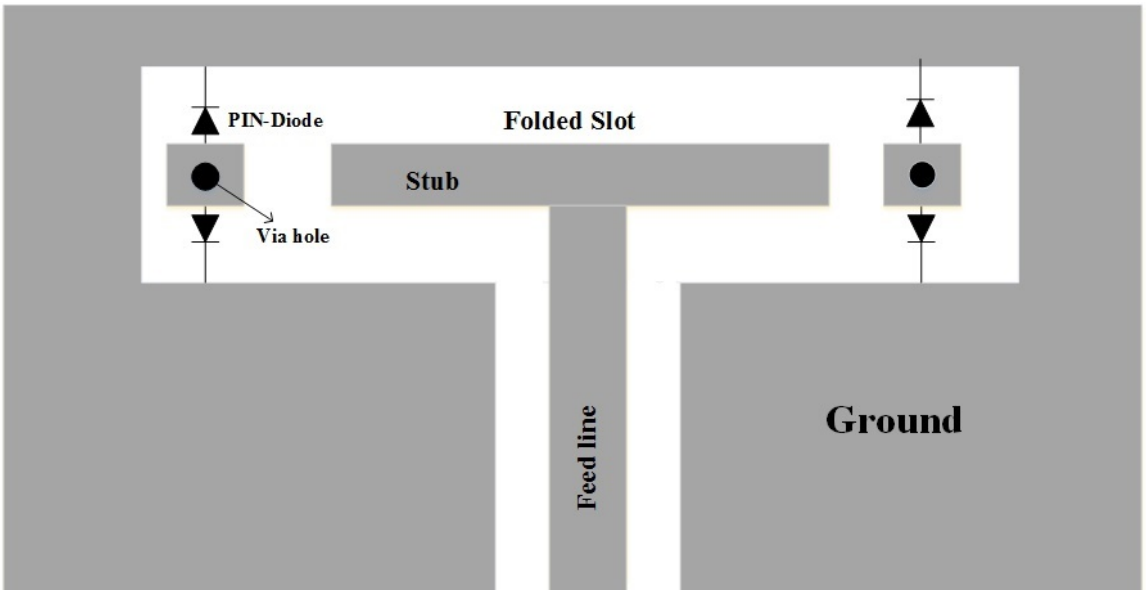

Figure 3.9: Reconfigurable Antenna of [32].

connected to the antenna surface to activate the PIN diodes. This may degrade the flexibility when the antenna is printed on a very thin flexible substrate. Instead, an alternative reconfiguration design was used here which minimizes the number of PIN diodes.

A new approach to reconfigure the folded slot antenna was undertaken and examined in this research. It is based on one PIN diode, as shown in Fig. 3.10(a), which is used to redirect and redistribute the current on the stub, and to adjust the stub length inside the slot to be symmetric or asymmetric with respect to the CPW feed line. The stub inside the slot is divided into left stub (T1) and right stubs (T2 and T3). The reconfiguration scenario is based on the status of the PIN diode where the switch is chosen to be in the middle of the right stub, as shown in Fig. 3.10(a). For reversed biased (OFF), the switch is used to redirect and redistribute the current on the internal stub, which results in a radiating dipole type of stub for a second resonant frequency with a polarization orthogonal to that of the slot. In this case,

the active stubs are T1 and T2, which form an asymmetrical stub with respect to the CPW feed line. To verify this assertion, the directions of the redirected and redistributed current distribution on stubs T1 and T2, are illustrated in Fig. 3.10(b). The diode is used to redirect the current on the right stub to be in-phase with current on the left stub. In this case, the proposed antenna resonates as a dual-band, linearly polarized with two different polarizations: one polarization is due to the slot while the other one (orthogonal to it) is due to the stub inside the slot (the stub acts as a dipole). For forward biasing (ON), an additional stub T3, is connected to stub T2 through the PIN diode, which is used to mismatch or eliminate the second resonant frequency. The active stubs are T1, T2 and T3 and they form one larger stub, which is symmetrical to the feed line. The current distribution on the stub is shown in Fig. 3.10(c) to illustrate that both sides of the stub have equal in magnitude but out of phase current distribution. In this case, the antenna has a single band with single linear polarization due only to the slot.

The proposed flexible reconfigurable antenna was designed, simulated and examined. Figs. 3.11 and 3.12 display the fabricated prototype and its bias circuit for the PIN diode. As discussed, the CPW feeding configuration makes the fabrication of flexible antennas and the integration of active devices onto flexible antennas easier. The proposed antenna is fed by a bias tee circuit, as shown in Fig. 3.12, which supplies both the RF signal for the radiator and the DC bias for the PIN diode (BAR64-03W) from Infineon. This is extremely useful for flexible radiators since no wires are connected to the antenna surface, which may degrade the flexibility and the radiation characteristics of the antenna. The chip RF choke inductor (56 nH) from Murata (LQW18AN56NG00D), has a Self-Resonant Frequency (SRF) of 2.4 GHz; the SRF was chosen at the operating frequency of the antenna. Another RF choke with a higher SRF (3.8 GHz) was also simulated, in place of the one with SRF of

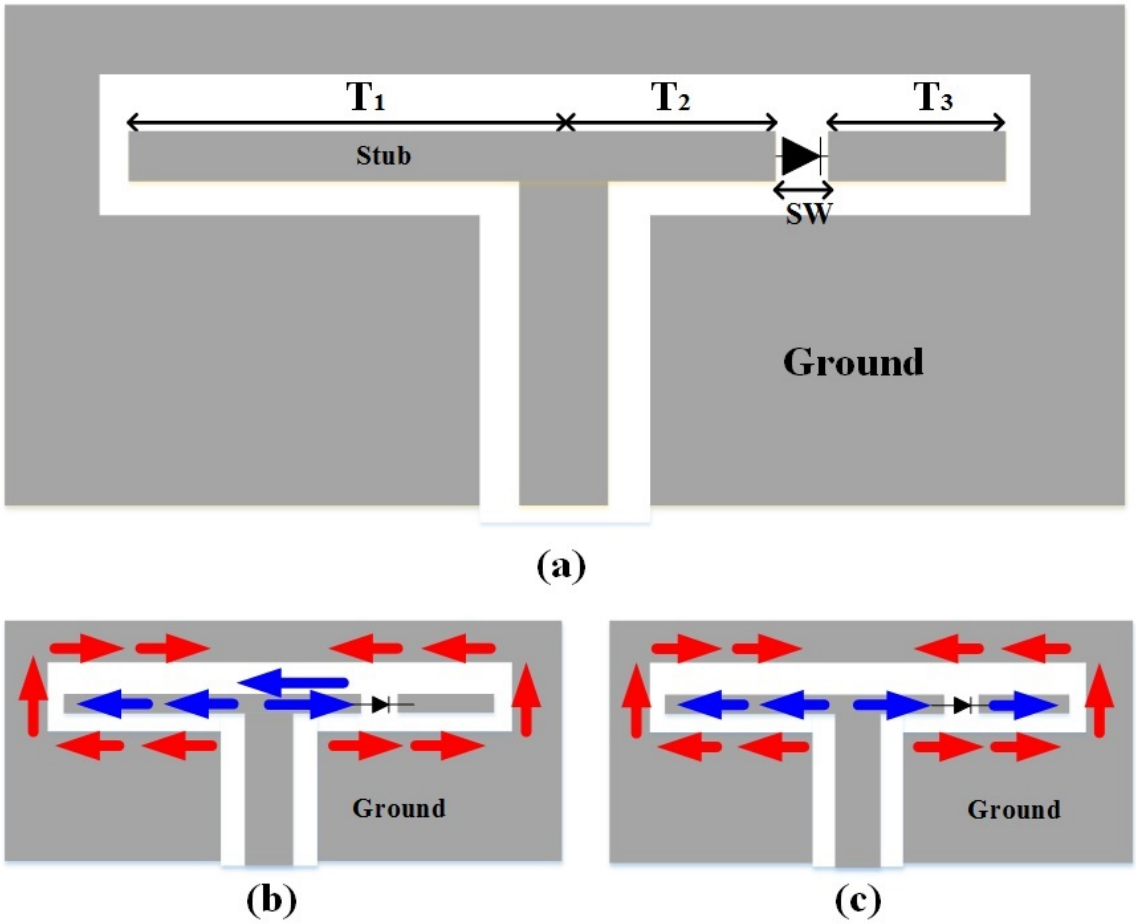

Figure 3.10: a) Reconfiguration Technique. b) Surface Current Directions for Reversed Biased. c) Surface Current Directions for Forward Biased.

2.4 GHz, and the reflection coefficients of the antenna performance for both RF chokes was nearly identical. The RF choke in this case is used to provide a DC ground to the cathode of the PIN diode and to block the RF signal from flowing to the ground. Both the PIN diode and the RF choke were soldered to the flexible substrate using low temperature tin-bismuth solder paste. It was required to have a temperature-controlled soldering iron to avoid burning the very thin PET material. The measurements were performed in the ElectroMagnetic Anechoic Chamber (EMAC) of Arizona State University (ASU).

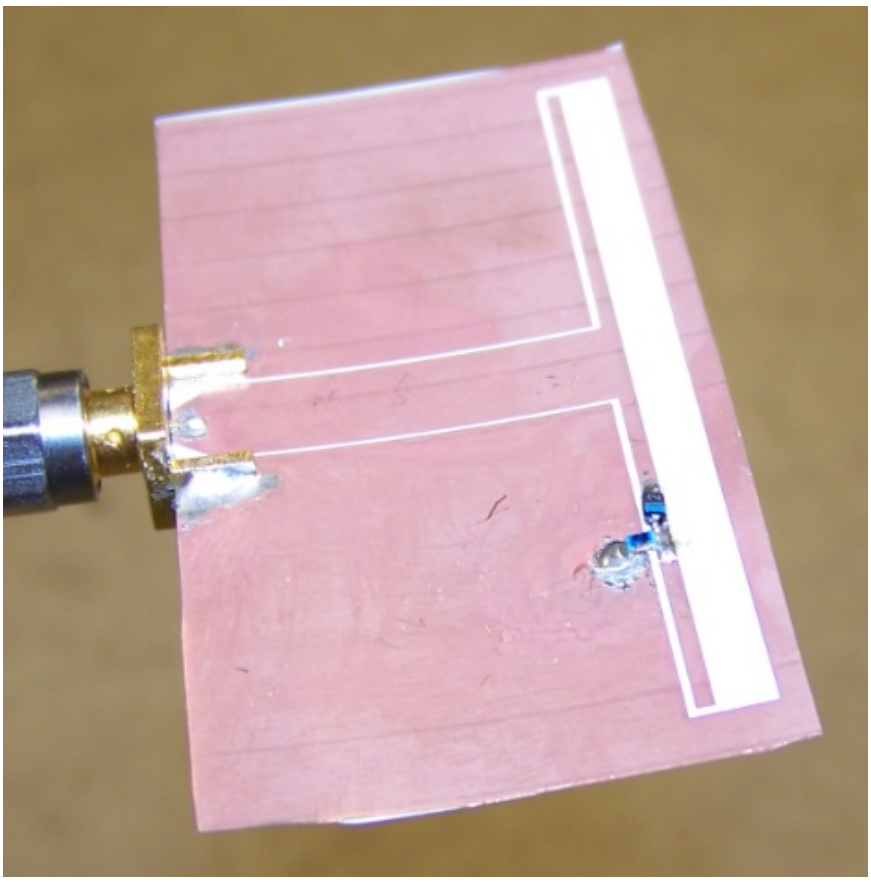

Figure 3.11: Fabricated Prototype of the Proposed Flexible Reconfigurable Antenna.

To ensure that the proposed antenna is a good radiator for conformal applications, the antenna was tested for reflection coefficients, amplitude patterns and gain, for both flat and curved configurations. For the two states of the PIN diode, the simulated and measured reflection coefficients for the flat configuration are shown in Figs. 3.13 and 3.14. The maximum currents for both the slot and the stub are shown in Figs. 3.15 and 3.16. The simulated and measured patterns for the flat configuration are displayed in Figs. 3.17, 3.18 and 3.19. It is observed that good agreements between measurements and simulations are achieved, and the antenna is well matched at the resonant frequencies. However, since the simulation does not include the parasitic

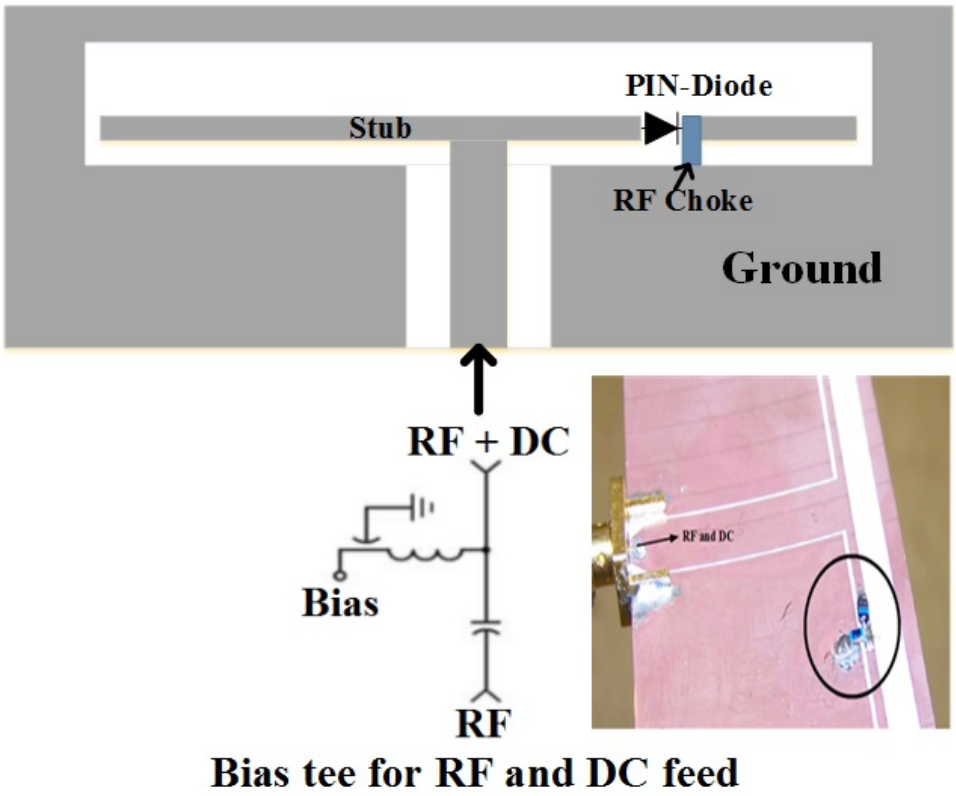

Figure 3.12: Bias Circuit of the Proposed Flexible Reconfigurable Antenna.

effects of the device packaging and also due to the alignment or metallization problems during the fabrication, there is a slightly shift in frequency between measured and simulated results.

To illustrate the polarization of the flat configuration of the proposed design, let us consider that the slot and the stub for the flat configuration are oriented horizontally and parallel to the XY plane based on the coordinate system in Fig. 3.1. When the PIN diode is forward biased (ON), the proposed antenna has a single band due to the slot at 2.42 GHz with a -10 dB measured impedance bandwidth of 0.16 GHz (2.34-2.5 GHz) for Wireless Local Area Network (WLAN) applications. The E plane (XZ plane) at 2.42 GHz is perpendicular to the horizontal slot and it is vertically polarized, while the H plane is the XY plane. When the PIN diode is reversed

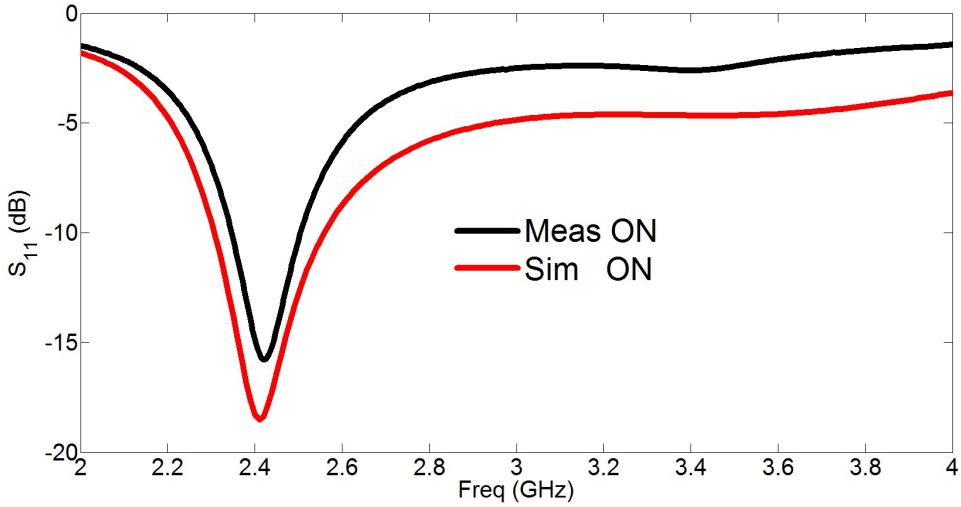

Figure 3.13: Comparison Between Measured and Simulated Reflection Coefficients for Forward (ON) Biased of the Flat Configuration.

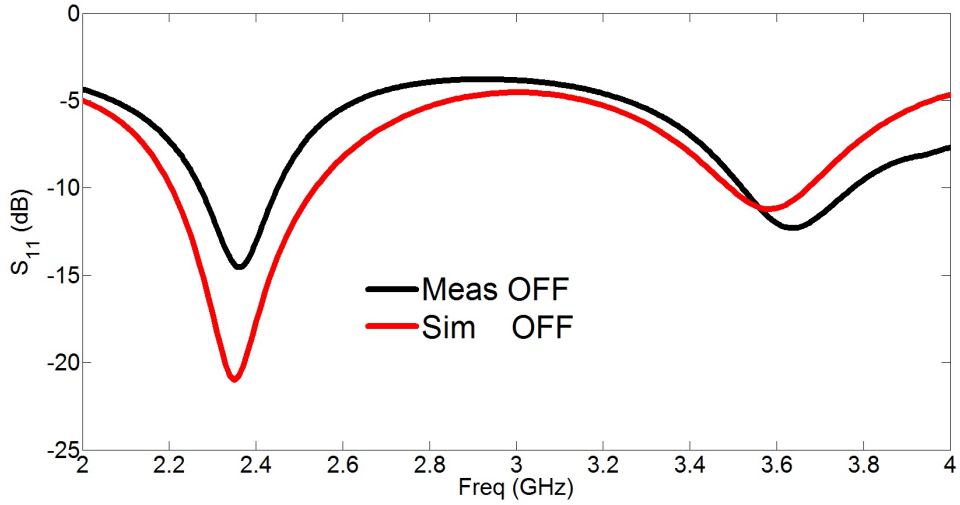

Figure 3.14: Comparison Between Measured and Simulated Reflection Coefficients for Reversed (OFF) Biased of the Flat Configuration.

biased (OFF), the proposed antenna is dual-band with two polarizations. One polarization is vertical due to the slot at 2.36 GHz with a -10 dB measured impedance bandwidth of 0.18 GHz (2.27-2.45 GHz), and the other polarization is horizontal due to the stub inside the slot at 3.64 GHz with a -10 dB measured impedance bandwidth

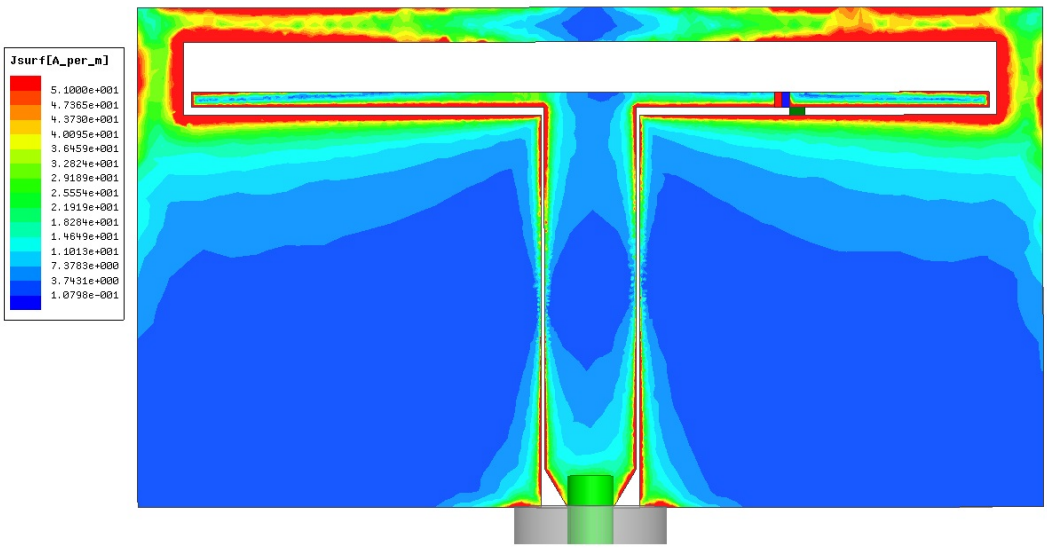

Figure 3.15: Simulated Maximum Current Distributions of the Slot at 2.4 GHz Resonance.

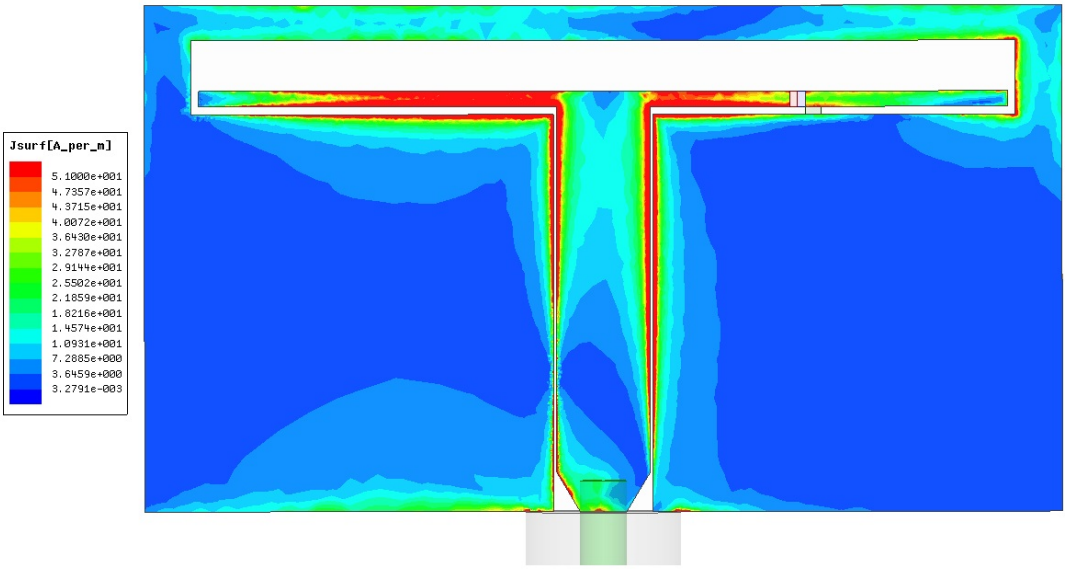

Figure 3.16: Simulated Maximum Current Distributions of the Stub at 3.6 GHz Resonance.

of 0.27 GHz (3.5-3.77 GHz). This provides WLAN and Worldwide Interoperability for Microwave Access (WiMAX) for wireless systems. The patterns at 2.36 GHz are identical to the forward biased case. However, since the stub acts as a dipole, the E plane, which is the XY plane, is parallel to the stub, and it is horizontally polarized. The H plane of the radiating stub is the XZ plane, which is perpendicular to the horizontal stub. The radiation patterns from the slot are dipole type, but with the E plane and H plane interchanged, which demonstrate the concept of the dipole being the complement of the slot according to Babinet's principle [10]. For clarity, the cross polarization is not shown in the presented patterns, but low-level of simulated cross polarization ($\leq$ -15 dB) was maintained for the forward biased case. However, for the reversed biased case, since the stub is radiating, a higher level of cross polarization was obtained.

Two curved configurations (circumferential and axial) [34], with a radius of $R = 25$ mm, were used to test the antenna for conformal applications. The circumferential configuration, as shown in Fig. 3.20(a), is when the length of the slot is perpendicular to the axis of the cylinder (z-axis), while the axial configuration, as shown in Fig. 3.20(b), is when the length of the slot is parallel to the axis of the cylinder (z-axis). For both circumferential and axial configurations, the measured and simulated reflection coefficients for the two states of the PIN diode, are shown in Figs. 3.21 and 3.22. The reflection coefficients are identical to those for the flat configuration, which indicates that the proposed antenna maintains its resonant frequencies for conformal applications. The patterns are also presented for the circumferential and axial configurations and compared in Fig. 3.23 with the flat configuration.

For conformal configurations, the pattern changes are expected since the entire surface of the antenna is not parallel to the principle axes. Thus, the changes in the null filing, symmetry and orientation of patterns are due to the non-planar structure

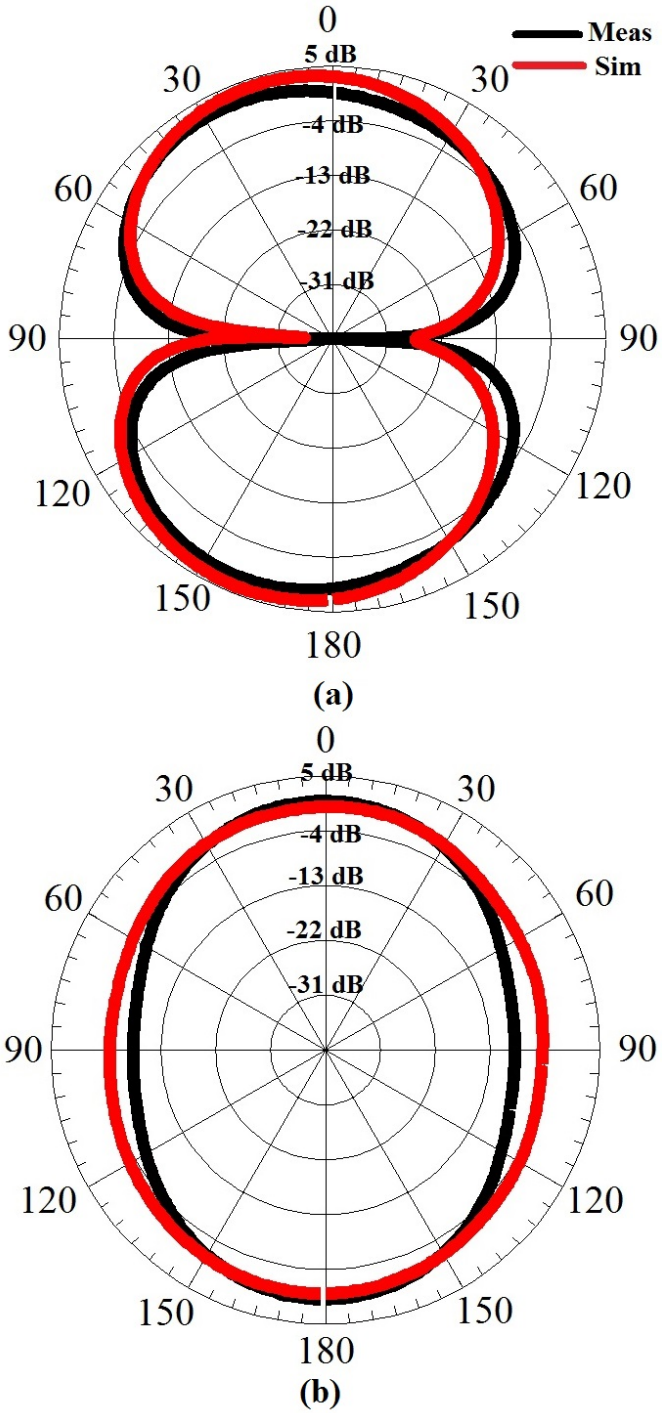

Figure 3.17: Measured and Simulated Radiation Patterns for the Flat Configuration of the Slot at 2.42 GHz (Diode Is ON): a) E Plane (XZ). b) H Plane (XY).

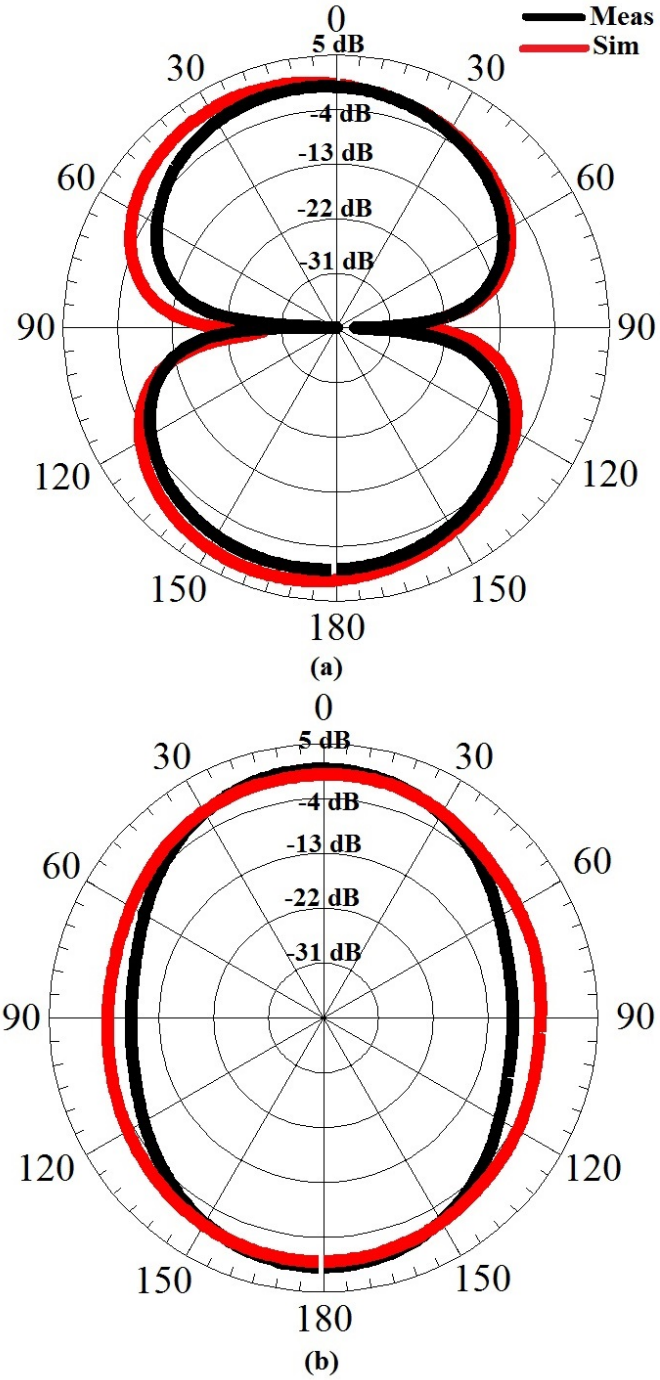

Figure 3.18: Measured and Simulated Radiation Patterns for the Flat Configuration of the Slot at 2.4 GHz (Diode Is OFF): a) E Plane (XZ). b) H Plane (XY).

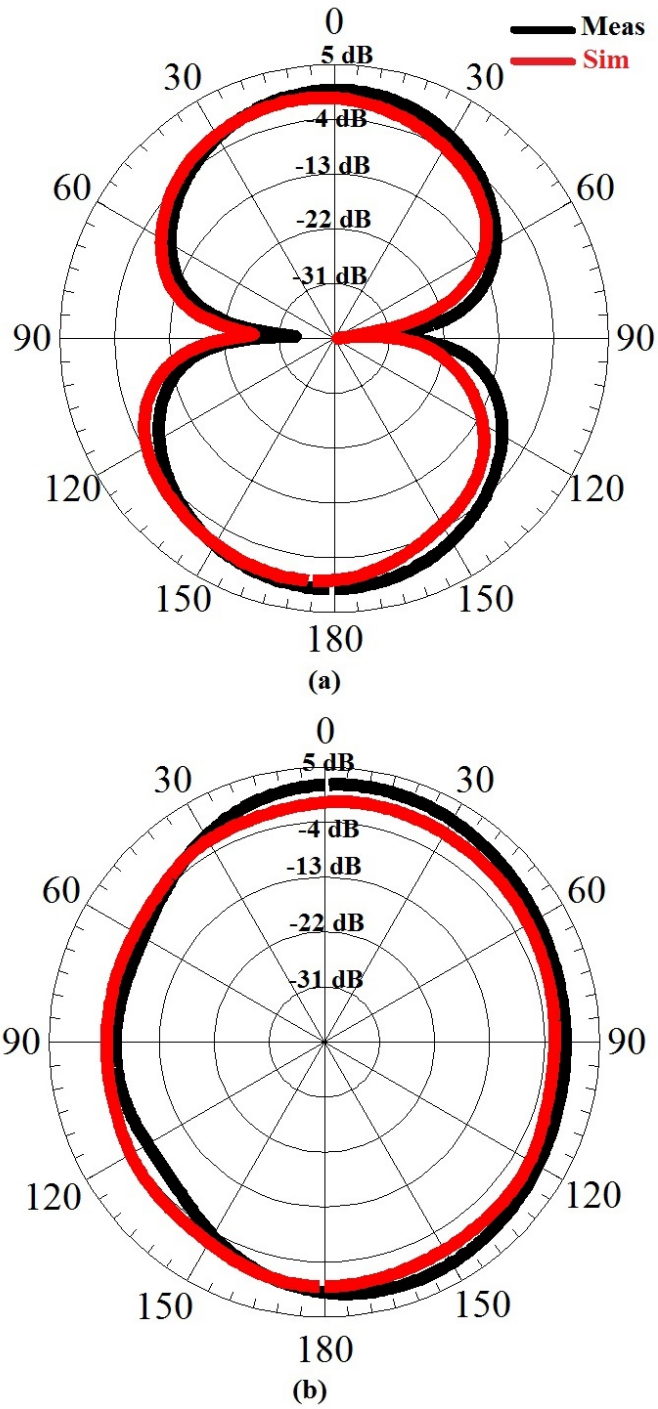

Figure 3.19: Measured and Simulated Radiation Patterns for the Flat Configuration of the Stub at 3.64 GHz (Diode Is OFF): a) E Plane (XY). b) H Plane (XZ).

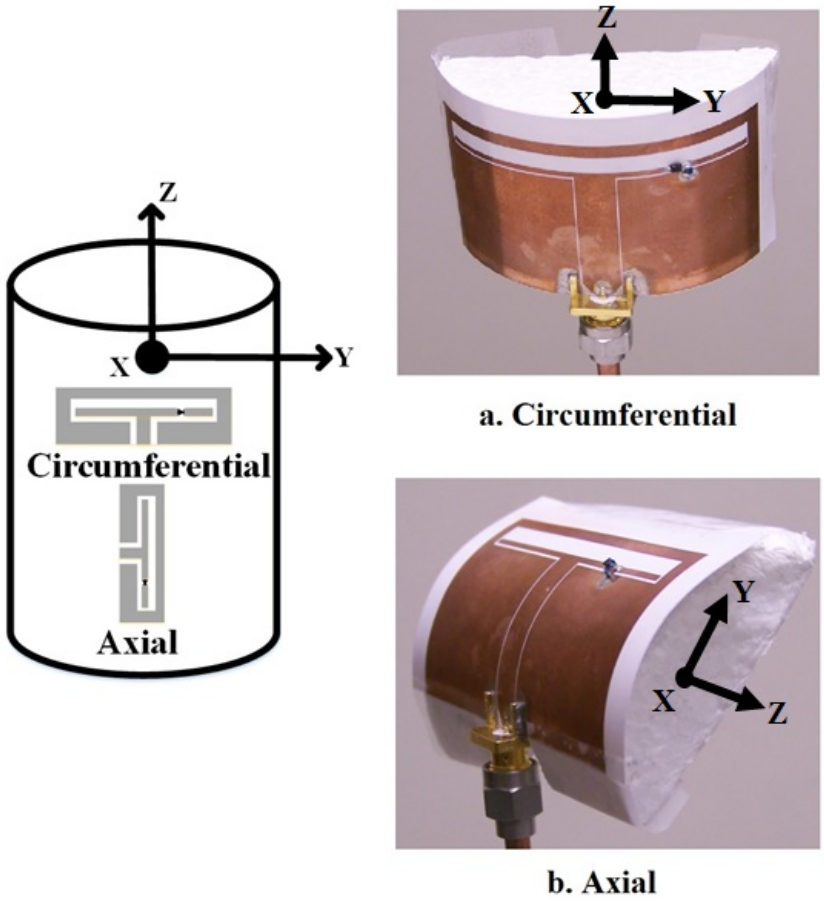

Figure 3.20: Fabricated Curved Prototype for Both Circumferential and Axial Configurations.

of the antenna, which contributes to the changes in the antenna patterns for both circumferential and axial configurations. When the antenna is mounted on a flat surface, the energy radiates primarily in the forward hemisphere. However, when the antenna is mounted on a cylinder, the antenna (slot and stub) is also curved and it radiates energy not only in the forward hemisphere but also sheds energy around the cylinder surface; thus the gain of the antenna (slot and stub) is influenced by its configurations (circumferential and axial) and the polarization of the respective E and H planes.

For the circumferential configuration, the E-plane of the slot is perpendicular to the curvature of the cylinder; so for both states of the PIN diode the intensity of the slot pattern in the back region, as shown in Fig. 3.23(a), is reduced resulting in slightly higher gain compared to the flat configuration. However, the E-plane of the stub is parallel to the curvature of the cylinder; therefore, its pattern, as shown in Fig. 3.23(b), is broader; thus the gain is decreased in comparison to the flat configuration.

Table 3.2: Gain Comparison Between Flat, Circumferential and Axial

Frequency (GHz)	Flat Gain(dB)	Circumf $R = 25$ mm Gain(dB)	Axial $R = 25$ mm Gain(dB)
2.42 (ON)	1	2	0.5
2.36 (OFF)	0.7	1.5	0.6
3.64 (OFF)	0.79	-3	1.75

For the axial configuration, the E plane of the slot is parallel to the curvature of the cylinder. Thus, as expected, for both states of the PIN diode, the pattern is slightly broader than the flat pattern, as shown in Fig. 3.23(a), and as a result the gain is slightly decreased. For the stub, the E plane is perpendicular to the curvature of the cylinder, and the intensity of the radiation pattern in the back region, as shown in Fig. 3.23(b), is reduced resulting in higher gain compared to the flat configuration. Table 3.2 tabulates a comparison between the measured gains at broadside for the flat, circumferential and axial configurations.

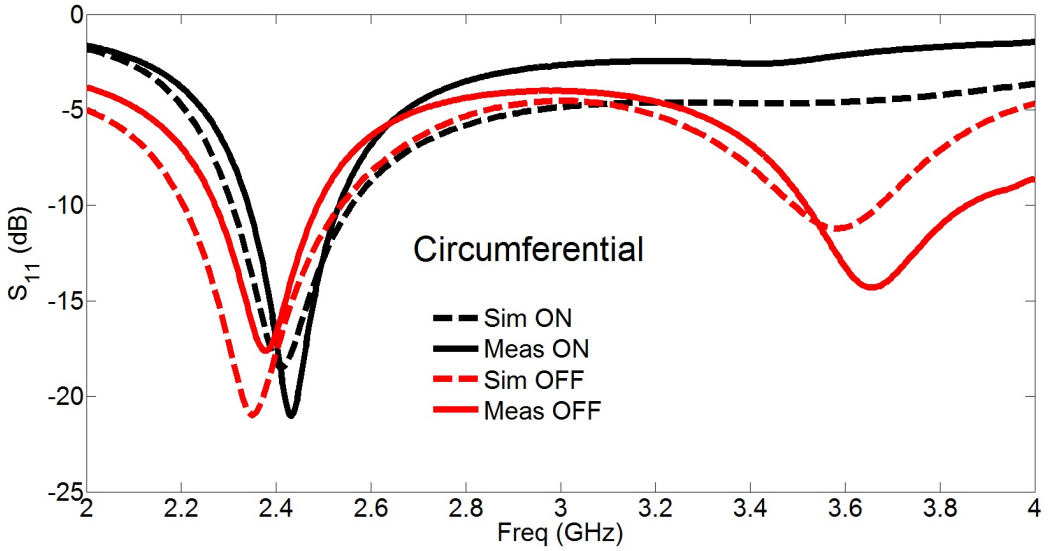

Figure 3.21: Measured and Simulated Reflection Coefficients for Circumferential Configuration ($R = 25$ mm) for Both Forward (ON) and Reversed (OFF) Biased.

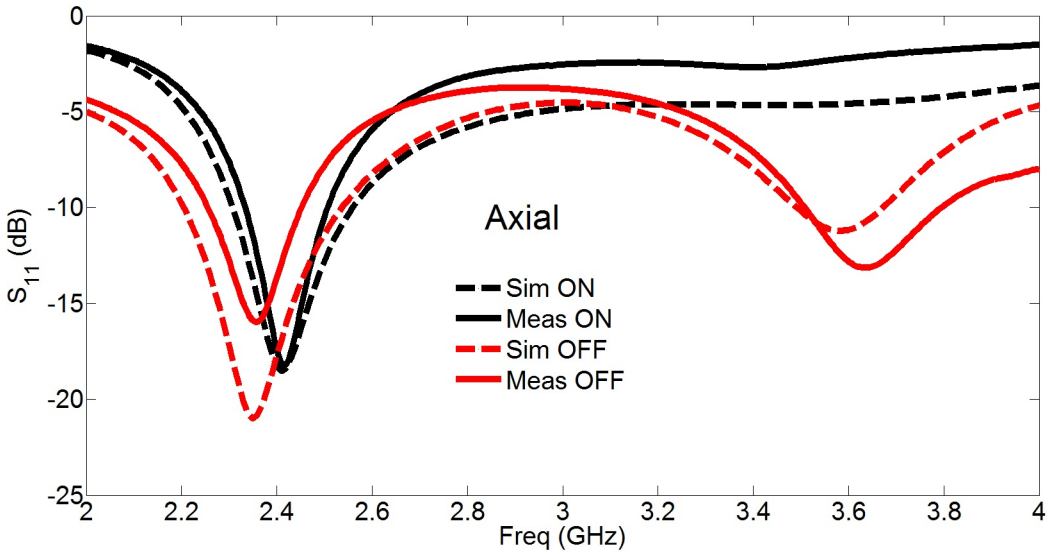

Figure 3.22: Measured and Simulated Reflection Coefficients for Axial Configuration ($R = 25$ mm) for Both Forward (ON) and Reversed (OFF) Biased.

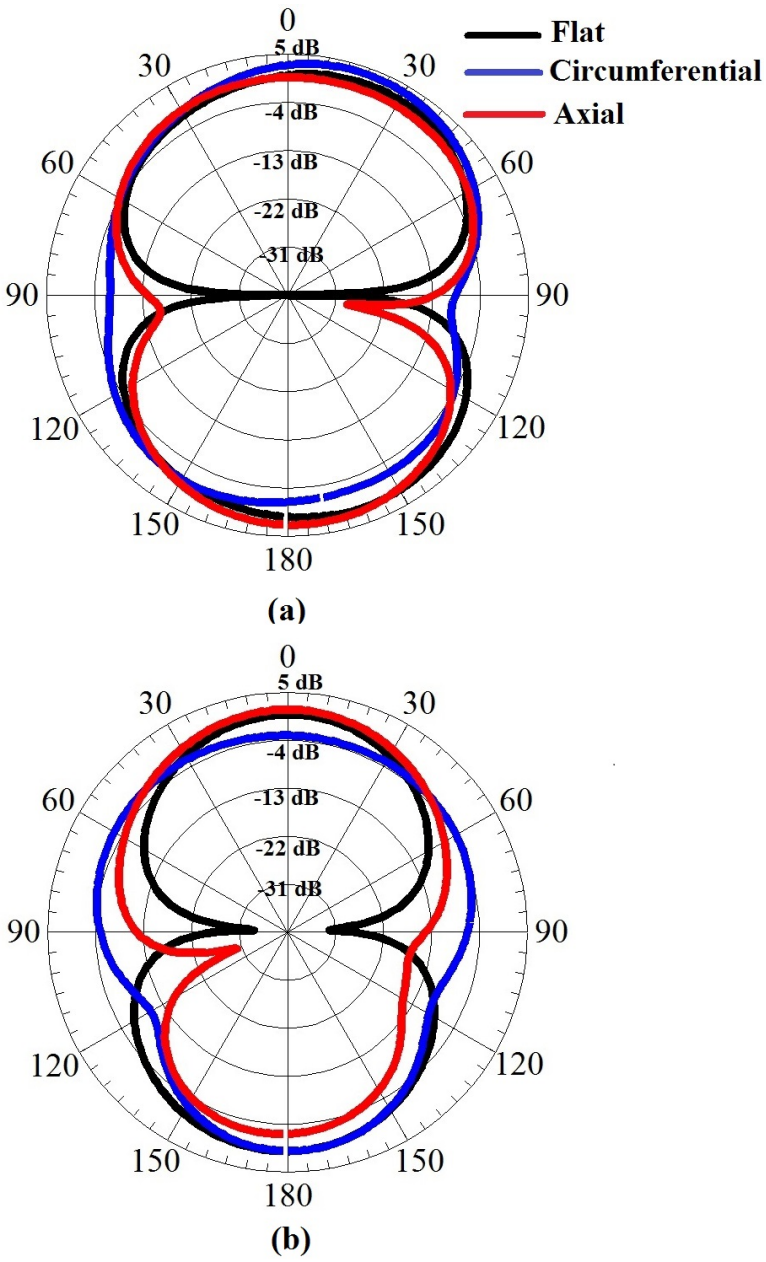

Figure 3.23: Comparison Between the Patterns for Flat, Axial and Circumferential Configurations ($R = 25$ mm): a) E Plane for the Slot. b) E Plane for the Stub.

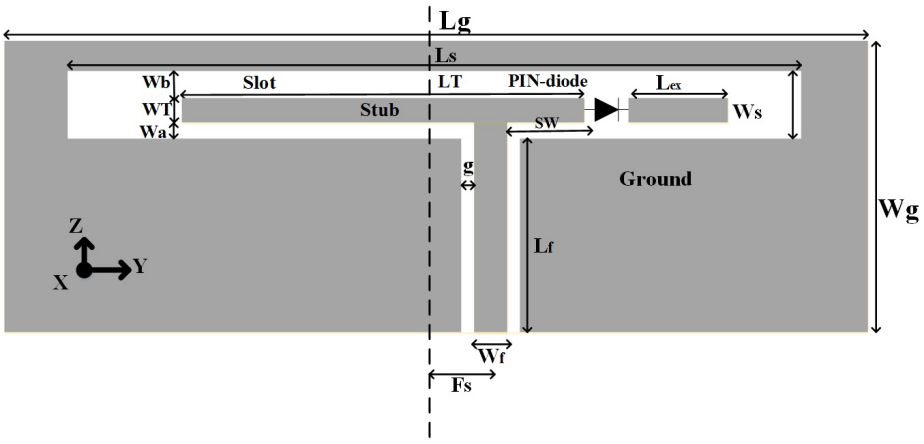

Figure 3.24: The Redesigned Reconfigurable Folded Slot Antenna Element.

3.4 Flexible Reconfigurable Antenna with MIMO Configuration

Multiple-Input Multiple-Output (MIMO) systems are used to improve the performance of wireless systems. They are also used to make antenna systems that improve the channel capacity and the diversity performance [35]. Reconfigurable MIMO antenna systems were previously reported in [36]-[37], where they can be used to enhance the diversity of conventional MIMO antenna systems and also can be used for future cognitive radio applications. A flexible reconfigurable MIMO antenna system is also proposed in this work, so that the antenna system is used for conformal applications. The previous reference antenna is redesigned on a flexible substrate Rogers (RO3003) [ϵ_r = 3, tan(δ) = 0.0013 and h= 1.52 mm], as shown in Fig. 3.24, to work either in single band at 2.4 GHz or dual-band at 2.4/5.2 GHz WLAN applications based on the state of the PIN diode. The dimensions of the new element are listed in Table 3.3. Fig. 3.25 illustrates the reflection coefficients of each single element while Fig. 3.26 displays the geometries of the proposed MIMO antenna system.

Since the antenna element consists of the slot and stub and both have orthogonal polarization to each other, this should be taken into consideration when placing the

Table 3.3: Dimensions of the Single Element of the MIMO Configuration

Parameters	Dimensions (mm)	Parameters	Dimensions (mm)
Lg	54.5	Lf	20.4
Wg	24	Wf	3.6
Ls	44.5	g	0.3
Ws	1.4	Wa	0.5
LT	20.4	Wb	0.4
WT	0.5	Fs	1.5
Lex	3	SW	8

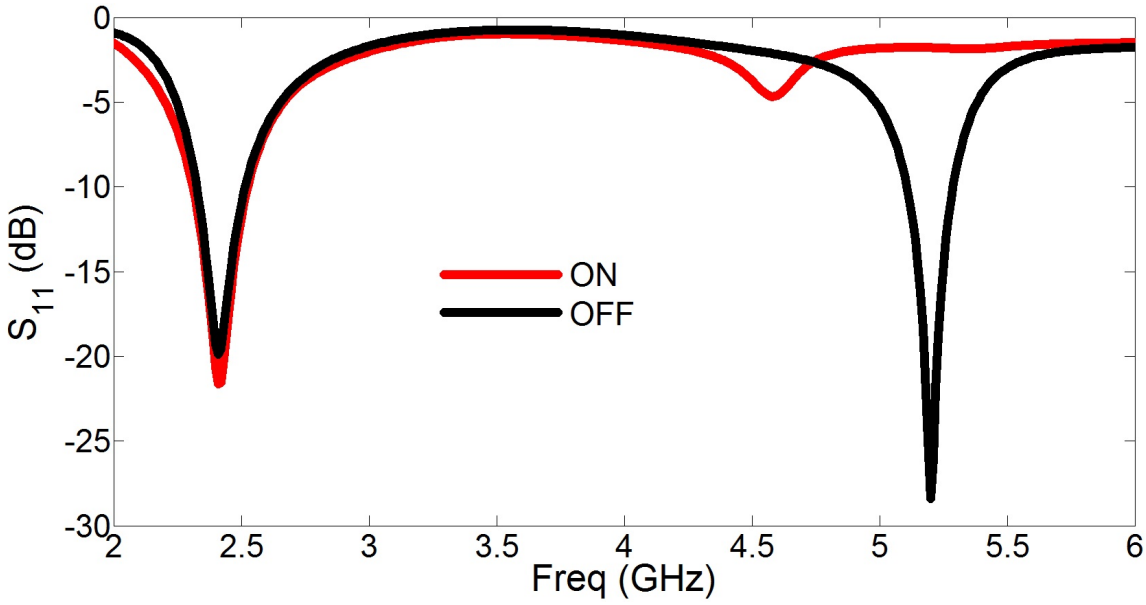

Figure 3.25: Simulated Reflection Coefficients of the Single Element for Both States (ON/OFF).

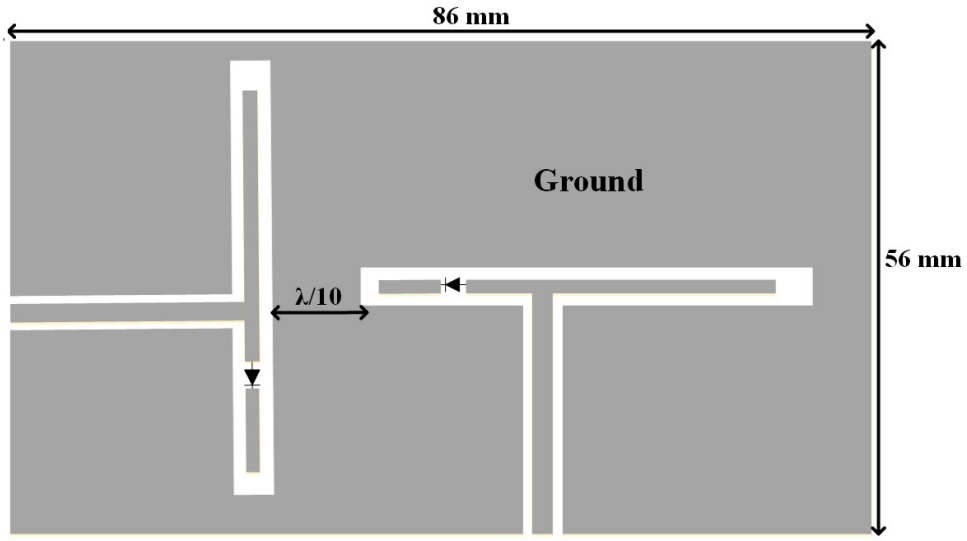

Figure 3.26: Reconfigurable MIMO Antenna Configuration.

MIMO antenna elements to maintain high isolation. Thus, to achieve better isolation, the two antenna elements are placed orthogonally, as shown in Fig. 3.26, to form the MIMO antenna configuration. The spacing distance between the antenna elements is about $\lambda/10$ at 2.4 GHz. The proposed MIMO antenna system is also designed on a flexible substrate so that it can be mounted on conformal structures.

Figs. 3.27 and 3.28 display the simulated reflection coefficients for the flat configuration of the proposed MIMO antenna system for both states of the PIN diode. The resonant frequencies from each antenna element are almost identical. As similar to the antenna element, the MIMO antenna system has either single band (2.4 GHz) or dual-band (2.4/5.2 GHz) operation based on the status of the PIN diode. The coupling (S_{12}) between the antenna elements is also studied, and it is observed that low coupling (below -15 dB) is achieved for both the slot and stub. The Envelope Correlation Coefficient (ECC), as discussed in [35], is also calculated using HFSS for both states of the PIN diode, as shown in Fig. 3.29. The values of ECC are below 0.1 for all resonant frequencies, which is excellent for MIMO antenna systems.

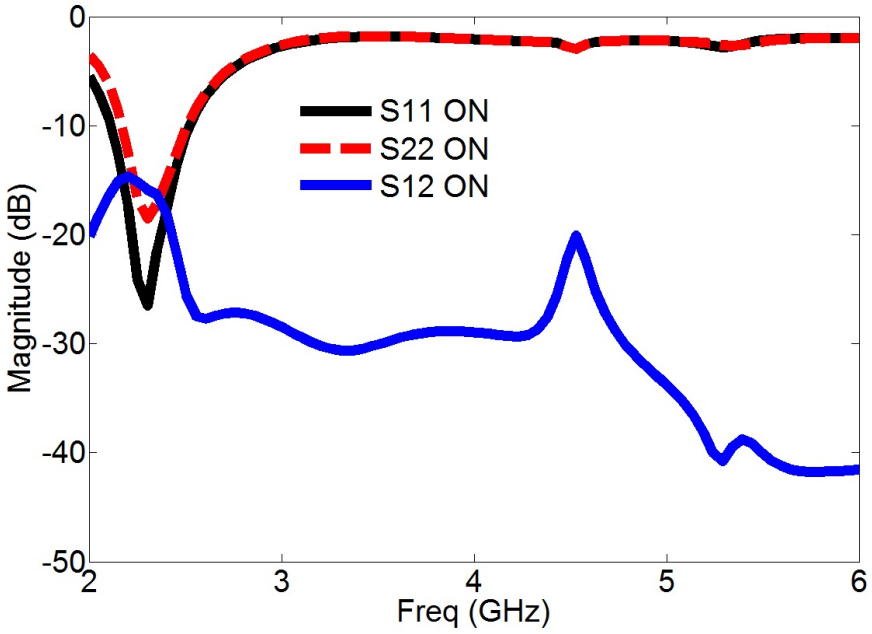

Figure 3.27: Simulated S-parameters of the Reconfigurable MIMO Antenna When the PIN Diode Is ON.

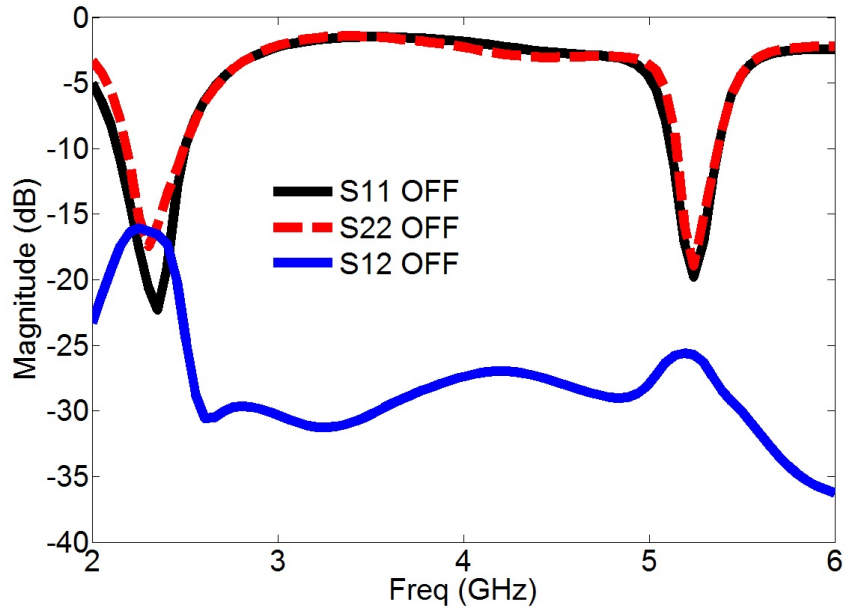

Figure 3.28: Simulated S-parameters of the Reconfigurable MIMO Antenna When the PIN Diode Is OFF.

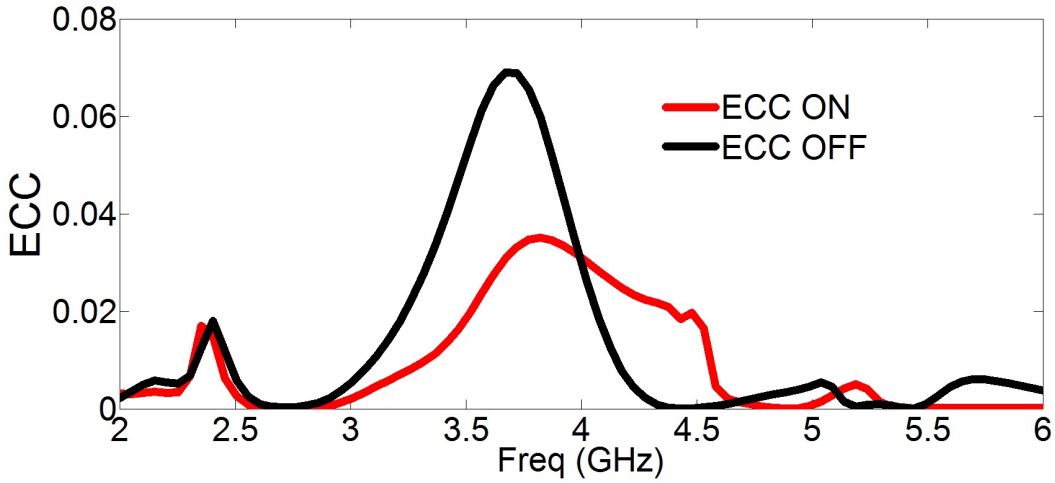

Figure 3.29: Simulated ECC Values for All Resonant Frequencies for Both States of the PIN Diode.

Chapter 4

WEARABLE FLEXIBLE RECONFIGURABLE ANTENNA

This chapter presents and discusses a wearable flexible reconfigurable folded slot antenna. The antenna is composed of a folded slot and a stub where the reconfigurability is achieved by turning a PIN diode ON and OFF, which alters the radiation characteristics of the stub. The operating frequency and polarization of the slot and stub are different. Hence, a polarization dependent dual-band AMC surface is integrated with the antenna to improve its radiation performance and to reduce the Specific Absorption Rate (SAR). The antenna is designed and fabricated on a flexible substrate, and its performance is measured for both flat and curved configurations. The measurements show an excellent agreement with the simulations. To examine its performance as a wearable antenna, it is placed and measured on a human body. Simulations show that the SAR level is reduced when the AMC surface is used as an isolator. The proposed wearable antenna structure can be used for Wireless Body Area Network (WBAN) and WiMAX body-worn wireless devices.

4.1 Introduction

Wireless Body Area Network (WBAN) is an active research topic, especially in the healthcare area, as it provides cost efficient and continuous monitoring of patients over a wide range of accessibility. In such a system, an array of body sensors is connected to a communication unit which collects the data and sends it to a health center [38]. This unit can either be located near or worn directly by the patient to minimize the impact on daily life activities. Hence, wearable antenna designs have attracted

considerable interest, to be utilized in similar on-body applications [39], [40]-[45]; however maintaining acceptable radiation characteristics with low levels of Specific Absorption Rate (SAR) is a challenging task. In addition, antennas are preferred to be flexible and conformal to the human body [6], [46]-[47]. The impact of the human body, which is considered as a lossy tissue, on the radiation efficiency is critical. Thus, it is recommended to use antennas that have uni-directional patterns, such as microstrips, or elements that have isolators to reduce the impact of the human body on their performance and to reduce the SAR level. Wearable antennas consisting of Perfect Electric Conductors (PECs) are not preferred for low profile applications due to the quarter wavelength height required to increase the radiation efficiency [10], which increases the overall size and also makes the flexibility and reconfigurability of the antenna more challenging.

AMC surfaces are being used as ground planes for low profile applications as discussed in [34], [48]-[50]. Thus, an AMC surface can be used as an isolator in wearable antenna applications, and they have been reported in the literature [42]-[45]. In [42], a dual-band textile antenna operating at 2.45 GHz and 5 GHz, which was printed on a dual-band EBG substrate, was proposed. The back radiation was reduced by 10 dB while the antenna gain increased by 3 dB. In [43], an inkjet-printed, low profile, Coplanar Waveguide (CPW) fed antenna was fabricated on a Jerusalem Cross AMC structure for bandwidth enhancement and SAR reduction. The front-to-back ratio and gain were increased by 8 dB and 3.7 dB, respectively, and a 64% reduction in SAR level was obtained. However, none of these antennas are reconfigurable.

In this chapter, we are proposing a novel flexible reconfigurable antenna for a wearable remote patient monitoring system, where the data transfer between the communication unit, the sensors and the health center is performed over WBAN and WiMAX bands, respectively. The reconfigurable antenna does not require a complex

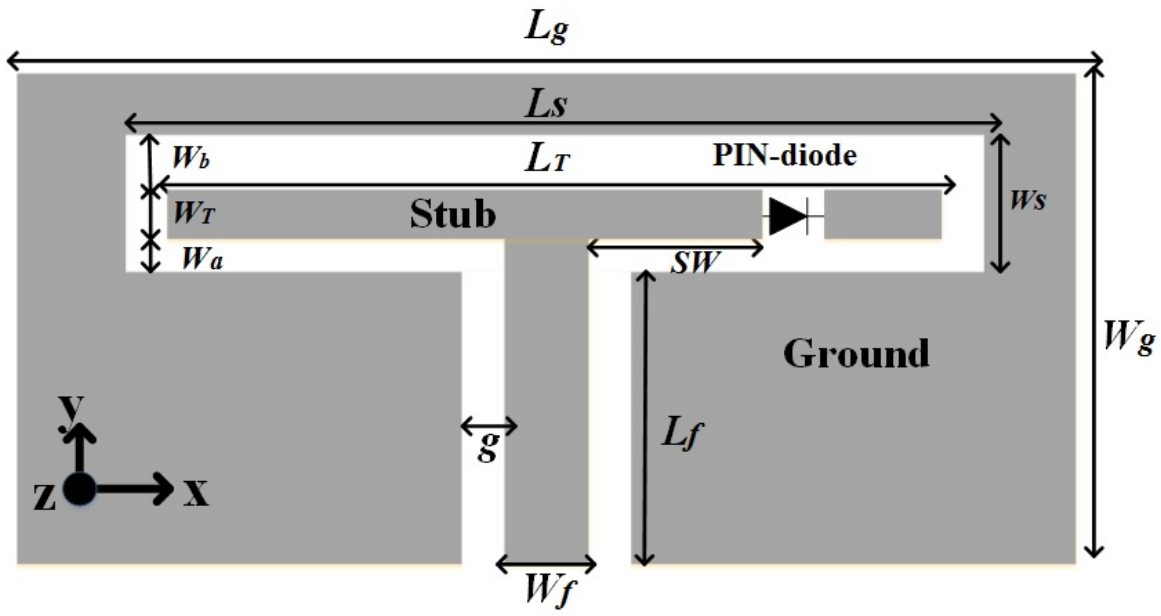

Figure 4.1: Reconfigurable Folded Slot Antenna.

bias circuitry, and it radiates orthogonally-polarized waves in the WBAN and WiMAX bands, which provides extra isolation. The SAR level is significantly reduced by the use of the dual-band, polarization dependent AMC surface.

4.2 Antenna and AMC Surface Design

The reference antenna element as discussed in Chapter 3 consists of three parts: a 50-ohm CPW feed line, a slot, and a stub, as shown in Fig. 4.1. It is redesigned to resonate over the AMC surface and its dimensions are listed in Table 4.1. If the stub inside the slot is symmetrical with respect to the CPW feed line, it does not radiate and the antenna has a single operating frequency from the slot only. On the other hand, if the stub is asymmetrical with respect to the feed line, then the current on the stub is redirected resulting in a dipole-type radiation. Thus, the folded slot antenna can be reconfigured by changing the length of the stub. This can be achieved

Table 4.1: Dimensions of the Reconfigurable Folded Slot Antenna

Parameters	Dimensions (mm)	Parameters	Dimensions (mm)
Lg	83	Lf	46
Wg	89	Wf	3.6
Ls	51	g	0.2
Ws	5.3	Wa	0.5
Lt	52	Wb	4
Wt	1	SW	8

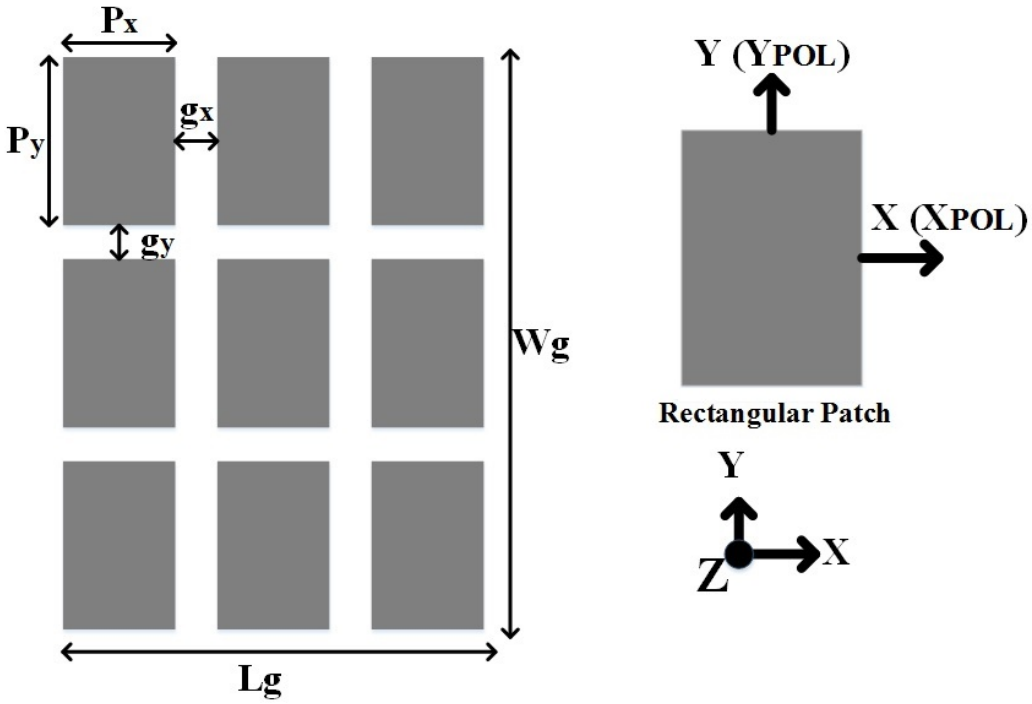

Figure 4.2: A Polarization-Dependent AMC Surface Design (3×3) Unit Cells. AMC Design Dimensions: Wg = 89 mm, Lg = 83 mm, Px = 23 mm, Py = 29 mm, gx = 3.5 mm, gy = 0.5 mm.

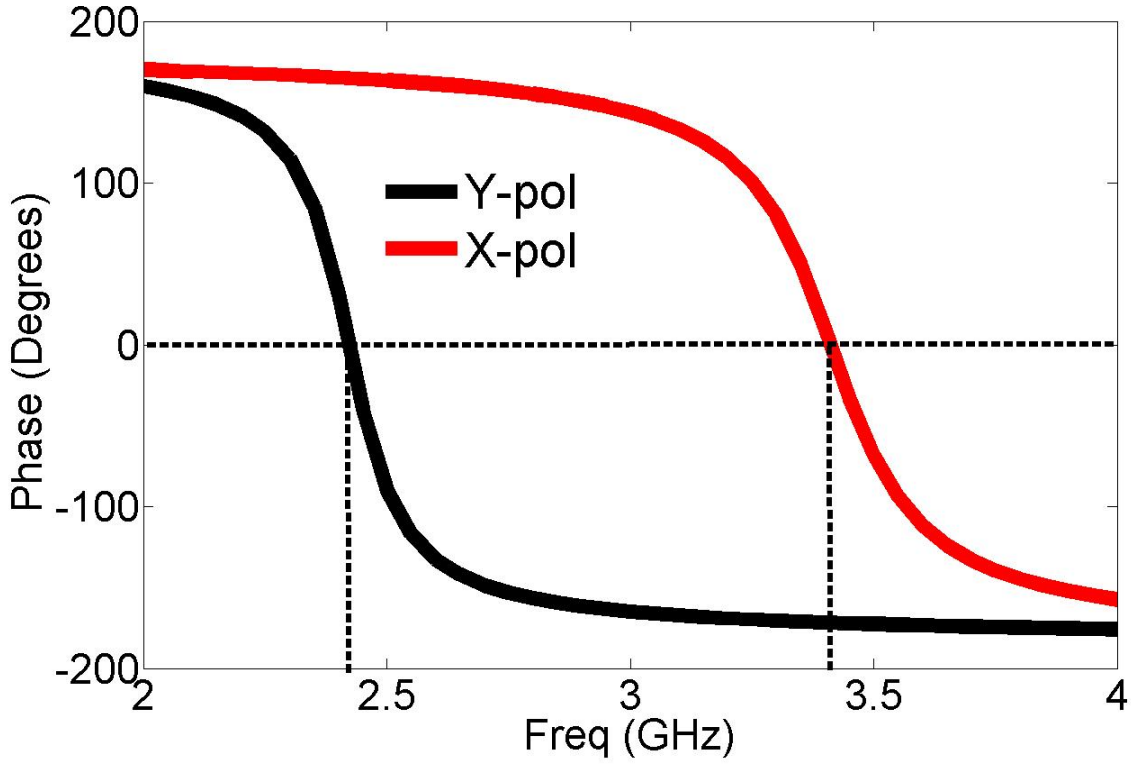

Figure 4.3: Reflection Phase of a Rectangular Patch Unit Cell of the AMC Surface.

by utilizing a PIN diode, and turning it ON and OFF, with the aid of a simple bias circuitry, as discussed in Chapter 3. If the diode is OFF, the antenna has dual-band operation and both the slot and the stub resonate with orthogonal polarizations, according to the Babinet's principle [10]. Based on the coordinate system of Fig. 4.1, the slot is y-polarized while the stub is x-polarized.

To reduce the backward radiation and lower the SAR level, the antenna is placed on an AMC surface, which considerably lowers the profile of the entire structure, compared to a PEC. Since the antenna has two operating bands with orthogonal polarizations, the AMC surface should also have two separate bands with different polarizations. To achieve this, a rectangular patch is utilized as the unit cell of the AMC, as shown in Fig. 4.2. The AMC surface consists of 9 unit cells (3x3) to

maintain a compact size and a reasonably low backward radiation. The total size of the structure measures approximately 0.71λ x 0.66λ at 2.4 GHz. The AMC has a zero reflection phase at 2.4 GHz and 3.4 GHz for y- and x-polarized normal incident plane waves, respectively. Fig. 4.3 displays the reflection phase of the proposed AMC surface.

The entire structure consists of 3 layers: the flexible reconfigurable antenna on top, the AMC surface on the bottom and a flexible foam material in between. Both the antenna and the AMC were fabricated, using an etching process, on Rogers RO3003 flexible substrate, with a dielectric constant and a loss tangent of 3 and 0.0013, respectively; the thickness of the substrate was 1.52 mm. The fabricated prototypes of the proposed antenna structure are displayed in Figs. 4.4 and 4.5.

Unlike a wire dipole, the CPW-fed folded slot antenna has a ground plane around the slot and if it is backed by an AMC surface, the coupling between the ground plane and the AMC may decrease the radiation efficiency and change the impedance matching. Hence, the antenna geometry and its height should be optimized to minimize the coupling and maintain good impedance matching. The antenna is placed approximately $\lambda/20$ at 2.4 GHz above the AMC surface, and a flexible foam material is used to fill the space between the radiating element and the AMC surface. The High Frequency Structure Simulator (HFSS) is used to design and simulate the entire antenna structure. Fig. 4.6 shows the simulated reflection coefficients, for different states of the PIN diode (ON/OFF), and with and without the (AMC/PEC) surfaces. It is observed that the matching is better when using the AMC surface.

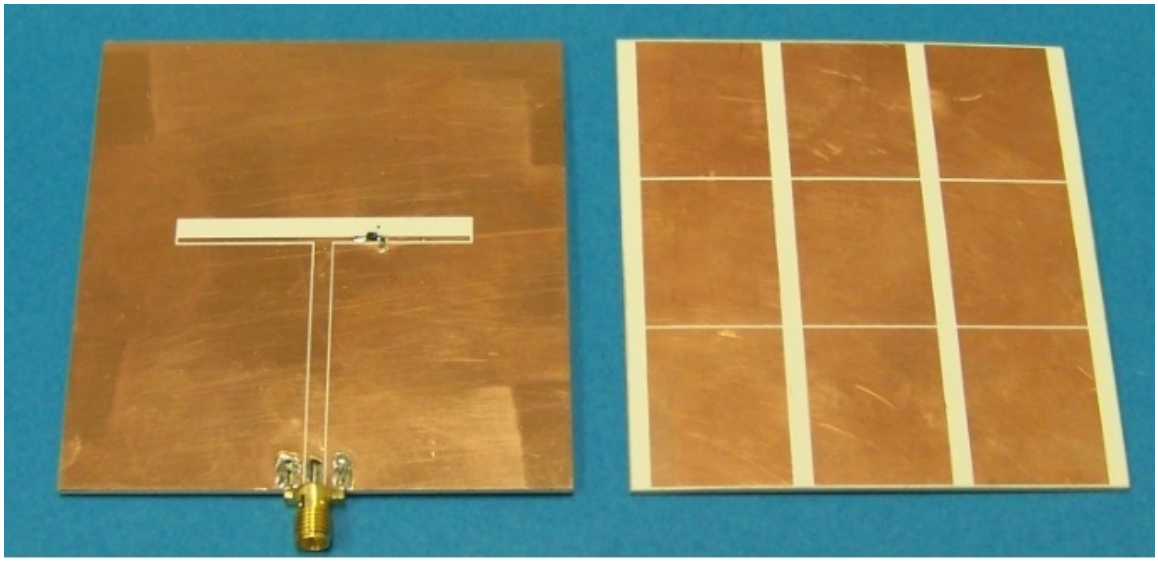

Figure 4.4: Fabricated Prototypes of the Antenna and AMC Surface.

4.3 Results and Discussion

To examine the performance of the proposed wearable antenna backed by an AMC surface, the radiation characteristics, such as the reflection coefficients and the radiation patterns, were measured and compared with the predicted results. In Figs. 4.7 and 4.8, a comparison between measured and simulated reflection coefficients of the proposed structure for different states of the PIN diode are displayed; an excellent agreement is achieved between simulations and measurements. The maximum currents for the folded slot antenna at 2.45 and 3.3 GHz are shown in Figs. 4.9 and 4.10, which illustrate that both the slot and the stub are resonating above the AMC surface. If the PIN diode is ON, the proposed antenna structure is single band from the slot, and it works at 2.45 GHz with a -10 dB measured impedance bandwidth of 0.1 GHz (2.4-2.5 GHz) for WBAN applications of wearable devices. However, if the PIN diode is OFF, the antenna structure is dual band from the slot at 2.45 GHz with a -10 dB measured impedance bandwidth of 0.17 GHz (2.35-2.52 GHz) and the

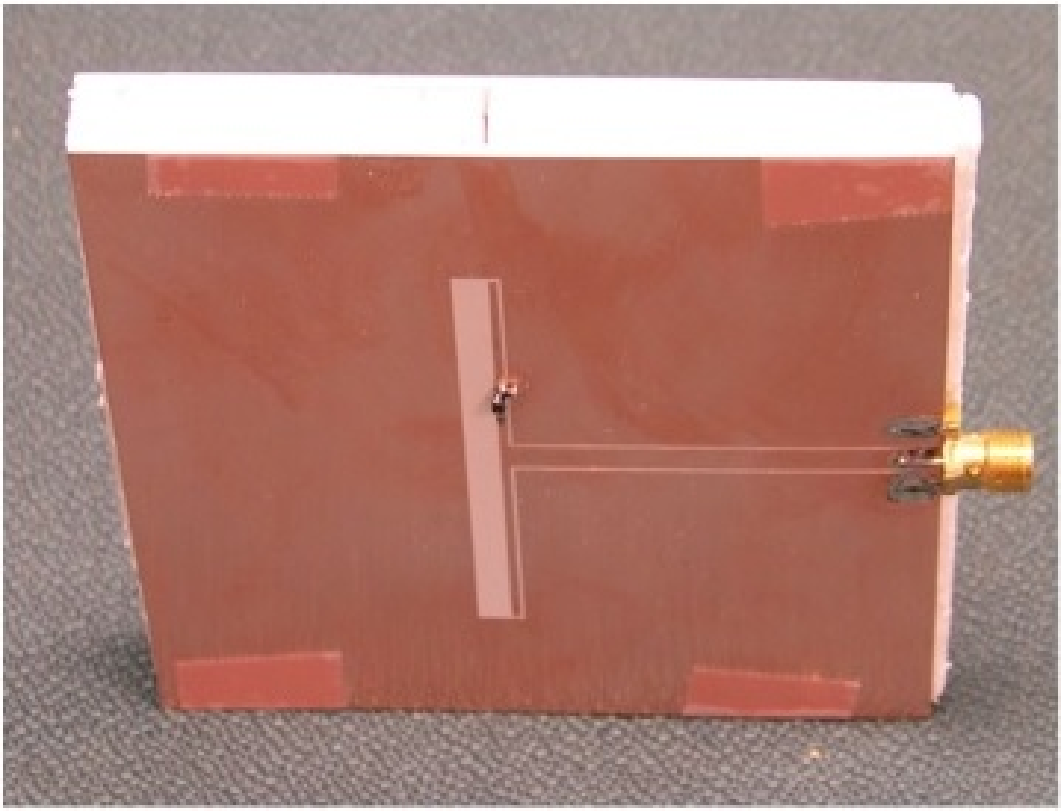

Figure 4.5: The Entire Antenna Structure.

stub at 3.3 GHz with a -10 dB measured impedance bandwidth of 0.1 GHz (3.28-3.38 GHz). In this case, the antenna can be used for both WBAN and WiMAX wireless applications. The measured and simulated radiation patterns for different states of the PIN diode of the proposed structure are displayed in Figs. 4.11, 4.12 and 4.13. It is clear that the AMC surface reduces the back radiation, which will result in SAR level reduction. Table 4.2 lists a comparison between the gains at broadside ($\theta = 0$), with and without the AMC surface. It is observed that with the AMC surface the gain of the antenna is enhanced by about 3.6 dB for the slot and 2.4 dB for the stub configurations.

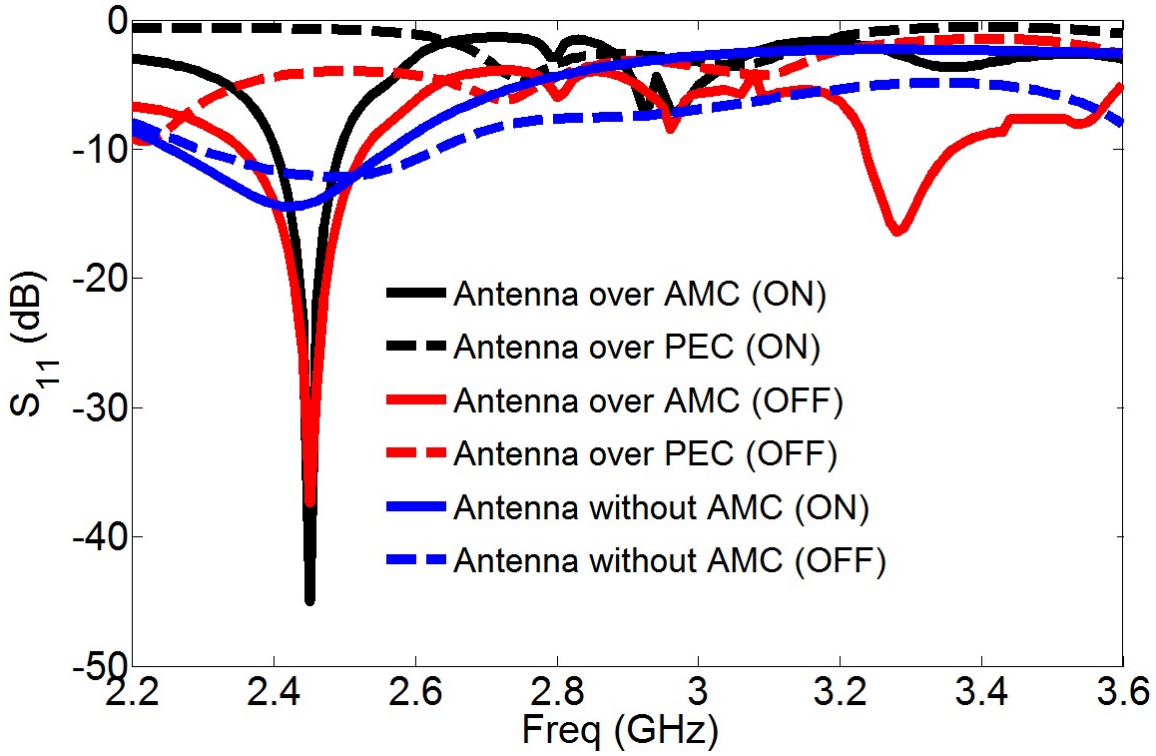

Figure 4.6: The Simulated Reflection Coefficients of the Proposed Antenna with and Without the (AMC/PEC) Surfaces.

It should be mentioned that if a larger AMC surface (more unit cells) is used, the antenna gain can be increased with further reduction in the back radiation. However, this will increase the overall size, which is not preferred.

For wearable applications, the flexibility test of the antenna is required to ensure that it can be worn or conformed on a human body. Figs. 4.14 and 4.15 illustrate the antenna when it is curved and mounted on a human body (leg). To ensure that the proposed antenna maintains its resonant frequencies when it is bent or conformed on a curved structure, it was tested for the reflection coefficients of the curved structure and compared with the reflection coefficients of the flat configuration. The comparison is displayed in Fig. 4.16, which indicates that the resonant frequencies for both flat and curved configurations are the same. The wearability of the proposed antenna,

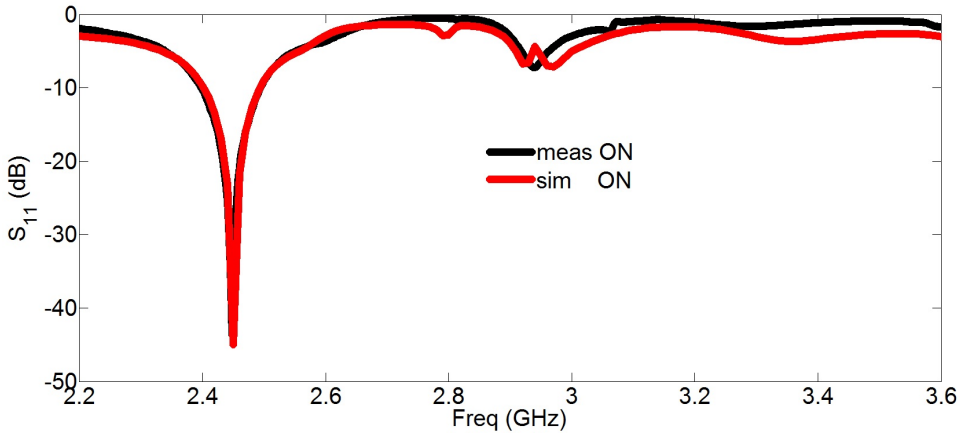

Figure 4.7: Measured and Simulated Reflection Coefficients of the Proposed Antenna Structure for the ON State of the PIN Diode.

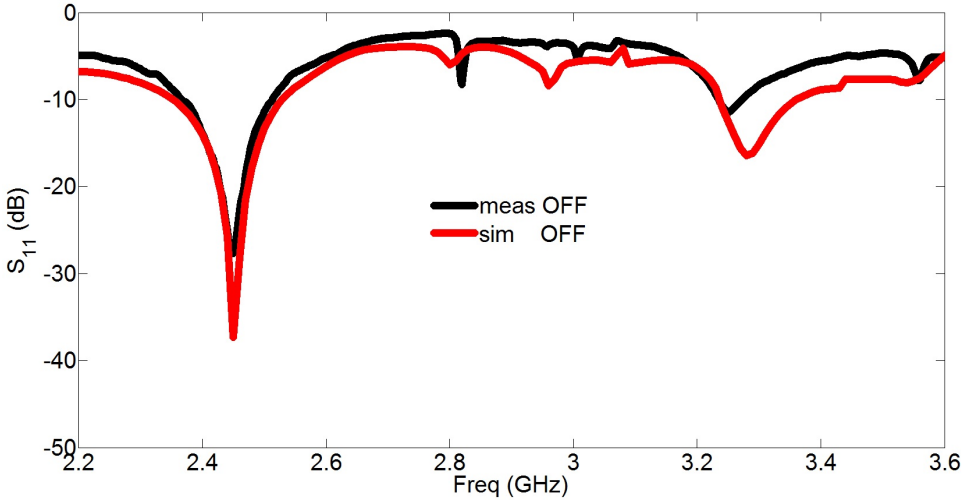

Figure 4.8: Measured and Simulated Reflection Coefficients of the Proposed Antenna Structure for the OFF State of the PIN Diode.

when it is mounted on human body tissue, as shown in 4.15, must be examined to test the impedance mismatch due the impact of human body tissue on its performance. The measured reflection coefficients are also shown in Fig. 4.16 for different states (ON/OFF) of the PIN diode; the antenna maintains its resonant frequencies.

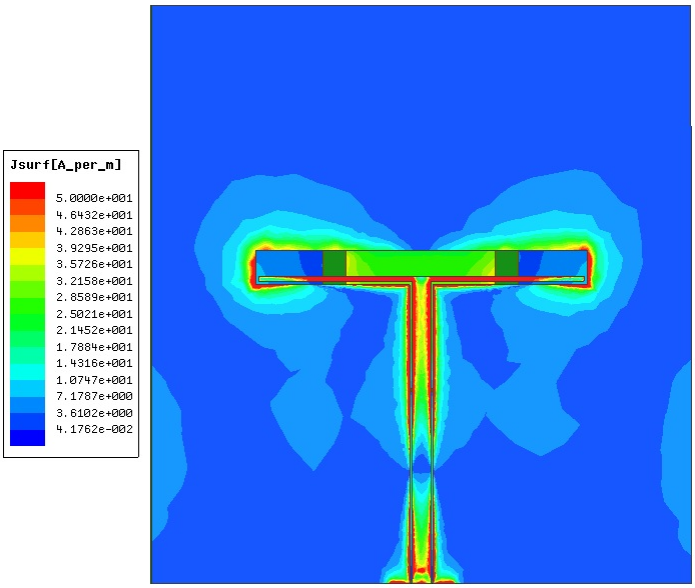

Figure 4.9: Simulated Maximum Current Distributions of the Slot at 2.45 GHz Resonance.

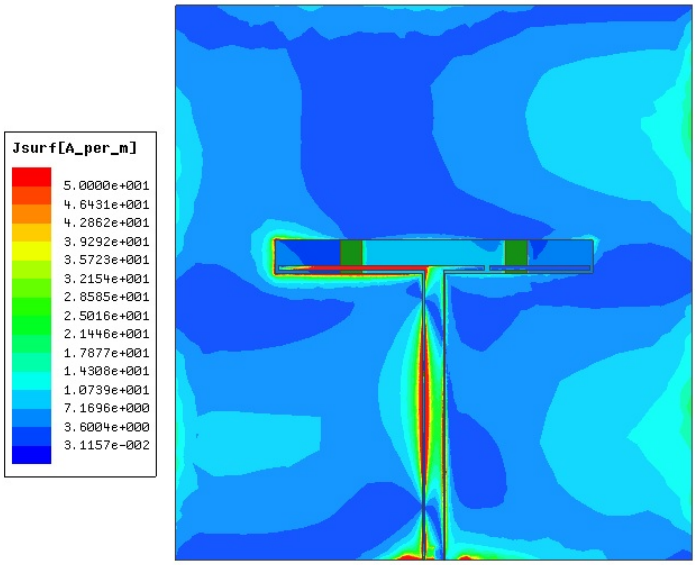

Figure 4.10: Simulated Maximum Current Distributions of the Stub at 3.3 GHz Resonance.

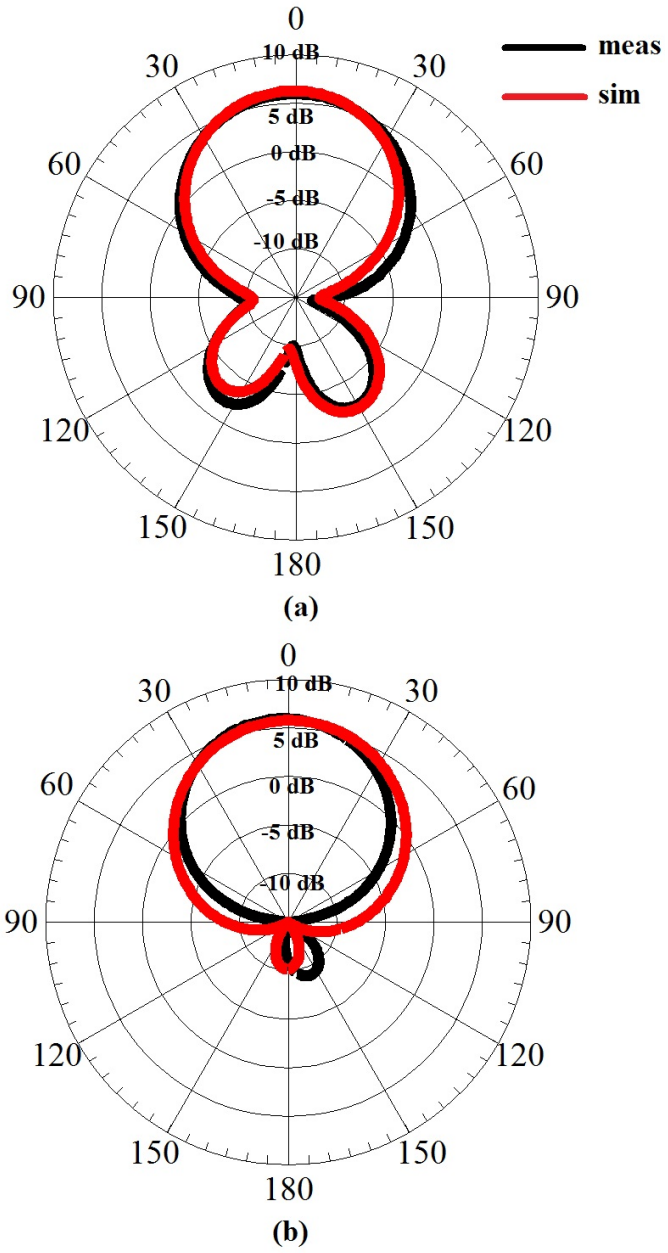

Figure 4.11: Measured and Simulated Radiation Patterns of the Proposed Structure at 2.45 GHz (Diode Is ON): a) E Plane. b) H Plane.

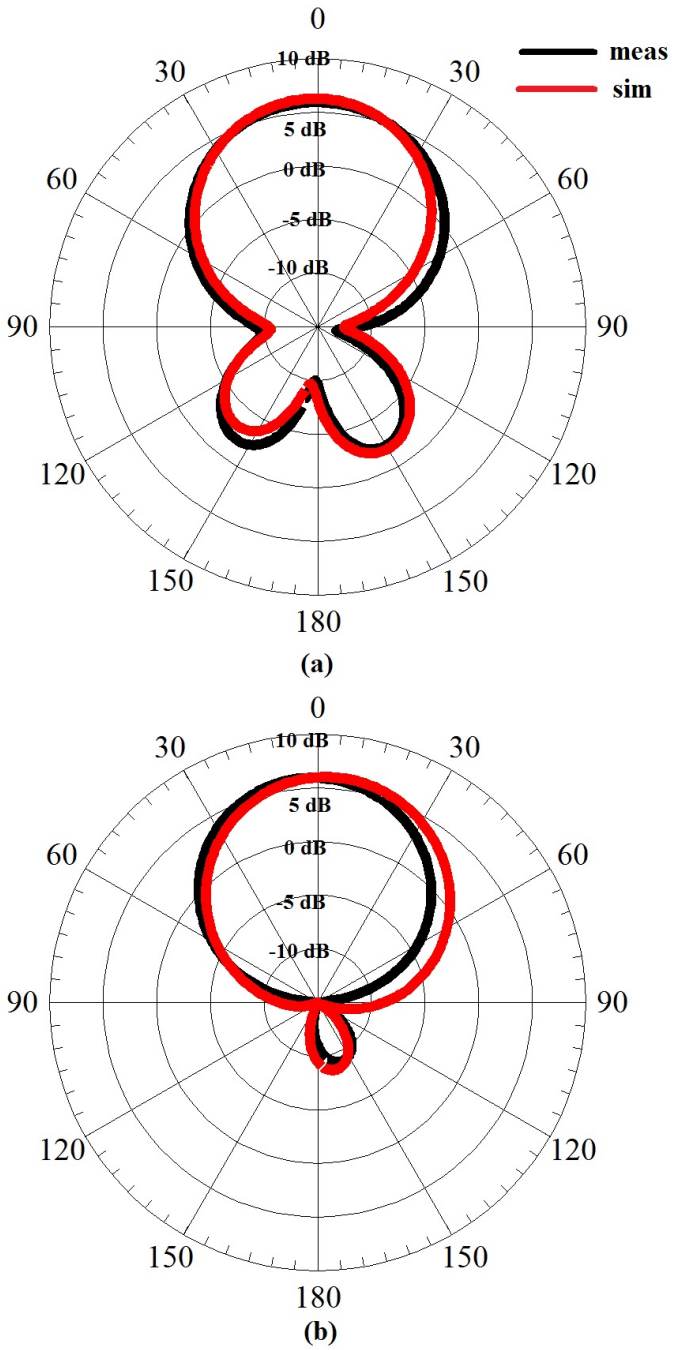

Figure 4.12: Measured and Simulated Radiation Patterns of the Proposed Structure at 2.45 GHz (Diode Is OFF): a) E Plane. b) H Plane.

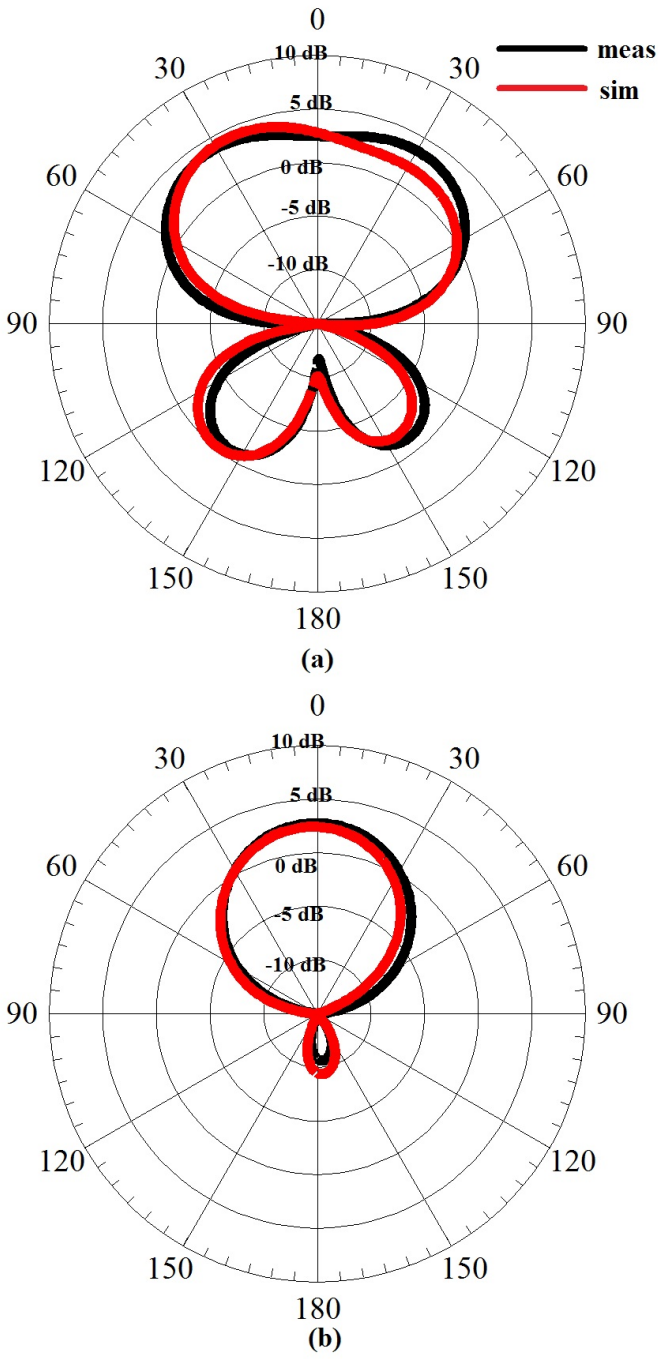

Figure 4.13: Measured and Simulated Radiation Patterns of the Proposed Structure at 3.3 GHz (Diode Is OFF): a) E Plane. b) H Plane.

Table 4.2: Gain Comparison With/Without the AMC

Frequency (GHz)	Antenna without AMC Gain (dB)	Antenna with AMC Gain (dB)
2.45 (ON)	2.7	6.4
2.45 (OFF)	2.6	6.2
3.3 (OFF)	0.6	3.0

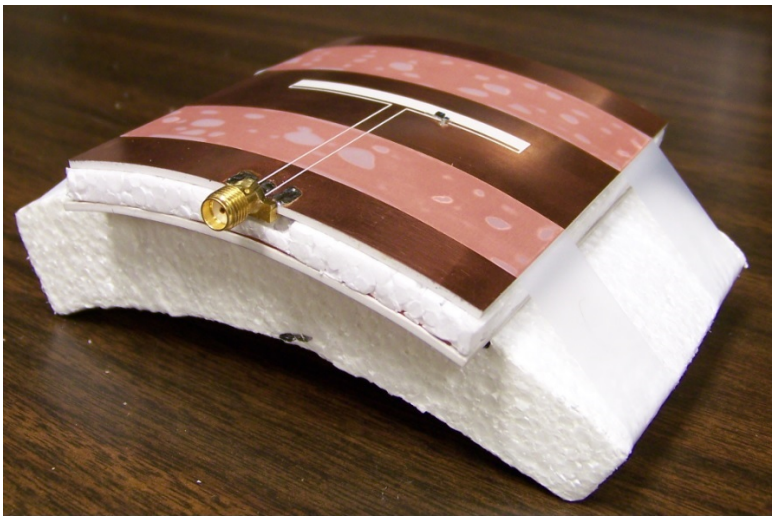

Figure 4.14: Fabricated Prototype of the Curved Antenna Structure.

Another performance metric is the SAR level, which is a factor or a standard that represents the amount of electromagnetic power absorbed by the human body. According to the Federal Communication Commission (FCC), the standard maximum permitted value of SAR level is about 1.6 W/kg in 1 gram of tissue [51]. The fundamental equation of calculating the SAR level is represented by (4.1), where σ is the conductivity and ρ is the mass density of the tissue, and E is the electric field [51]:

Figure 4.15: Fabricated Prototype of the Antenna Structure Placed on Human Body.

$$SAR = \frac{\sigma |E^2|}{\rho} \tag{4.1}$$

The SAR level of the proposed antenna was examined by modeling a human head in HFSS, as illustrated in Fig. 4.17, with a dielectric constant (ϵ_r) of 39.2, a conductivity (σ) of 1.8 S/m and a mass density of 1000 kg/m^3 [51]. The accepted power by the antenna is about 0.1 W, and the distance between the antenna (with/without the AMC surface) and the human head is about 1 mm. Figs. 4.18, 4.19 and 4.20 show the averaged SAR values over 1 gram without the AMC surface for two states of the diode (ON/OFF) and the antenna resonates at 2.45 GHz and 3.3 GHz. It is clear that the SAR is above 1.6 W/kg, which is not preferred for wearable applications. Figs. 4.21, 4.22 and 4.23 display the averaged SAR values over 1 gram with the presence of the AMC surface; it is evident that a significant SAR reduction is obtained by using the AMC surface. Based on the scale in the figures, the maximum SAR value is reduced from 2 W/kg to 0.29 W/kg after using the AMC surface as an isolator.

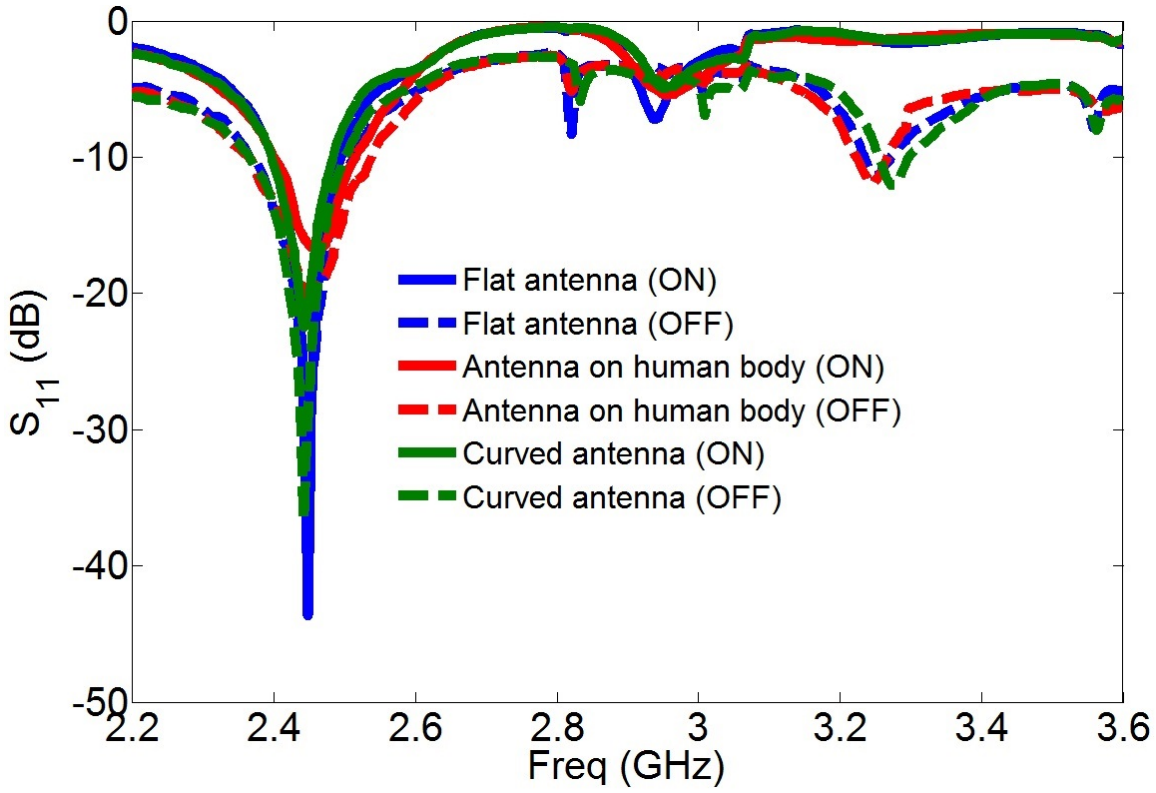

Figure 4.16: The Measured Reflection Coefficients of the Proposed Antenna Structure for Different Configurations: Flat, Curved and Antenna on Human Body (Leg).

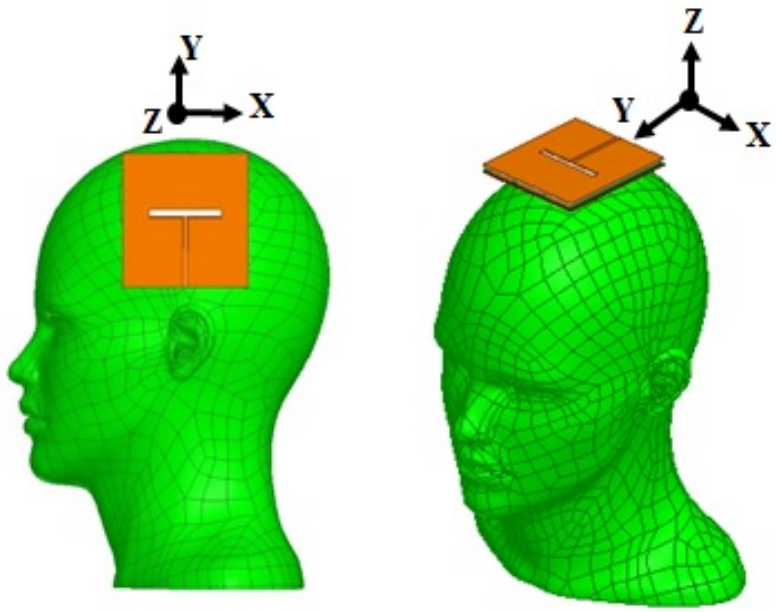

Figure 4.17: The SAR Simulation Setup in HFSS.

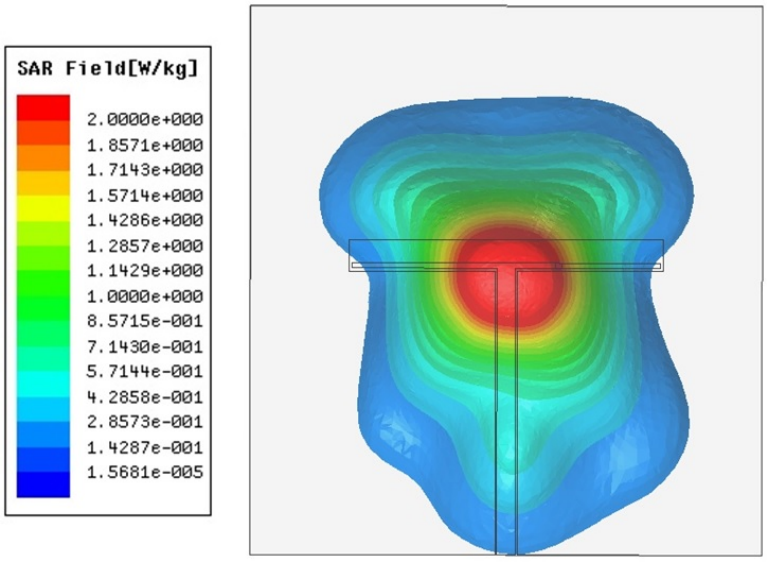

Figure 4.18: The Averaged SAR Values at 2.45 GHz of the Antenna Without AMC Surface (Diode Is ON).

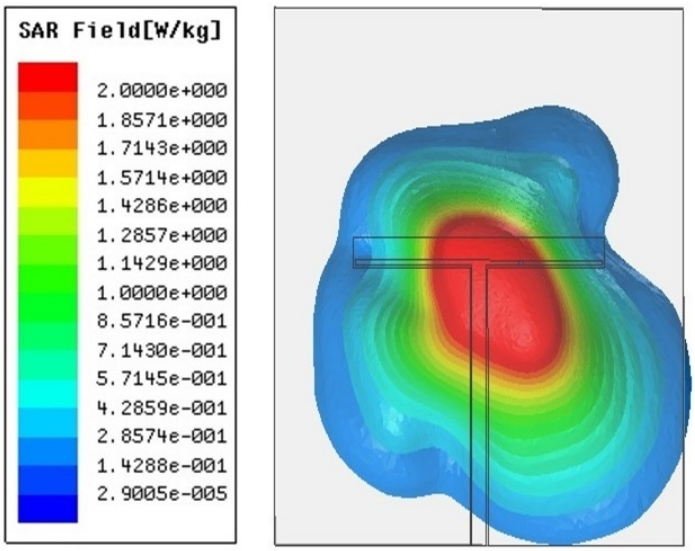

Figure 4.19: The Averaged SAR Values at 2.45 GHz of the Antenna Without AMC Surface (Diode Is OFF).

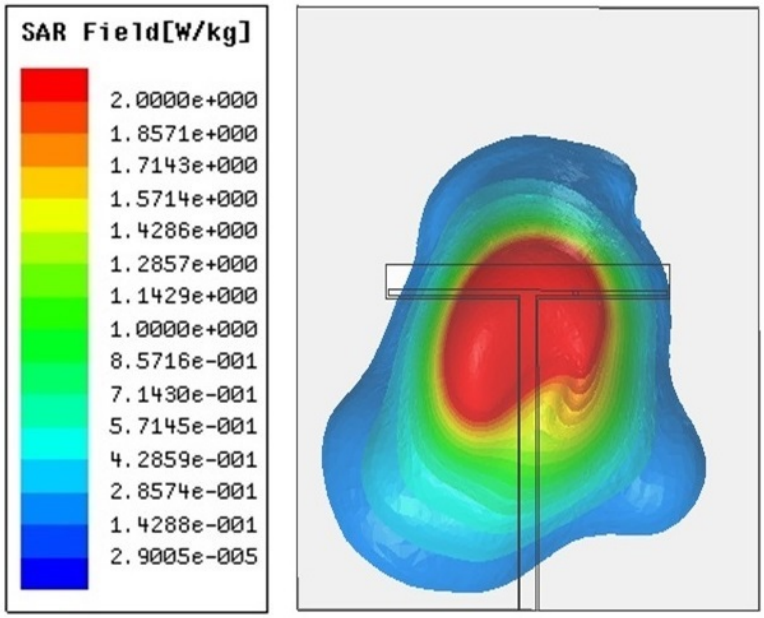

Figure 4.20: The Averaged SAR Values at 3.3 GHz of the Antenna Without AMC Surface (Diode Is OFF).

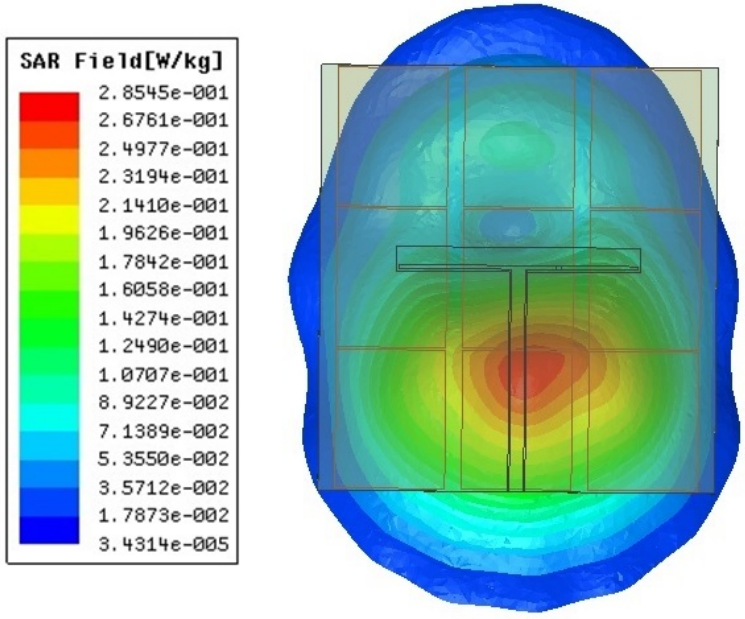

Figure 4.21: The Averaged SAR Values at 2.45 GHz of the Antenna with AMC Surface (Diode Is ON).

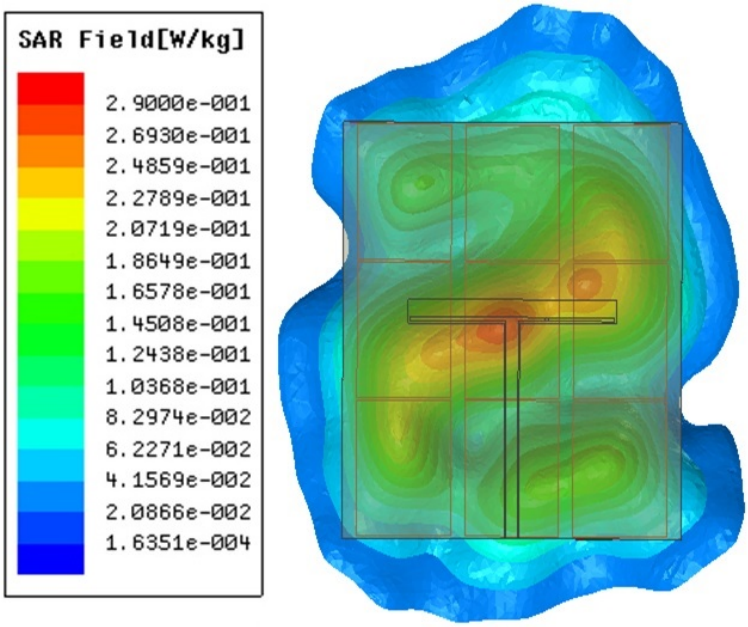

Figure 4.22: The averaged SAR values at 2.45 GHz of the Antenna with AMC Surface (Diode Is OFF).

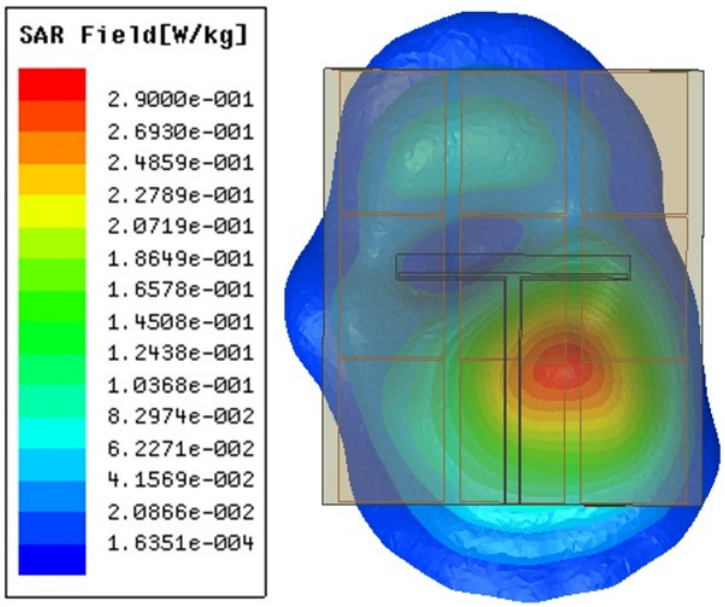

Figure 4.23: The Averaged SAR Values at 3.3 GHz of the Antenna with AMC Surface (Diode Is OFF).

Chapter 5

FLEXIBLE PERFORATED HIGH IMPEDANCE SURFACE

Electromagnetic bandgap (EBG) structures are used to suppress the Surface Wave (SW) propagation in printed antenna systems. Although there are several different types of EBG structures, not all of them can be utilized in flexible electronic applications. As a promising flexible EBG structure, Perforated High Impedance Surfaces (PHISs), which also function as Artificial Magnetic Conductor (AMC) surfaces, are reported. This chapter presents a PHIS, which suppresses SWs in more than one direction. The geometry of the perforations and patches are optimized to overlap the reflection phase and the SW suppression bands. The coupling between two microstrip antennas, each placed on other side of the PHIS, is discussed and a square loop radiator is also designed and simulated over the surface, which show that the proposed design can be used for both coupling reduction between radiating elements and as a ground plane for low profile applications.

5.1 Introduction

For most antenna applications, Surface Waves (SWs) are not desirable since they may reduce the performance of wireless systems. To name a few, they may distort the radiation patterns and can introduce scan blindness in antenna array applications [34], [52]. To overcome this problem, Electromagnetic Band Gap (EBG) structures have been proposed for SW reduction. For example, mushroom surfaces with vias behave as two dimensional left-handed structures where they reduce the SW propagation within a certain band gap [48]. However, it is known that vias increase the cost and

complexity of fabrication. Moreover, EBG structures with vias are not recommended for flexible applications since then limit the flexibility.

In the literature, several other EBG structures without vias are reported [53]. In these structures, the patches are designed to create an equivalent inductance which reduces the propagation of SWs without the need of vias. Other possible designs, which suppress the SWs in the absence of vias, are Defected Ground Structures (DGSs) [54]-[55]. In DGSs, the perforations on the ground plane are used to obtain a band gap for SWs suppression. One drawback of these structures is that either they do not behave as a High Impedance Surface (HIS) or their reflection phase and SW bands do not overlap. As a solution to this issue, Perforated High Impedance Surfaces (PHISs) were reported in [56]-[58]. PHISs are capable of reducing SW propagation and also the reflection phase band is overlapped with the band of SW suppression. Therefore, in this work, a PHIS is reported where the SWs can be suppressed in more than one direction due to the rotational symmetry of the structure. In this chapter, we address the scattering and SW propagation properties of PHIS by unit-cell reflection phase/magnitude and microstrip antenna coupling analyses.

In the literature, HISs were previously reported in [50], [59]-[62] where they are being used as ground planes for radiating elements which are placed in close proximity to those surfaces; and results in antenna design miniaturization. Furthermore, these surfaces improve the radiation characteristics of antennas because they behave as AMC surfaces over a band of frequencies. For the proposed PHIS design, it is desired for the surface to reduce the SWs propagation between antennas and also to be used as a ground plane for low profile applications. Thus, a square loop element is designed over the PHIS to demonstrate the in-phase reflection characteristic of the surface.

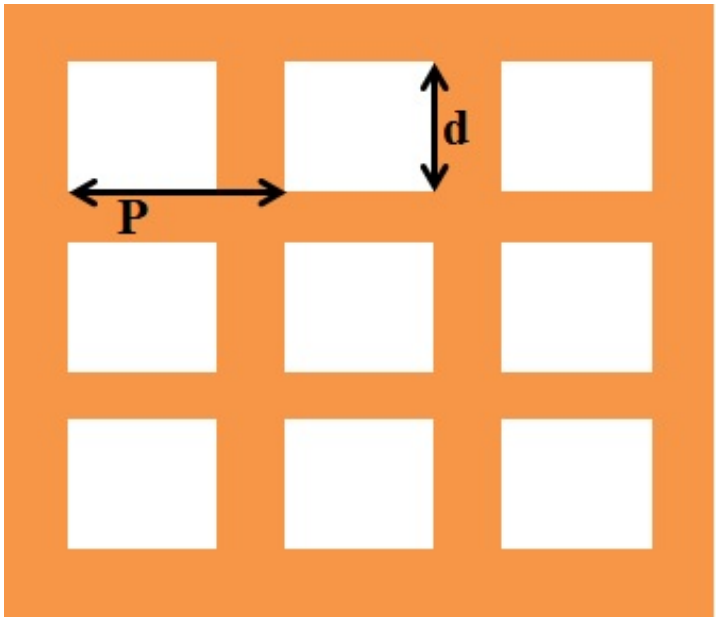

Figure 5.1: Geometry of DGS With Square Slots.

5.2 Design Procedure of a PHIS

The proposed PHIS can be considered as a DGS. As shown in Fig. 5.1, the ground plane of the structure is periodically perforated by square slots whose width (d) is smaller than the period (P). For this type of structure, the suppression of SW is due to Bragg diffraction [63]. When the periodicity is $P = \lambda/2$, the fields that are reflected from each slot interact constructively leading to a strong reflection. This significantly reduces the SW propagation.

In [58], a PHIS with dumbbell shaped slots is reported, where SW suppression is achieved in only one direction. Here we adopt square shaped defects which allow the structure to be symmetrical; hence SW suppression can be achieved in more than one direction. Fig. 5.2 depicts a unit cell of the PHIS where the dashed and solid lines outline the square slots on the ground and the patches on the top surface, respectively. Fig. 5.3 displays the geometry of the proposed PHIS. It is known

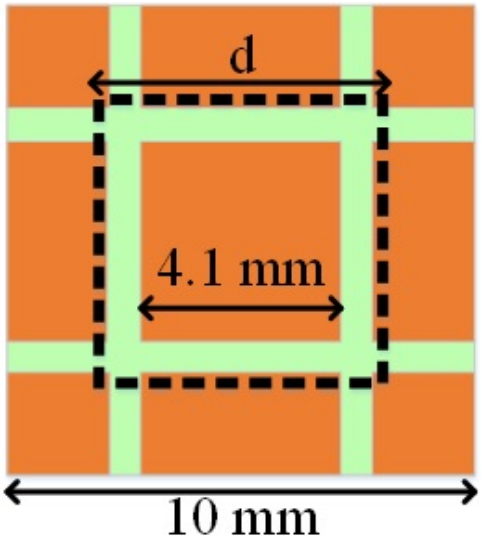

Figure 5.2: Geometry of the Unit-cell of Modified Surface.

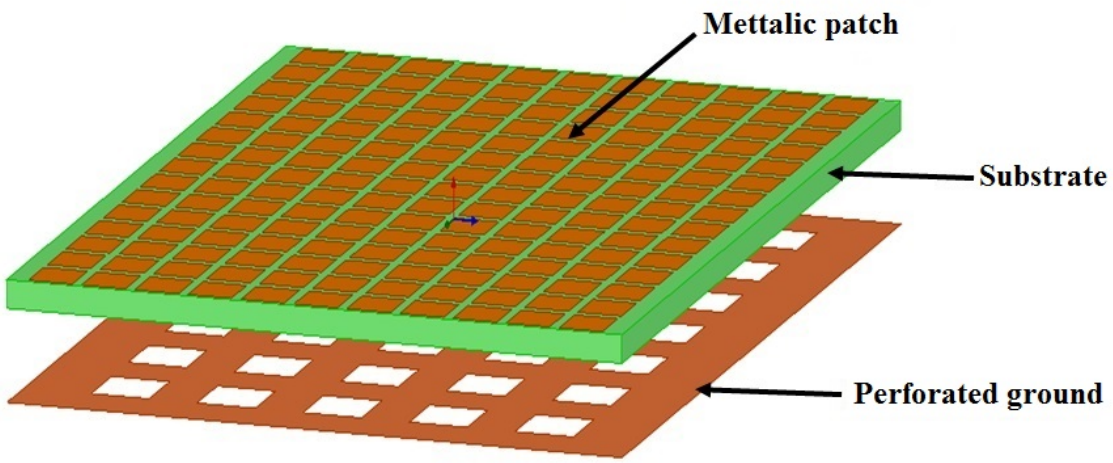

Figure 5.3: Geometry of Perforated High Impedance Surface.

that the reflection phase and SW suppression bands depend on the geometries of the patches and perforations. Therefore, the dimensions of the perforations and patches are chosen carefully to overlap these bands of the reflection phase and the SW suppression. Since the PHIS is proposed as a promising flexible EBG structure where the metallic vias are eliminated but still the surface can still be used for SWs

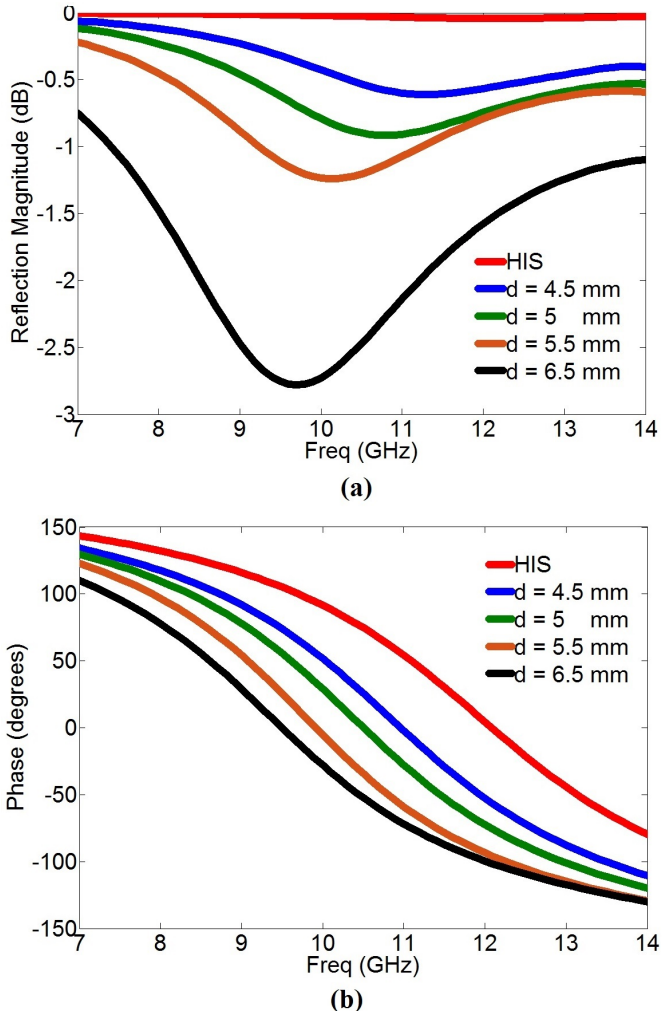

Figure 5.4: a) Reflection Magnitude of the Unit Cell. b) Reflection Phase of the Unit Cell.

suppression, it is designed and simulated on a flexible substrate Rogers (RO3003) [$\epsilon_r = 3$, $\tan(\delta) = 0.0013$ and h = 1.52 mm]. Fig. 5.4 illustrates the numerical results for the reflection phase and magnitude of the unit cell for different perforation widths (d). It can be seen that the center frequency decreases when the slot size increases. Likewise, the magnitude of the reflection coefficient is smaller when the perforation size is larger. Furthermore, the bandwidth is larger when the size of the perforations increases due to the additional inductance from the perforations. For

a conventional HIS surface, the center frequency and bandwidth are proportional to $1/\sqrt{(LC)}$ and $\sqrt{(L/C)}$, respectively [49]. Thus, for the PHIS unit cell, the center frequency decreases and the bandwidth increases if the perforation size increases, and this is due to the additional inductance. Since the structure is rotationally symmetric, the reflection phase is polarization independent. For the dimensions given in Fig. 5.2 and the optimized perforation size is (d = 5.5 mm), the surface has a center frequency (zero reflection phase) at 9.9 GHz and the reflection phase band is 3.6 GHz (36%). The magnitude of the reflection coefficient is around -1.25 dB at the center frequency due to the presence of the perforations.

To demonstrate the SWs suppression of the proposed PHIS, the mutual coupling between two microstrip patches (placed on either side of the PHIS) is simulated. The schematic drawing of the simulation geometry to demonstrate the coupling reduction between the microstrip patch antennas is displayed in Fig. 5.5. The PHIS is placed between two coax-fed microstrip patches which each has a resonant frequency of 10.2 GHz, as shown from the simulated return loss (S_{11}) in Fig. 5.6, and the ground plane is not perforated. A comparison of the mutual coupling (S_{12}) between the antennas is displayed in Fig. 5.6; there are no patches or perforations between the microstrip antennas for the reference case. As indicated in the figure, the proposed PHIS reduces the mutual coupling by about 40 dB. To examine the surface for conformal applications, it is simulated when it is curved with a radius of curvature of about 2λ. Fig. 5.7 shows the schematic drawing of the simulated curved PHIS where two microstrip elements are used to study the coupling of the curved configuration. A comparison between the coupling of the flat and curved configurations are displayed in Fig. 5.8. It is observed that the curved PHIS maintains the SW suppression and the coupling is also reduced.

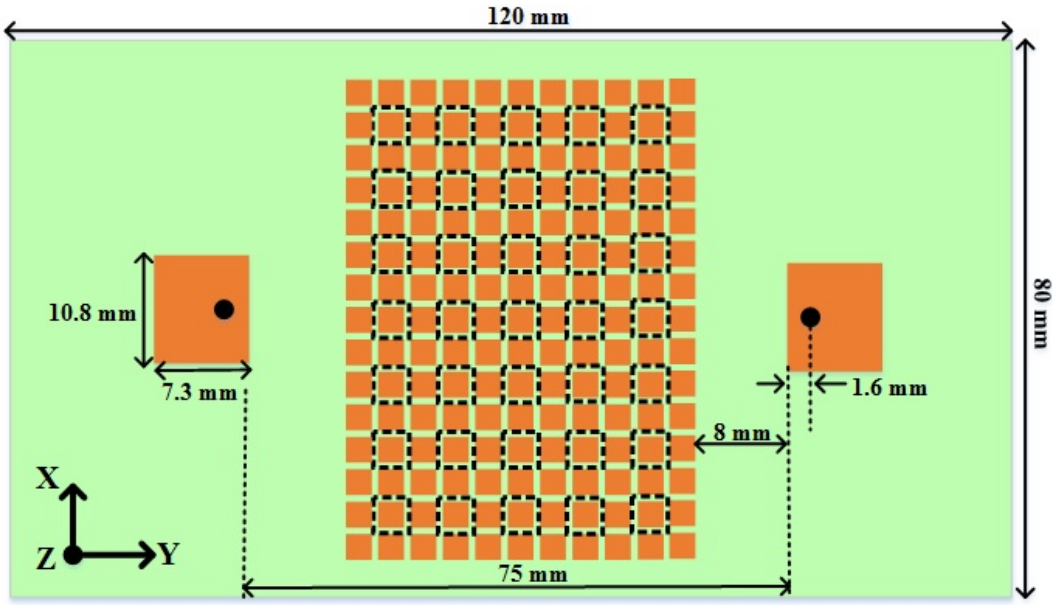

Figure 5.5: Schematic Drawing of the Simulation Geometry to Demonstrate the Coupling Reduction Between the Patch Antennas.

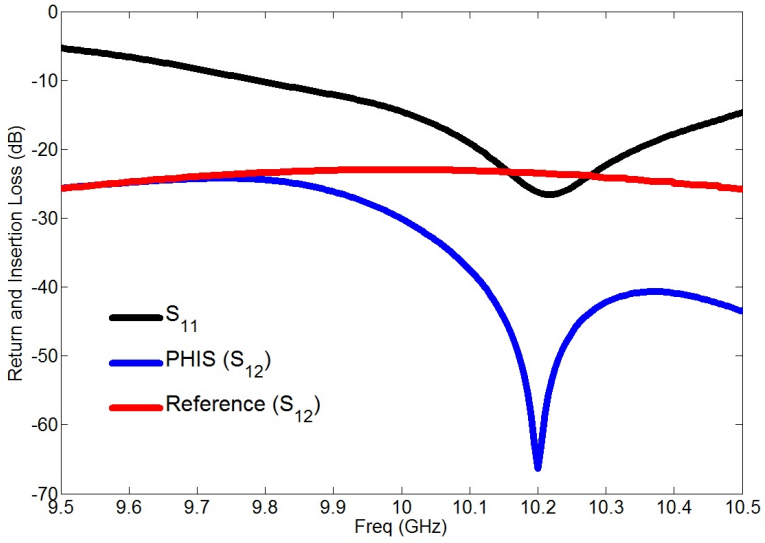

Figure 5.6: Mutual Coupling Reduction Between Two Patch Antennas.

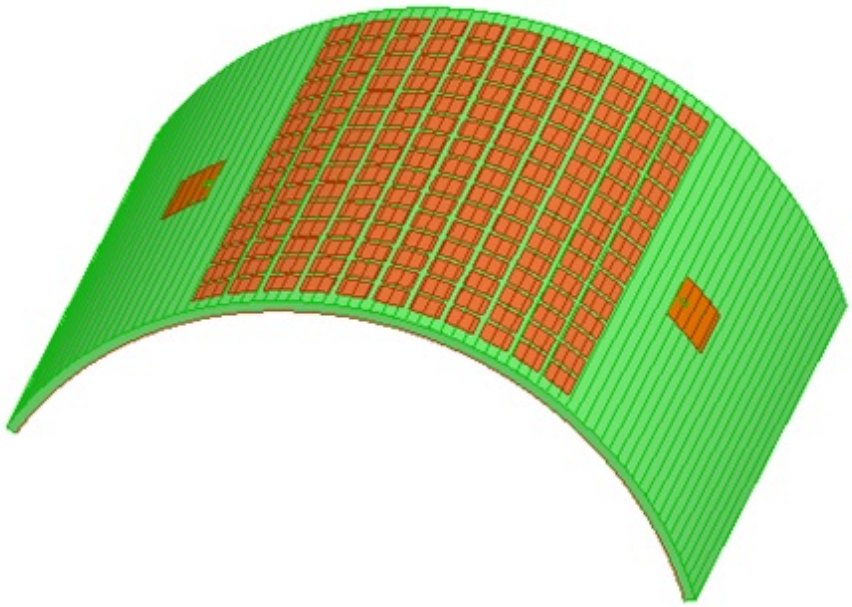

Figure 5.7: Curved Configuration of the Proposed PHIS.

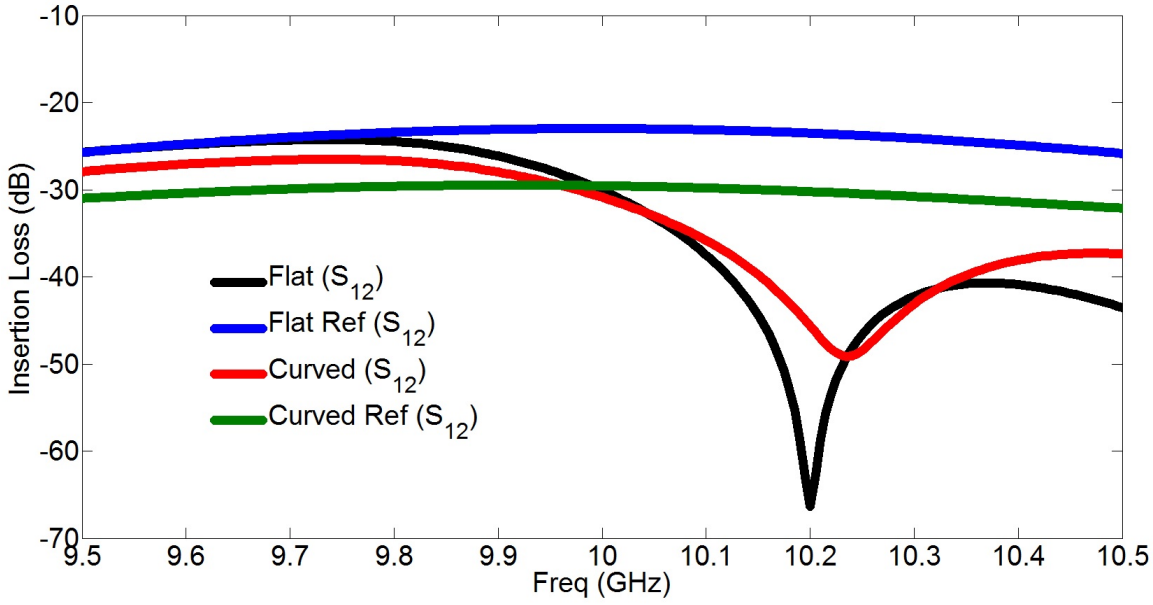

Figure 5.8: A Comparison Between the Coupling Reduction of the Flat and Curved Configurations.

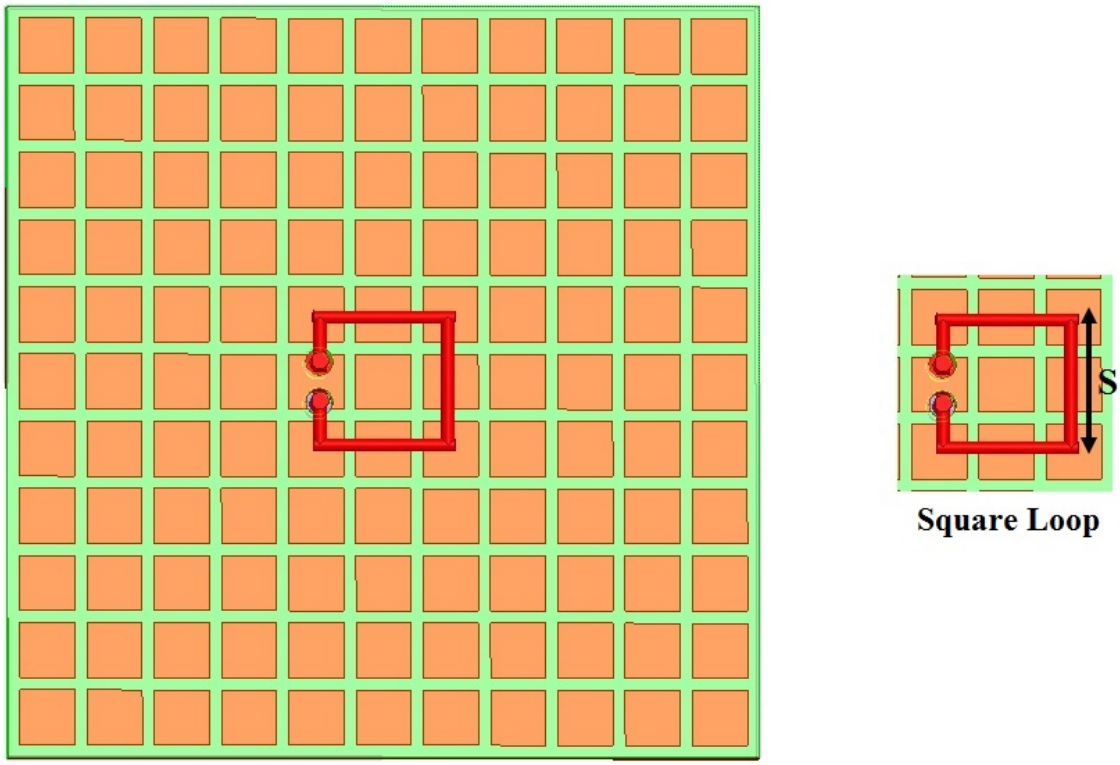

Figure 5.9: Square Loop Antenna over PHIS.

5.3 A Square Loop Antenna over PHIS

As discussed earlier, the artificial ground planes, such as HISs, have been used extensively for low-profile antenna applications. Therefore, the proposed PHIS is also designed to be utilized as a ground plane for antennas. To demonstrate this characteristic, a square loop element is placed in the vicinity of the PHIS, which is considered as a square size ground plane (55.9 mm $\times$ 55.9 mm) with 25 unit-cells (5x5), and the dimensions of each unit-cell are shown in Fig. 5.2. Fig. 5.9 displays the loop radiator over a PHIS ground plane where the side length of the square loop is denoted by S.

To obtain the operational bandwidth of the PHIS, the side length (S) of the square loop was varied. The frequency interval where the return loss is below -10 dB is the

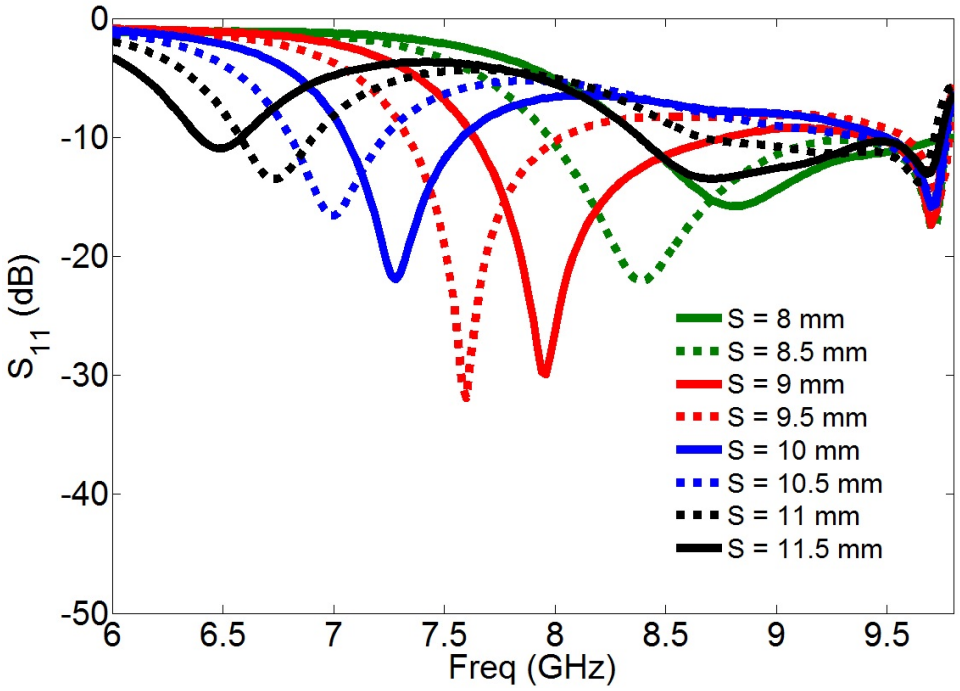

Figure 5.10: Return Loss of the Loop Antenna with Different Side Lengths (S).

considered operational bandwidth of the PHIS. The square loop antenna is placed at a height of 0.025λ over the surface, where the center frequency is 7.9 GHz. Fig. 5.10 exhibits the return loss of the square loop antenna with different side lengths, and it indicates that the -10 dB operational bandwidth of the PHIS is about 41.7%. The performance of the loop antenna is also examined over a Perfect Electric Conductor (PEC) and compared with the PHIS. Fig. 5.11 shows a comparison between the return loss of the antenna over PEC and PHIS ground planes. When PEC surface is used as a ground plane, the return loss of the antenna is about - 2.5 dB at the 7.9 GHz center frequency because the PEC has 180 degree reflection phase where the current of the image is in the opposite direction and ideally it cancels the direct radiation resulting in very low radiation efficiency. However when the PHIS is used, which has a reflection phase that varies from 180 to -180 degrees with frequency, the return loss is about -30 dB and the loop radiator is well matched at the center frequency.

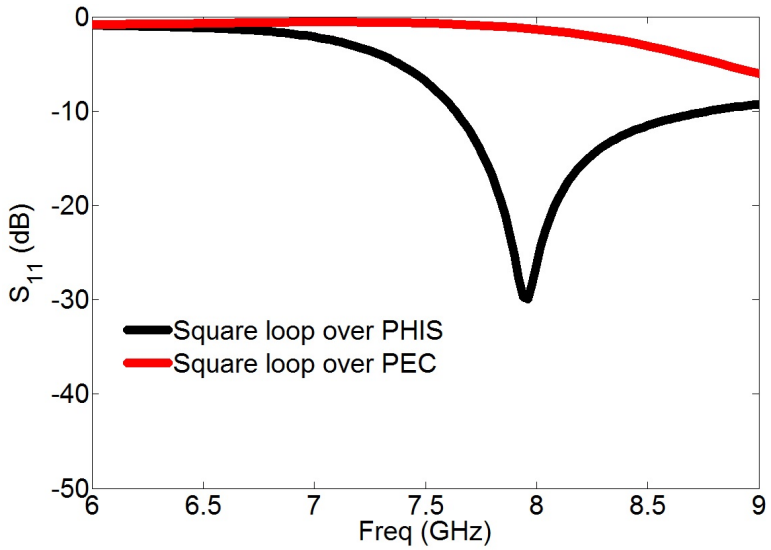

Figure 5.11: A Comparison Between the Return Loss of Square Loop Antenna (S = 9 mm) over PHIS and PEC Ground Planes.

This indicates that the proposed PHIS serves as a desired ground plane for low profile antenna applications. The input impedance of the antenna over PHIS is also displayed in Fig. 5.12, and it validates that the antenna is matched to a 50-ohm coaxial cable feed; the gain radiation pattern of the antenna over PHIS is also considered and shown in Fig. 5.13. Since the antenna is mounted on a ground plane, most of the energy is radiated in the forward hemisphere while the back radiation is reduced. However, due to the perforations on the ground plane, there is some energy leakage producing back radiation but still the front-to-back ratio is high around 19.5 dB for the designed surface. Thus, the designer must consider the size of the perforations and the unit-cell dimensions in order to reduce the amount of leakage. For the proposed design, the peak gain of the antenna over PHIS at broadside ($\theta = 0$) is about 7 dB which is considered a good gain for a square loop radiator above the PHIS ground plane.

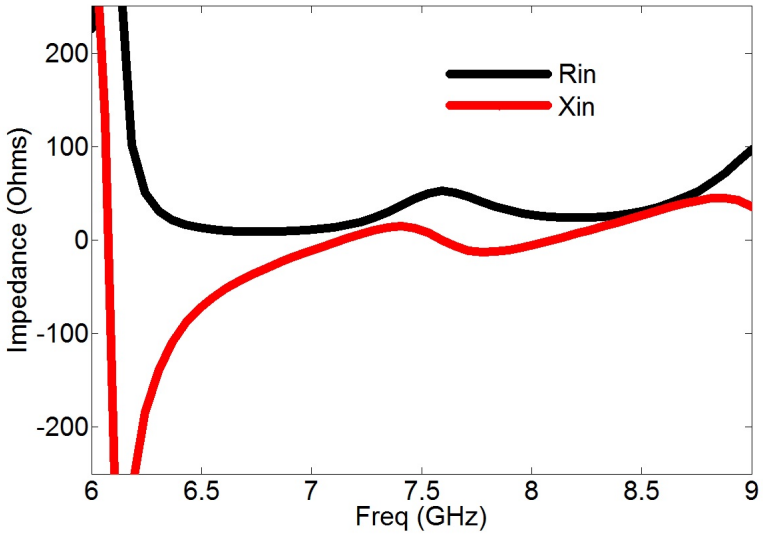

Figure 5.12: Input Impedance of the Square Loop Antenna (S = 9 mm).

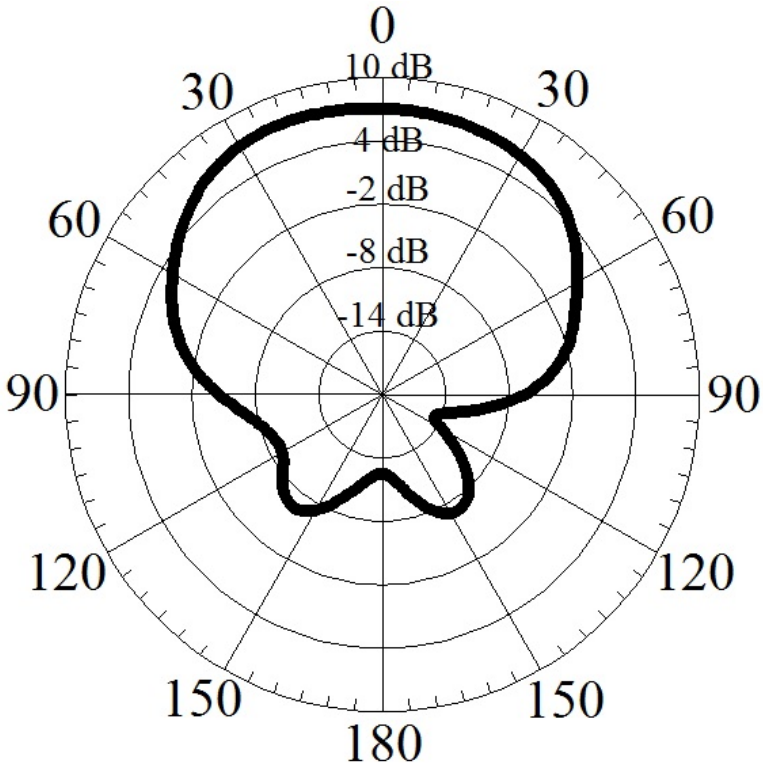

Figure 5.13: Gain Pattern of the Square Loop Antenna over PHIS at the Center Frequency 7.9 GHz.

Chapter 6

CONCLUSIONS

In this research work, the flexibility and the reconfigurability of antennas were investigated and merged. A literature review on flexible radiating elements and substrates was performed to review the design techniques and requirements for them. Another literature review was undertaken on reconfigurable antennas and their applications. Since the proposed flexible antenna is based on the concept of CPW-fed folded slot antennas, the concept of slot radiating elements and their complimentary dipole elements were reviewed and compared. It was concluded that the printed folded slot antenna is a good candidate as a reference radiator in this work due to their attractive radiation characteristics, such as a large bandwidth. Also, they can be used to match and reduce the slot impedance as discussed in Chapter 2. Another advantage is the CPW technique, where the radiating element and ground plane are printed on the same side of the substrate. This is recommended for the integration of active devices to antennas printed on very thin flexible substrates.

The proposed inkjet-printed flexible reconfigurable antenna was designed and fabricated on a flexible PET substrate, to be used for wireless conformal applications as discussed in Chapter 3 [47], [64]-[65]. It was fabricated using inkjet-printing technology due its fast, simple and inexpensive fabrication process. After that, a new reconfiguration approach for folded slot antennas was proposed to reconfigure the antenna. The approach is mainly based on using one PIN diode to adjust the stub length inside the slot to change its symmetry with respect to the CPW feed line. When the PIN diode is ON, the antenna has a single band operation at 2.42 GHz for WLAN wireless applications, and the radiation is mainly from the slot itself. When

the PIN diode is OFF, the antenna has a dual-band operation with two orthogonal polrizations. The first resonant frequency is at 2.36 GHz and it is belonged to the slot. The second resonant frequency is at 3.64 GHz, and it is mainly from the asymmetric stub. The antenna maintains a sufficient bandwidth to be used for WLAN and WiMAX wireless applications. It was designed and examined for both flat and curved configuration where it was mounted on circumferential and axial cylindrical configurations to examine its performance when it used for conformal applications. It was observed that the proposed radiating element maintained its flexibility and reconfigurability and good agreement was achieved between measured and simulated results. The MIMO configuration of the proposed flexible reconfigurable radiator was also designed [66]. The radiating element was redesigned at either single band (2.4 GHz) or dual band (2.4/5.2 GHz) to be used for high speed internet applications. Two orthogonal folded slot antennas are used to form the MIMO antenna system which has a good isolation. The antenna system has a single band or dual-band operation based on the state of the PIN diode. The proposed system can be used for WLAN conformal wireless devices.

So far the flexible reconfigurable antenna was designed for WLAN and WiMAX wireless devices where the radiating element is required to have omni-directional radiation patterns. However, the back radiation is not preferred for devices worn on the human body. Thus, the proposed radiator has to be integrated with an isolator to protect the human body from the back radiation. For that reason, the wearability of the radiating element was investigated. A novel antenna design that merges the flexibility, reconfigurability and wearability of antennas in one design is proposed as discussed in Chapter 4 [67]-[68]. Hence, the previous design has either single band or dual band with two orthogonal polarizations based on the state of the PIN diode. It was integrated with a polarization dependent AMC surface that also has

dual band reflection phase with two orthogonal polarizations. The proposed antenna structure has a good impedance matching at the resonant frequencies. It was tested for different configurations: flat, curved and antenna on human body. It was observed that the proposed antenna maintains its performance and has excellent radiation characteristics. The AMC ground plane reduces the SAR level resulting in good isolation between the antenna and the human body. The proposed radiating device is flexible, reconfigurable and wearable and it can be used for WBAN (2.45 GHz) and WiMAX (3.3 GHz) body-worn wireless devices.

The reflection phase and SW suppression properties of the proposed PHIS are investigated as discussed in Chapter 5 [69]. It is shown that the choice of perforations and patches geometries is critical to overlap the bands of SW suppression and reflection phase. Using two microstrip patches on either side of the PHIS validates that SW suppression can be achieved with the PHIS. Furthermore, a square loop radiator is mounted over the surface to examine its performance as a ground plane for low-profile antenna applications. The results indicate that the proposed structure is a good candidate for flexible antenna applications since the metallic vias are eliminated.

Chapter 7

FUTURE WORK

The recommendations and the future work of the current research on flexible, wearable and reconfigurable antennas are discussed as the following:

- The MIMO configuration of the proposed flexible reconfigurable antenna was investigated. Its performance was examined for the flat configuration using HFSS simulations only. The next step is to examine its performance for the curved configuration. Measurements and fabrication of the proposed MIMO design are also required. It is also recommended to characterize the proposed design in order to examine the diversity performance. Since the coupling between the MIMO elements is critical, the Frequency Selective Surfaces (FSSs) can be utilized to reduce the coupling and to improve the performance of the MIMO antennas.

- The printed folded slot antenna antenna has a ground plane itself and when the antenna mounted over the AMC surface, the coupling between the ground plane of the antenna and the AMC surface may impact the behaviour of the AMC. It may also impact the radiation efficiency of the antenna. So far the height of the antenna over the AMC and the geometry of the element were optimized to overcome this design issue. Another recommended design is to reduce the size of the ground plane and to redesign the antenna over the AMC surface.

- Since MIMO technology is widely used for wireless communication systems as discussed in Chapter 3, the design of wearable reconfigurable MIMO antennas which are integrated over AMC or EBG surfaces is recommended. EBG/AMC

surfaces can be used to isolate the human body from the radiating elements and to reduce the coupling between the radiators.

- So far the proposed PHIS was only designed and simulated using HFSS simulator. The surface needs to be fabricated to compare and verify the simulation results with the measurements. Also, since the main goal of this surface is to use it for flexible antenna applications, the surface is designed on a flexible substrate and it is recommended to be examined and measured for conformal configurations. Moreover, the surface can be used as a ground plane for low-profile antenna applications; and one square loop antenna was mounted on the surface as discussed in Chapter 5. The next step is to design and mount more than one element on the proposed surface, and to examine its performance as an artificial ground plane to those antennas and to reduce the coupling between the radiating elements.

REFERENCES

[1] D. E. Schwartz et al., "Flexible Hybrid Electronic Circuits and Systems," *IEEE Journal on Emerging and Selected Topics in Circuits and Systems*, vol. 7, no. 1, pp. 27-37, Mar. 2017.

[2] W. Wong and A. Salleo, *Flexible Electronics: Materials and Applications*, NewYork, NY: Springer Science & Business Media, 2009.

[3] H. R. Khaleel, "Design and Fabrication of Compact Inkjet Printed Antennas for Integration Within Flexible and Wearable Electronics," *IEEE Transactions on Components, Packaging and Manufacturing Technology*, vol. 4, no. 10, pp. 1722-1728, Oct. 2014.

[4] E. Moradi et al., "Miniature Implantable and Wearable On-body Antennas: Towards the New Era of Wireless Body-centric Systems [Antenna Applications Corner]," *IEEE Antennas and Propagation Magazine*, vol. 56, no. 1, pp. 271-291, Feb. 2014.

[5] D. E. Anagnostou, A. A. Gheethan, A. K. Amert and K. W. Whites, "A Direct-Write Printed Antenna on Paper-Based Organic Substrate for Flexible Displays and WLAN Applications," *Journal of Display Technology*, vol. 6, no. 11, pp. 558-564, Nov. 2010.

[6] A. C. Durgun, C. A. Balanis, C. R. Birtcher and D. R. Allee, "Design, Simulation, Fabrication and Testing of Flexible Bow-Tie Antennas," *IEEE Trans. Antennas Propag.*, vol. 59, no. 12, pp. 4425-4435, Dec. 2011.

[7] J. So, J. Thelen, A. Qusba, G. J. Hayes, G. Lazzi and M. D. Dickey, "Reversibly Deformable and Mechanically Tunable Fluidic Antennas," *Advanced Function Materials*, vol. 19, no. 22, pp. 3632-3637, Oct. 2009.

[8] H. R. Khaleel, H. M. Al-Rizzo and D. G. Rucker, "Compact Polyimide-Based Antennas for Flexible Displays," *Journal of Display Technology*, vol. 8, no. 2, pp. 91-97, Feb. 2012.

[9] G. A. Casula, G. Montisci and G. Mazzarella, "A Wideband PET Inkjet-Printed Antenna for UHF RFID," *IEEE Antennas and Wireless Propagation Letters*, vol. 12, pp. 1400-1403, Oct. 2013.

[10] C. A. Balanis, *Antenna Theory: Analysis and Design*, 4th ed., Hoboken, NJ, USA: Wiley, 2016.

[11] V. Lakafosis, A. Rida, R. Vyas, Y. Li, S. Nikolaou and M. M. Tentzeris, "Progress Towards the First Wireless Sensor Networks Consisting of Inkjet-Printed, Paper-Based RFID-Enabled Sensor Tags," *Proceedings of the IEEE*, vol. 98, no. 9, pp. 1601-1609, Sep. 2010.

[12] J. Bernhard, "Reconfigurable Antennas," Synthesis Lectures on Antennas, vol. 2, no. 1, pp. 1-66, 2007, Morgan & Claypool Publishers.

[13] D. Schaubert, "Frequency-Agile Polarization Diversity Microstrip Antennas and Frequency Scanned Arrays," *U.S. Patent 4367474*, Jan. 1983.

[14] D. Peroulis, K. Sarabandi and L. P. B. Katehi, "Design of Reconfigurable Slot Antennas," *IEEE Trans. Antennas Propag.*, vol. 35, no. 2, pp. 645-654, Feb. 2005.

[15] J. Costantine, Y. Tawk and C. Christodoulou, "Design of Reconfigurable Antennas Using Graph Models," Synthesis Lectures on Antennas, vol. 5, no. 1, pp. 1-148, 2013, Morgan & Claypool Publishers.

[16] J. Costantine, "Design, Optimization, and Analysis of Reconfigurable Antennas," Ph.D. Dissertation, Dept. Elect. Eng., Univ. of New Mexico, Albuquerque, NM, 2009.

[17] J. Costantine, S. Saeed, Y. Tawk, F. Ayoub and C. Christodoulou, "A New Reconfigurable Meander Line Antenna," IEEE Antennas and Propagation Society International Symposium (APSURSI), Orlando, FL, pp. 388-389, July 2013.

[18] J. Chang, L. Ming and F. De Flaviis, "Reconfigurable Scan-Beam Single-Arm Spiral Antenna Integrated With RF-MEMS Switches," *IEEE Trans. Antennas Propag.*, vol. 54, no. 2, pp. 455-463, Feb. 2006.

[19] J. Costantine, Y. Tawk and C. Christodoulou, "A Varactor-Based Reconfigurable Filtenna," *IEEE Antennas and Wireless Propagation Letters*, vol. 11, no. 2, pp. 716-719, Jun. 2012.

[20] Solutions, Skyworks. "Design with PIN Diodes.," Application Note APN1002.

[21] J. Kraus, R. Marhefka and A. Khan, *Antennas for All Applications*, 3rd ed. New York, NY: McGraw, 2002.

[22] H. G. Booker, "Slot Aerials and Their Relation to Complementary Wire Aerials," *J. Inst. Elect. Eng.*, part III A, pp. 620-626, 1946.

[23] R. Garg, *Microstrip Antenna Design Handbook*, 1st ed., Noorwood, MA: Artech House, 2001.

[24] S. K. Sharma, L. Shafai and N. Jacob, "Investigation of Wide-band Microstrip Slot Antenna," *IEEE Trans. Antennas Propag.*, vol. 52, no. 3, pp. 865-872, Mar. 2004.

[25] N. Behdad and K. Sarabandi, "A Wide-band Slot Antenna Design Employing a Fictitious Short Circuit Concept," *IEEE Trans. Antennas Propag.*, vol. 53, no. 1, pp. 475-482, Jan. 2005.

[26] R. H. Chen and Yi-Cheng Lin, "Miniaturized Design of Microstrip-Fed Slot Antennas Loaded With C-Shaped Rings," *IEEE Antennas and Wireless Propagation Letters*, vol. 10, no. 2, pp. 203-206, Dec. 2011.

[27] Huan-Shang Tsai and R. York, "FDTD Analysis of CPW-Fed Folded-Slot and Multiple-Slot Antennas on Thin Substrates," *IEEE Trans. Antennas Propag.*, vol. 44, no. 2, pp. 217-226, Feb. 1996.

[28] N. Lopez-Rivera and R. A. Rodriguez-Solis, "Impedance Matching Technique for Microwave Folded Slot Antennas," *IEEE Antennas and Propagation Society International Symposium*, vol. 3, pp. 450-453, Jun. 2002.

[29] T. M. Weller, L. P. B. Katehi and G. M. Rebeiz, "Single and Double Folded-Slot Antennas on Semi-Infinite Substrates," *IEEE Trans. Antennas Propag.*, vol. 43, no. 12, pp. 1423-1428, Dec. 1995.

[30] A. A. Gheethan and D. E. Anagnostou, "Broadband and Dual-Band Coplanar Folded-Slot Antennas (CFSAs)," *IEEE Antennas and Propagation Magazine*, vol. 53, no. 1, pp. 80-89, Feb. 2011.

[31] A. Pourghorban Saghati, J. Singh Batra, J. Kameoka and K. Entesari, "Miniature and Reconfigurable CPW Folded Slot Antennas Employing Liquid-Metal Capacitive Loading," *IEEE Trans. Antennas Propag.*, vol. 63, no. 9, pp. 3798-3807, Sept. 2015.

[32] D. E. Anagnostou and A. A. Gheethan, "A Coplanar Reconfigurable Folded Slot Antenna Without Bias Network for WLAN Applications," *IEEE Antennas and Wireless Propagation Letters*, vol. 8, pp. 1057-1060, Mar. 2009.

[33] Gang Chen, Xiao-lin Yang and Yan Wang, "Dual-Band Frequency-Reconfigurable Folded Slot Antenna for Wireless Communications," *IEEE Antennas and Wireless Propagation Letters*, vol. 11, pp. 1386-1389, Jan. 2012.

[34] C. A. Balanis, *Advanced Engineering Electromagnetics*, 2nd ed., Hoboken, NJ, USA: Wiley, 2012.

[35] M. S. Sharawi, M. U. Khan, A. B. Numan and D. N. Aloi, "A CSRR Loaded MIMO Antenna System for ISM Band Operation," *IEEE Trans. Antennas Propag.*, vol. 61, no. 8, pp. 4265-4274, Aug. 2013.

[36] R. Hussain and M. S. Sharawi, "A Cognitive Radio Reconfigurable MIMO and Sensing Antenna System," *IEEE Antennas and Wireless Propagation Letters.*, vol. 14, no. 2, pp. 257-260, 2015.

[37] Y. Tawk, J. Costantine and C. G. Christodoulou, "Reconfigurable Filtennas and MIMO in Cognitive Radio Applications," *IEEE Trans. Antennas Propag.*, vol. 62, no. 3, pp. 1074-1083, Mar. 2014.

[38] D. P. Tobn, T. H. Falk and M. Maier, "Context Awareness in WBANs: a Survey on Medical and Non-medical Applications," *IEEE Wireless Communications*, vol. 20, no. 4, pp. 30-37, Aug. 2013.

[39] G. A. Conway and W. G. Scanlon, "Antennas for Over-Body-Surface Communication at 2.45 GHz," *IEEE Trans. Antennas Propag.*, vol. 57, no. 4, pp. 844-855, Apr. 2009.

[40] K. Koski, L. Sydnheimo, Y. Rahmat-Samii and L. Ukkonen, "Fundamental Characteristics of Electro-Textiles in Wearable UHF RFID Patch Antennas for Body-Centric Sensing Systems," *IEEE Trans. Antennas Propag.*, vol. 62, no. 12, pp. 6454-6462, Dec. 2014.

[41] B. Hu, G. P. Gao, L. L. He, X. D. Cong and J. N. Zhao, "Bending and On-Arm Effects on a Wearable Antenna for 2.45 GHz Body Area Network," *IEEE Antennas Wireless Propag. Lett.*, vol. 15, pp. 378-381, 2016.

[42] S. Zhu and R. Langley, "Dual-Band Wearable Textile Antenna on an EBG Substrate," *IEEE Trans. Antennas Propag.*, vol. 57, no. 4, pp. 926-935, Apr. 2009.

[43] H. R. Raad, A. I. Abbosh, H. M. Al-Rizzo and D. G. Rucker, "Flexible and Compact AMC Based Antenna for Telemedicine Applications," *IEEE Trans. Antennas Propag.*, vol. 61, no. 2, pp. 524-531, Feb. 2013.

[44] S. Yan, P. J. Soh and G. A. E. Vandenbosch, "Low-Profile Dual-Band Textile Antenna With Artificial Magnetic Conductor Plane," *IEEE Trans. Antennas Propag.*, vol. 62, no. 12, pp. 6487-6490, Dec. 2014.

[45] B. S. Cook and A. Shamim, "Utilizing Wideband AMC Structures for High-Gain Inkjet-Printed Antennas on Lossy Paper Substrate," *IEEE Antennas and Wireless Propagation Letters*, vol. 12, pp. 76-79, 2013.

[46] H. R. Khaleel, H. M. Al-Rizzo and A. I. Abbosh, "Design, Fabrication, and Testing of Flexible Antennas," in Advancement in Microstrip Antennas With Recent Applications, A. Kishk, Ed., InTech, Vienna, Austria, 2013.

[47] **S. M. Saeed**, C. A. Balanis and C. R. Birtcher, "Inkjet-Printed Flexible Reconfigurable Antenna for Conformal WLAN/WiMAX Wireless Devices," *IEEE Antennas and Wireless Propagation Letters*, vol. 15, pp. 1979-1982, 2016.

[48] D. Sievenpiper, High-Impedance Electromagnetic Surfaces, Ph.D. Dissertation, Department of Electrical Engineering, UCLA, 1999.

[49] A. Durgun, Analysis, Design, Simulation, and Measurements of Flexible High Impedance Surfaces, Ph.D. Dissertation, School of Electrical, Computer and Energy, ASU, 2013.

[50] Y. Fan and Y. Rahmat-Samii, "Reflection Phase Characterizations of the EBG Ground Plane for Low Profile Wire Antenna Applications," *IEEE Trans. Antennas Propag.*, vol. 51, no. 10, pp. 2691-2703, 2003.

[51] IEEE Recommended Practice for Determining the Peak Spatial-Average Specific Absorption Rate (SAR) in the Human Head from Wireless Communications Devices: Measurement Techniques - Redline," in IEEE Std 1528-2013 (Revision of IEEE Std 1528-2003) - Redline, pp.1-500, Sept. 2013.

[52] Y. Fu and N. Yuan, "Elimination of Scan Blindness in Phased Array of Microstrip Patches Using Electromagnetic Bandgap Materials," *IEEE Antennas and Wireless Propagation Letters*, vol. 3, no.1, pp. 63-65, 2004.

[53] R. Coccioli, F.-R. Yang, K.-P. Ma, and T. Itoh, "Aperture-Coupled Patch Antenna on UC-PBG Substrate," *IEEE Trans. Microw. Theory Tech.*, vol. 47, no. 11, pp. 2123-2130, 1999.

[54] T.-Y. Yun and K. Chang, "Uniplanar One-dimensional Photonic-bandgap Structures and Resonators," *IEEE Trans. Microw. Theory Tech.*, vol. 49, no. 3, pp. 549-553, 2001.

[55] C. Caloz, H. Okabe, T. Iwai, and T. Itoh, "A Simple and Accurate Model for Microstrip Structures with Slotted Ground Plane," *IEEE Microwave and Wireless Components Letters*, vol. 14, no. 4, pp. 133-135, 2004.

[56] A. C. Durgun, C. A. Balanis, and C. R. Birtcher, "A Novel HIS with a Perforated Ground Plane for Miniaturization and Bandwidth Enhancment," *in Antenna and Propagation Society International Symposium (APSURSI)*, 2012.

[57] A. C. Durgun, C. A. Balanis, and C. R. Birtcher, "Surface Wave Suppression Properties of Perforated Artificial Impedance Surfaces," *in Antenna and Propagation Society International Symposium (APSURSI)*, 2013.

[58] A. C. Durgun, C. A. Balanis, and C. R. Birtcher, "High-Impedance Surfaces With Periodically Perforated Ground Planes," *IEEE Trans. Antennas Propag.*, vol. 62, no. 9, pp. 4510-4517, 2014.

[59] A. Vallecchi, J. R. De Luis, F. Capolino, and F. De Flaviis, "Low Profile Fully Planar Folded Dipole Antenna on a High Impedance Surface," *IEEE Trans. Antennas Propag.*, vol. 60, no. 1, pp. 51-60, 2012.

[60] M. Z. Azad and M. Ali, "Novel Wideband Directional Dipole Antenna on a Mushroom Like EBG Structure," *IEEE Trans. Antennas Propag.*, vol. 65, no. 5, pp. 1242-1250, 2008.

[61] A. C. Durgun, C. A. Balanis, and C. R. Birtcher, "Reflection Phase Characterization of Curved High Impedance Surfaces," *IEEE Trans. Antennas Propag.*, vol. 61, no. 12, pp. 6030-6038, 2013.

[62] M. A. Amiri, C. A. Balanis, and C. R. Birtcher, "Analysis, Design, and Measurements of Circularly Symmetric High-Impedance Surfaces for Loop Antenna Applications," *IEEE Trans. Antennas Propag.*, vol. 64, no. 2, pp. 618-629, 2016.

[63] A. M. E. Safwat, S. A. Tretyakov, and A. V. Raisanen, "High-Impedance Wire," *IEEE Antennas and Wireless Propagation Letters*, vol. 6, pp. 631-634, 2007.

[64] **S. M. Saeed**, C. A. Balanis and C. R. Birtcher, "A Flexible and Reconfigurable Antenna for Wearable Conformal Applications," *in AMTA 37th Annual Meeting and Symposium*, Long Beach, California, pp. 1-4, 2016.

[65] **S. M. Saeed**, C. A. Balanis and C. R. Birtcher, "Radiation Characteristics of Flexible Reconfigurable Antenna With Curved Cylindrical Configurations," *in 2016 IEEE Antennas and Propagation International Symposium*, Fajardo, Puerto Rico, pp. 1433-1434, 2016.

[66] **S. M. Saeed**, C. A. Balanis and C. R. Birtcher, "Flexible Reconfigurable Antenna With MIMO Configuration," *in 2017 IEEE Antennas and Propagation International Symposium*, San Diego, CA, pp. 1643-1644, 2017.

[67] **S. M. Saeed**, C. A. Balanis and C. R. Birtcher, "A Wearable and Reconfigurable Folded Slot Antenna for Body-Worn Devices," *in 2017 IEEE Antennas and Propagation International Symposium*, San Diego, CA, pp. 575-576, 2017.

[68] **S. M. Saeed**, C. A. Balanis and C. R. Birtcher, A. C. Durgun and H. N. Shaman, "Wearable Flexible Reconfigurable Antenna Integrated With Artificial Magnetic Conductors," *IEEE Antennas and Wireless Propagation Letters*, vol. 17, 2017.

[69] **S. M. Saeed**, C. A. Balanis and C. R. Birtcher, "Reflection Phase and Surface Wave Propagation Characteristics of a Symmetrical Perforated High Impedance Surfaces," *in 2016 IEEE Antennas and Propagation International Symposium*, Fajardo, Puerto Rico, pp. 1963-1964, 2016.